AN ABSTRACT OF THE THESIS OF

Yip Chun for the degree of Master of Science in Oceanography presented on September 9, 1988.

Title: Geochemistry of Thorium in Natural Water Systems

Redacted for Privacy

Abstract approved: Chih-An Huh

^{232}Th is non-radiogenic and hence is supplied to natural water systems only by the weathering of crustal rocks. Like most other trace metals, it is delivered to the ocean by the usual fluvial and aeolian pathways. Therefore, ^{232}Th can serve as a connection between trace metals and radiogenic thorium isotopes (i.e., ^{234}Th, ^{230}Th, and ^{228}Th). Knowledge of the distribution of ^{232}Th in natural waters can therefore enhance the value of information on the distributions of the other Th isotopes when they are applied to various geochemical and geochronological studies.

The activities of ^{230}Th and ^{232}Th in continental water (river and lake), seawater, and hydrothermal solutions are determined by neutron activation analysis (NAA) and isotope dilution mass spectrometry (IDMS). Concentrations of dissolved and particulate ^{230}Th and ^{232}Th are presented for the Columbia River, the confluence of the John Day and Columbia Rivers, Crater Lake, Lost Lake, Oregon, and the Saanich Inlet, Canada. This data set indicates that there are large variations of thorium content in natural waters and of its partitioning between the dissolved and particulate forms. In surface waters, dissolved ^{232}Th concentrations range from 0.021 to 0.708 dpm/10^3kg, and dissolved ^{230}Th

concentrations range from 0.039 to 0.917 dpm/10^3kg. Concentration ranges of particulate ^{232}Th and ^{230}Th are 0.0083 to 18.65 dpm/10^3kg and 0.03 to 51.75 dpm/10^3kg, respectively. The concentration levels in fresh waters are one (for dissolved Th) to four (for particulate Th) orders of magnitude larger than in seawater. Thorium is a very particle-reactive element. The partitioning of Th on particulates in the fresh waters are about 2 to 20 times higher than in seawater, reflecting higher particle concentration in fresh waters.

Vertical profiles are reported for three sampling sites: Crater Lake, Saanich Inlet, and off the coast of Washington and Oregon. A subsurface maximum of ^{232}Th is observed in Crater Lake and Saanich Inlet, which may be produced by vertical particulate transport. The profiles in Saanich Inlet also show systematic trends along the oxic/anoxic interface; dissolved ^{232}Th and ^{230}Th increase with depth while particulate ^{232}Th and ^{230}Th decrease with depth. Chemical changes across the redox boundary strongly affect the partitioning of thorium between solution and suspended particles. When settling particles cross the redox boundary, Th is released into solution, enhancing the dissolved Th concentration in the anoxic water. The profile of ^{232}Th in coastal seawater clearly indicates a surface source of ^{232}Th and its scavenging throughout the water column. In addition, the remobilization and enhanced scavenging at land-sea boundaries may have a significant influence on thorium distribution, which suggests that fluvial input is more important in coastal regions, whereas aeolian input dominates in the open ocean.

The concentrations of ^{232}Th in hydrothermal solution from the Juan de Fuca Ridge range from 0.08 to 3.1 dpm/10^3kg. Correlation between ^{232}Th concentration and other properties indicates that the hydrothermal end-member is highly enriched in ^{232}Th relative to deep seawater. Thus, hydrothermal vents should constitute a source of ^{232}Th to the deep ocean.

Geochemistry of Thorium in Natural Water Systems

by

Yip Chun

A THESIS

submitted to

Oregon State University

in partial fulfillment of
the requirements for the
degree of

Master of Science

Completed September 9, 1988

Commencement June 1989

APPROVED:

Redacted for Privacy

Assistant Professor of Oceanography in charge of major

Redacted for Privacy

Head of department of Oceanography

Redacted for Privacy

Dean of Graduate School

Date thesis is presented September 9, 1988

ACKNOWLEDGEMENTS

First of all, I am indebted to all the people who edited this manuscript. Special thanks to Dabra Zahnle for her proofreading and helpful comments on the first draft of this manuscript. Thanks to Collin Roesler, Annette de Charon, Calven Mordy, and my host family Danetta and Mario Cordova for their emotional support, culture guidance and English editing.

Most of all I am indebted to Chih-An Huh for his financial support, scientific guidance, and his valuable time. Whenever I needed his advice, he always made time for me, no matter how busy he was. I couldn't have finished without his help. I would like to thank Fredrick G. Prahl for his constructive comments, advice and encouragement. Special thanks to Robert W. Collier for providing Crater Lake samples and data, suggestions, careful reading of the manuscript and helpful critique. I would also like to thank to David C. Kadko for supplying hydrothermal solution samples from the Juan de Fuca Ridge.

Last, but not least, I would like to thank my husband, Ken Kwong for his understanding, patience, and the times he worked through the night with me on our computer. Without his emotional support and computer knowledge, I couldn't have finished this thesis.

This research was supported by NSF grants OCE-8515631.

This thesis is dedicated to my mother who devotes all her life to her children.

TABLE OF CONTENTS

LIST OF FIGURES

LIST OF TABLES

GEOCHEMISTRY OF THORIUM IN NATURAL WATER SYSTEMS

INTRODUCTION

Applications of thorium (Th) isotopes to various studies in marine geochemistry have long received wide attention. In the ocean, radiogenic Th isotopes have been studied intensively and applied to explain various geochemical and geochronological phenomena. Radiogenic Th isotopes are generated in the water column at known rates. Thus they are of special value as natural tracers for studying the general scavenging process and as clocks to determine the rates of important biogeochemical processes. However, when using radiogenic Th isotopes as proxies to study the general scavenging of other non-radiogenic trace metals, they cannot be compared directly due to their very different source terms and pathways of input to the oceans (Nozaki and Horibe, 1983; Huh and Bacon, 1985a,b). ^{232}Th is nonradiogenic and is delivered to the ocean from continents through the fluvial and aeolian pathways, like most other trace metals (Huh and Bacon 1985a,b); and possibly through hydrothermal vents as well. In order to provide a link between the radiogenic Th isotopes and other particle-reactive trace metals, it is necessary to study the distribution of nonradiogenic ^{232}Th in seawater and its partitioning between dissolved and particulate forms. It has been suggested that the knowledge of concentration and distribution pattern of ^{232}Th in seawater can enhance our understanding of the transport pathways and biogeochemistry of Th, as well as many other particle-reactive trace metals, in the ocean (Huh and Moore, 1988). Moreover, by comparing ^{232}Th with other radiogenic Th isotopes, further benefits can be gained in certain applications, such as their geochemical cycling and sources of input. Thus, our knowledge of the distribution of ^{232}Th is not only of

fundamental importance to the marine geochemistry of this actinide element, but also is essential to improve applications of other Th isotopes.

^{232}Th is supplied by the weathering of crustal rocks (Broecker et al., 1973). The major pathway by which most products of chemical weathering on land reach the sea is riverine transport (Ivanovich and Harmon, 1982). The amount of input is usually determined by the biogeochemical reactions occurring on deteriorated materials transported along fluvial trails toward the ocean. Thus, knowledge of the behavior and distribution of ^{232}Th in fresh water systems is very important for constructing its geochemical balance and evaluating its crustal weathering and supply to the ocean.

Very little is known, however, about the distribution and partitioning of Th isotopes in rivers and lakes. Several types of chemical reactions may take place in fresh water environments. Rivers and lakes are highly variable in pH and alkalinity. Since thorium adsorption in the water column is a function of pH and carbonate alkalinity and adsorption of Th increases with increasing pH and decreasing carbonate alkalinity (LaFlame and Murray, 1986; Langmuir & Herman,1980), the rate and mechanism of Th scavenging will vary.

The purpose of this research is to understand factors controlling the distribution and geochemistry of Th in natural water systems of such different environmental settings as fresh water (i.e., river and lake), seawater, and hydrothermal waters. Specific study areas included the Columbia River, the confluence of the John Day and Columbia Rivers, Lost Lake and Crater Lake, Oregon, the coast of Washington and Oregon, Saanich Inlet, Canada (Fig. 1.1) and the Juan de Fuca Ridge.

The Columbia River, which flows over a 1950-km course through the Cascade Mountains to the Pacific Ocean from its headwaters in Canada, is the largest river in western North America. It drains a basin of 667,000 km^2 and

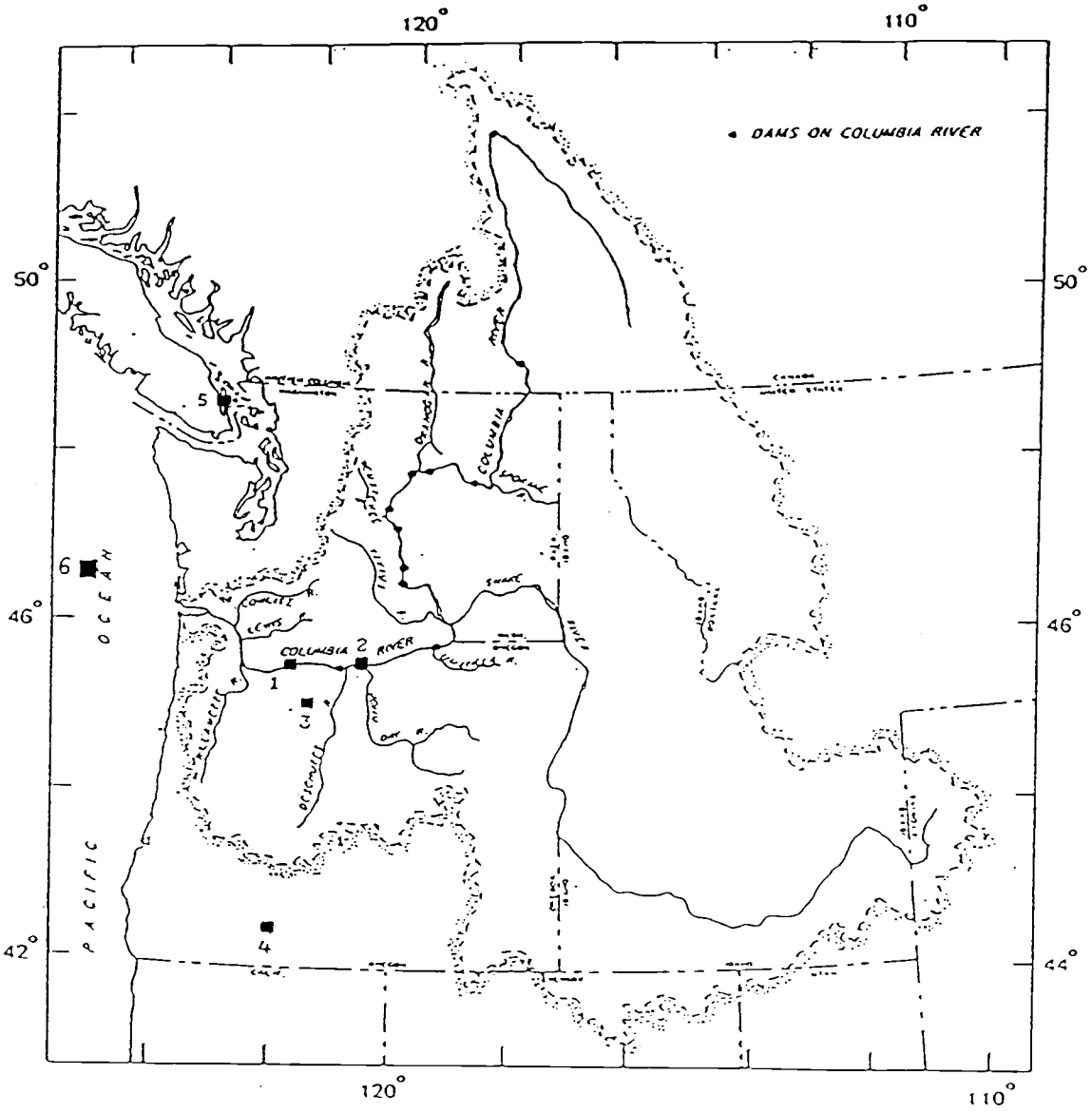

Figure 1.1. Map showing water sampling locations (solid square). 1. Bonneville Dam; 2. Confluence of the John Day & Columbia Rivers; 3. Lost Lake; 4. Crater Lake; 5. Saanich Inlet, Vancouver, B.C; and 6. Washington and Oregon coast

discharges 7,300 m^3/sec of freshwater into the northeast Pacific Ocean (Jay and Sherwood, 1984). It has been recognized that the Columbia River plume has great influence on the hydrodynamics and sedimentation processes of the Washington and Oregon Coasts and the northeast Pacific (Pruter and Alverson, 1972). Hence, to study Th concentrations in Columbia River is a good way to understand the behavior of Th in an estuary and coastal region. The John Day River is one of the main tributaries entering the Columbia River in Oregon, thus it should have certain contribution to and influence on the chemical compositions of the Columbia River. Thorium tends to form strong organic complexes (Langmuir and Herman, 1980). The organic fraction of the Columbia River is dominated by dissolved organic carbon (DOC); and our sampling time was during its maximum season (Dahm et al., 1981). Lost Lake is an oligotrophic lake located in the Cascade Mountains and surrounded by intense coniferous forest. It is interesting to compare the concentrations of Th in those waters and to learn the environmental influence on Th behaviors.

Crater Lake has many unique features. It is a very young volcanic lake formed about 7000 years ago (Volchok et al., 1970) by the eruption and collapse of Mt. Mazama. It is the deepest freshwater body in the U.S. (590 m), and has 53 km^2 of surface area with no outflowing streams (Williams and Von Herzen, 1983). Seepage (approximately 0.5% of the volume of the lake) and evaporation are the only means of water loss from Crater Lake (Simpson, 1970). About 78% of the total annual supply ($1.2x10^{11}$ liters) of water, mainly in the form of snowfall, is directly deposited onto the lake surface (Volchok et al., 1970; Williams and Von Herzen, 1983). The total volume of Crater Lake, about $17x10^{12}$ liters, has remained relatively constant for the last 75 years (Volchok et al., 1970 and references therein). The lake water is extraordinarily pure and clear, and has very low particle content (Williams and Von Herzen, 1983), which

will certainly affect scavenging of thorium, and hence its concentration and distribution in the lake. In addition, Crater Lake is also influenced by hydrothermal activity. The studies of Collier and Dymond (1987) have suggested the existence of hydrothermal vents in the southwest basin of the Lake.

The samples collected from hydrothermal vents on the Juan de Fuca Ridge should allow us to evaluate and study the behavior of Th in hydrothermal solutions. The solutions emerging from the hot spring are of very different chemistry from the original waters (Richards and Strens, 1985). It has been shown that hydrothermal processes provide an important source of certain elements (Edmond et al., 1982 and references therein) while removing a quantitative amount of some other elements (Chen et al., 1986a and references therein). Thus, the hydrothermal input and its interaction with overlying water will significantly alter the chemistry of the water. In order to better understand the marine geochemistry of thorium, it is fundamentally important to measure Th concentrations in hydrothermal solutions so as to assess their role as potential sources or sinks of Th in the ocean.

The study area off Washington coast, located approximately 100 km northwest of the mouth of the Columbia River, is influenced by Columbia River effluence due to the predominant north-northwest transport toward the Quinault canyon (Nittrouer et al., 1979). Analyses of the major elements and composition of suspended particulate matter in the waters off the coast of Washington indicate that suspended particulate matter from the mouth of the Columbia River to the base of the continental slope were chemically homogeneous (Baker, 1976), suggesting that Columbia River-derived particles are dominant at this site. Therefore, the study area is uniquely positioned to intercept substantial portions of Columbia River discharges, and is well suited for a study of the fate of thorium, including sources, sinks and removal processes.

Saanich Inlet is an intermittently anoxic fjord on the southeast side of Vancouver Island at 48°29'- 48°41'N and 123°28'- 123°32'W. The water depth is about 220 m and the sill depth is at 75 m (Sanchez, et al. 1986). A seasonal cycle of anoxia is caused by the isolation of water behind the sill during late winter and summer, which is followed by dense oxygenated water overflowing the sill in the fall due to strong coastal upwelling (Anderson and Devol, 1973). There is a well established oxygen-hydrogen sulfide interface observed at a depth of 130-140m (Tebo, Personal communication) at the time of our sample collection. Thorium distribution within a changing redox front is expected to vary, because Th-Fe-Mn hydroxyl complexing is different in reducing water where particulate Mn (IV) and Fe (III) are reduced to dissolved Mn (II) and Fe (II), respectively.

These sampling sites are characterized by a variety of geological and climatic conditions and, as a consequence, the waters have distinct chemical compositions. This research then is expected to result in a data set describing the distributions of thorium in natural waters of various chemical make-up. These particular sampling sites will allow an evaluation of the supply of Th isotopes from continents to the ocean, an observation of thorium concentrations in variety of environments such as in fresh water, seawater, and hydrothermal solution, and a study of the behaviors of Th across a redox boundary.

In this study, ^{230}Th and ^{232}Th were determined on samples collected from above mentioned environmental settings by neutron activation analysis (for ^{232}Th only) and isotope dilution mass spectrometry (for both ^{230}Th and ^{232}Th). In order to determine the partitioning of Th between dissolved and particulate forms, all the samples were filtered, except the hydrothermal solutions from the Juan de Fuca Ridge and the samples from the station off Washington and Oregon coast.

LITERATURE REVIEW

2.1 Thermodynamic Properties of Thorium

Knowledge on the thermodynamic properties of dissolved thorium species and thorium compounds may help us understand the mechanisms controlling Th concentrations in natural waters. Thorium is widely distributed in the earth's crust with an average concentration of 8 ppm, although it is only rarely encountered in appreciable concentrations (Ryabchikov and Gol'braikh, 1963). Continental igneous rocks are enriched in thorium by up to two orders of magnitude over oceanic basalt (Ivanovich and Harmon, 1982). Thorium content in basic rocks is considerably lower than that in acidic rocks (Ryabchikov and Gol'braikh, 1963) because of its enrichment in the accessory minerals crystallized only in the late stages of magma differentiation. Such minerals (e.g. monazite, thorite, thorianite, zircon, etc.) are highly resistant to natural weathering, so that there is little tendency for a concentration of this metal in secondary minerals. Thus it is expected that the solubility and concentration of this metal in natural waters, particularly in seawater, should be extremely low, and is mostly transported in a form bound to insoluble resistant minerals or is adsorbed onto the surface of clay minerals.

Thorium is an electropositive element found in nature only as a tetravalent cation (Langmuir and Herman, 1980; Fuger and Oetting, 1976). Due to the chemical properties dictated by its electronic configuration (i.e.$[Rn]6d^27s^2$), thorium tends to form complexes rather than strict ionic bonds (Cotton and Wilkinson, 1972). Thermochemical data suggest that dissolved thorium in natural waters is almost invariably complexed with hydroxyl, anions of various salts and organic anions (Ryabchikov and Gol'braikh, 1963; Langmuir and Herman, 1980).

Table 1 gives reaction constants for complex formation of thorium ion with various anions. Formation of the Th complex is controlled by the properties of ligands and is dependent upon ionic strength (I). Stability constants are high for $H_2PO_4^-$, SO_4^{2-}, F^-, OH^-, HPO_4^{2-} and the organic species (Log K = 10 ~ 40), indicating that thorium in natural waters is strongly complexed with these anions. In contrast, the formation constant of thorium carbonate complex is low (Log K = 1.36), although it has been shown that carbonate alkalinity will increase Th concentration in solution by competing surface sites (LaFlamme and Murray, 1987). Due to the lack of thermodynamic data in the literature, thorium-carbonate relations remain unclear to date.

Equilibrium constants (K) of the complexes versus the charge of Th complex and the ionic strength of the medium are plotted in Fig. 2.1. In general, when considering the same complexing ligand, the equilibrium constants increase as positive charges of the thorium complex decreases and the ionic strength of the medium decreases. Comparing thorium-hydroxy complexes, the Log K value increases linearly to the maximum as the complex reaches neutral from positive charges (Fig. 2.1a). EDTA forms a strong complex with thorium (Table 1) because it is a multidentate organic chelating agent and one EDTA group can completely satisfy the coordination requirements of the Th^{4+} ion. It has been suggested that EDTA may be equivalent in complexing ability to some aqueous humic species (Langmuir and Herman, 1980). Therefore, EDTA is used here to represent a strong complexing ligand rather than as a specific constituent in natural waters.

Application of the stability constant data shows that organic ligands bind thorium to a greater extent than most major inorganic ligands (Fig. 2.2). Most organic matter (mainly humic substances) acts as a chelating ligand binding mainly via phenolate and carboxylate groups (Reuter and Perdue, 1977). The

TABLE 1. Equilibrium constants for complex formation of the thorium ion with various anions

Reaction	Log K	I	References
$Th^{4+} + OH^- = [ThOH]^{3+}$	10.8	0	[72]
$Th^{4+} + 2OH^- = [Th(OH)_2]^{2+}$	21.07	0	[72]
$Th^{4+} + 3OH^- = [Th(OH)_3]^{+}$	30.3	0	[72]
$Th^{4+} + 4OH^- = [Th(OH)_4]^{0}$	40.1	0	[72]
$Th^{4+} + HF = [ThF]^{3+}$	8.03	0	[72]
	4.70	0.5	[112]
$Th^{4+} + 2HF = [ThF_2]^{2+}$	14.25	0	[72]
	7.49	0.5	[112]
$Th^{4+} + 3HF = [ThF_3]^{+}$	18.93	0	[72]
$Th^{4+} + 4HF = [ThF_4]^{0}$	22.31	0	[72]
$Th^{4+} + Cl^- = [ThCl]^{3+}$	1.09	0	[72]
	0.30	0.5	[112]
	0.25	0.7	[112]
	0.18	1.0	[112]
	0.08	2.0	[112]
	0.32	6.0	[112]
$Th^{4+} + 2Cl^- = [ThCl_2]^{2+}$	0.80	0	[72]
	-1	2.0	[112]
	-0.88	4.0	[112]
	-0.26	6.0	[112]
$Th^{4+} + 3Cl^- = [ThCl_3]^{+}$	1.65	0	[72]
	-0.70	2.0	[112]
	-1.16	4.0	[112]
	-0.46	6.0	[112]
$Th^{4+} + 4Cl^- = [ThCl_4]^{0}$	1.26	0	[72]
	-1.80	4.0	[112]
$Th^{4+} + 5CO_3^{2-} = [Th(CO_3)_5]^{6-}$	1.36		[69]
$Th^{4+} + HPO_4^{2+} = [ThHPO_4]^{2+}$	10.8	0.35	[72]
$Th^{4+} + 2HPO_4^{2+} = [Th(HPO_4)_2]^{0}$	22.8	0.35	[72]
$Th^{4+} + 3HPO_4^{2+} = [ThHPO_4]^{2-}$	31.3	0.35	[72]

TABLE 1. (cont'd)

$Th^{4+} + H_2PO_4^- = [ThH_2PO_4]^{3+}$	4.52 2.18	0 2	[72] [112]
$Th^{4+} + 2H_2PO_4^- = [Th(H_2PO_4)_2]^{2+}$	8.88 3.90	0 2	[72] [112]
$Th^{4+} + H_3PO_4 = [ThH_3PO_4]^{4+}$	1.91	2	[72]
$Th^{4+} + SO_4^{2-} = [ThSO_4]^{2+}$	5.45 2.20	0 2	[72] [112]
$Th^{4+} + 2SO_4^{2-} = [Th(SO_4)_2]^0$	9.73 3.45	0 2	[72] [112]
$Th^{4+} + 3SO_4^{2-} = [Th(SO_4)_3]^{2-}$	10.50	0	[72]
$Th^{4+} + 4SO_4^{2-} = [Th(SO_4)_4]^{4-}$	8.48	0	[72]
$Th^{4+} + NO_3^- = [Th(NO_3)]^{3+}$	0.94 0.67 0.45	0 0.5 5.97	[72] [112] [112]
$Th^{4+} + 2NO_3^- = [Th(NO_3)_2]^{2+}$	1.97 0.15	0 5.97	[72] [112]
$Th^{4+} + (C_2O_4)^{2-} = [ThC_2O_4]^{2+}$	9.30	0	[72]
$Th^{4+} + 2(C_2O_4)^{2-} = [Th(C_2O_4)_2]^0$	18.54	0	[72]
$Th^{4+} + 3(C_2O_4)^{2-} = [Th(C_2O_4)_3]^{2-}$	25.73	0	[72]
$Th^{4+} + (C_6H_5O_7)^{3-} = [ThC_6H_5O_7]^+$	13.00	0.5	[72]
$Th^{4+} + 2(C_6H_5O_7)^{3-} = [Th(C_6H_5O_7)_2]^{2-}$	20.97	0.5	[72]
$Th^{4+} + HEDTA^{3-} = [ThHEDTA]^+$	17.02	0.1	[72]
$Th^{4+} + EDTA^{4-} = [ThEDTA]^0$	25.30	0.1	[72]
$Th^{4+} + (C_5H_7O_2)^- = [THC_5H_8O_2]^{3+}$	7.85	0.01	[112]
$Th^{4+} + 2(C_5H_7O_2)^- = [TH(C_5H_7O_2)_2]^{2+}$	15.58	0.01	[112]
$Th^{4+} + 3(C_5H_7O_2)^- = [TH(C_5H_7O_2)_3]^+$	21.86	0.01	[112]
$Th^{4+} + 4(C_5H_7O_2)^- = [TH(C_5H_7O_2)_4]^0$	26.86	0.01	[112]

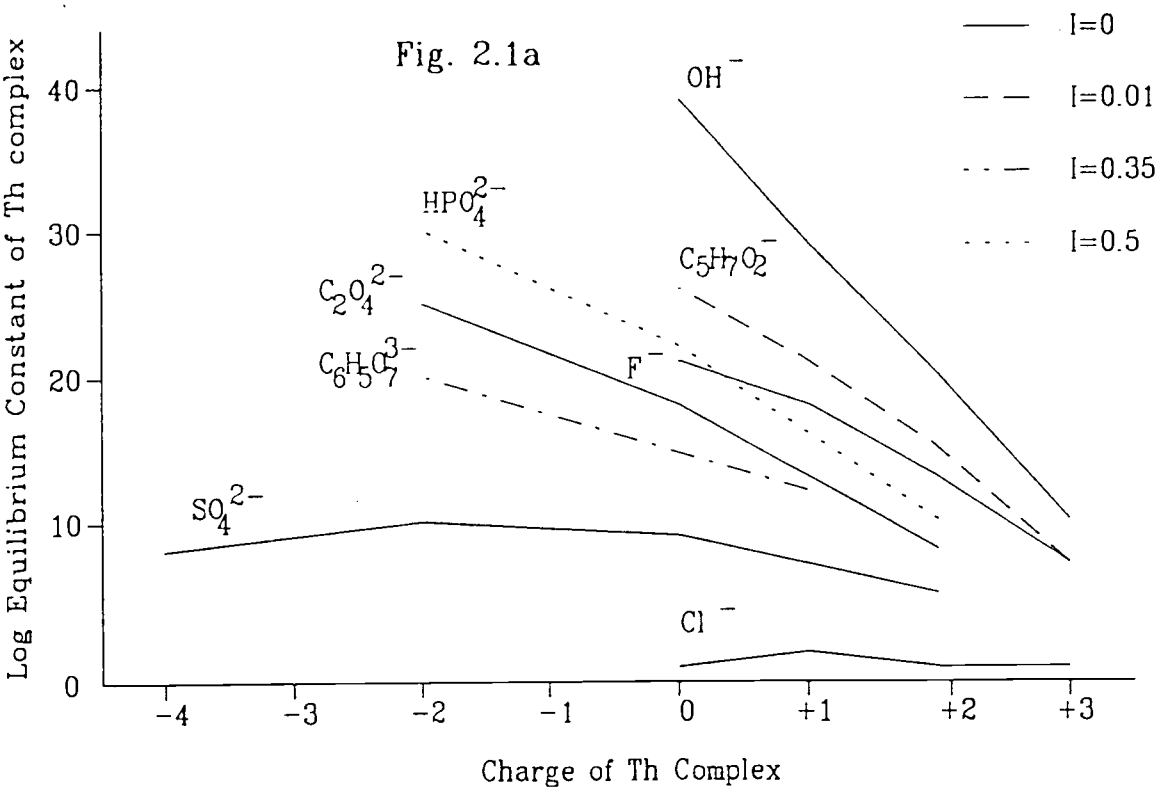

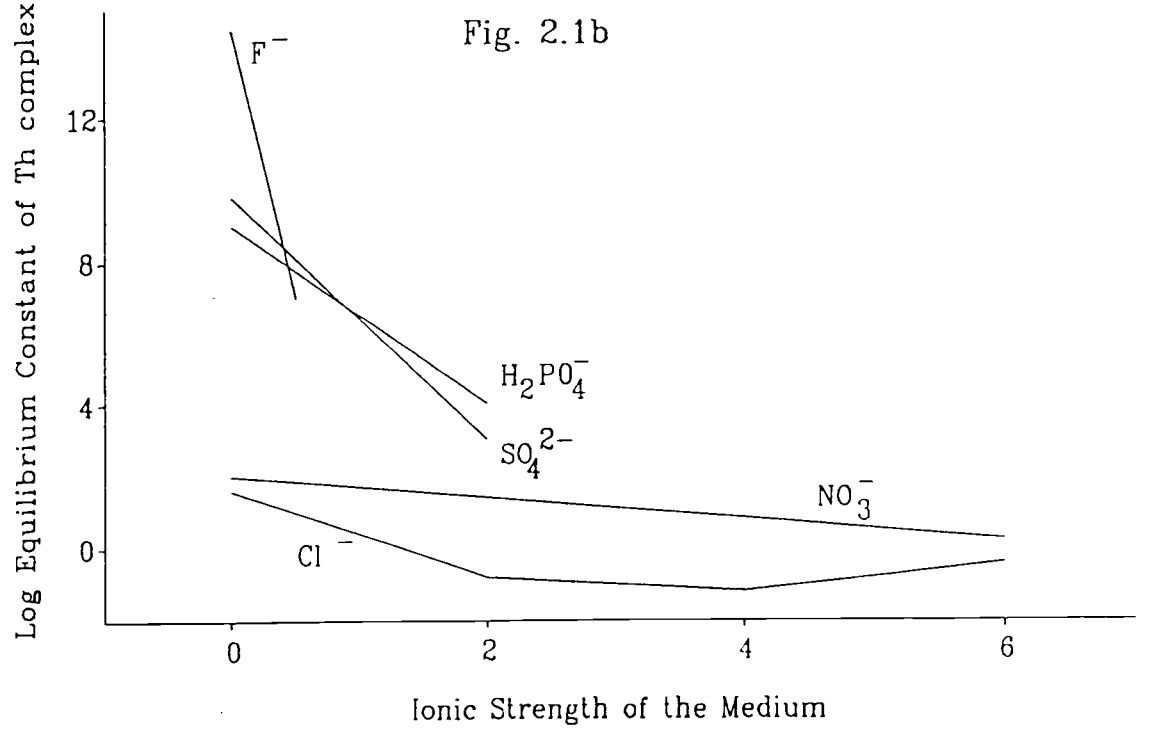

Figure 2.1. Equilibrium constants of the complexes versus (a) the charge of Th complex, and (b) the ionic strength of the medium (data source given in Table 1). Different lines indicate specific ionic strength

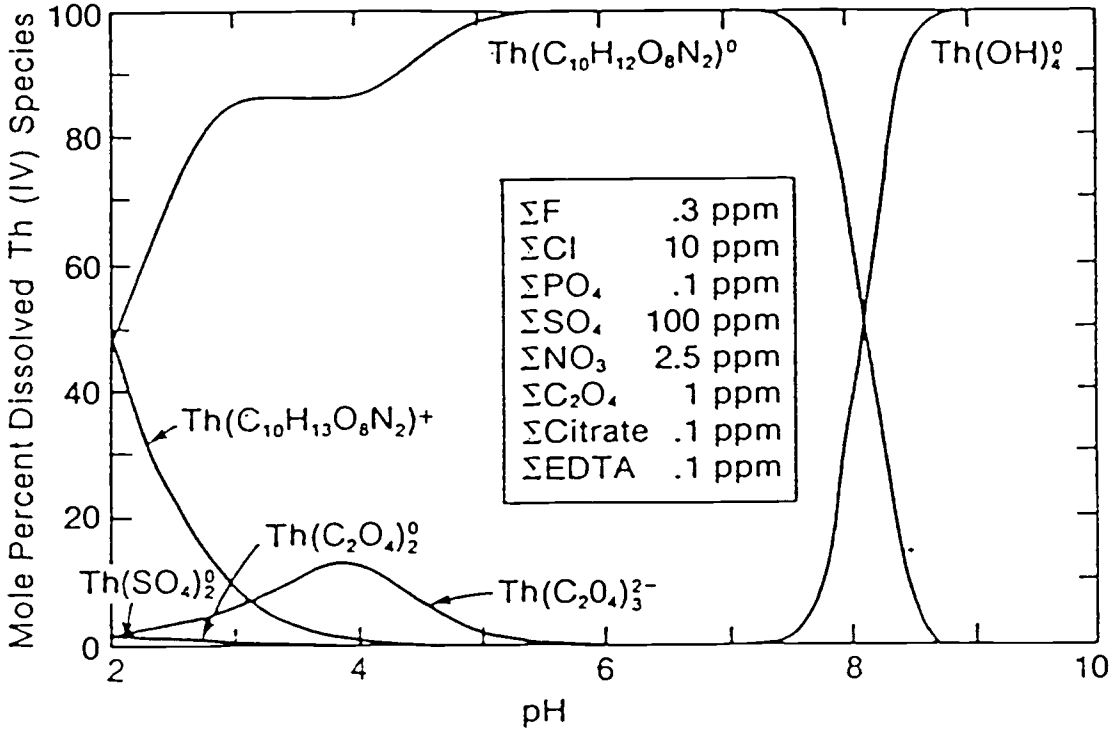

Figure 2.2. Distribution of Th complexes versus pH in a solution containing inorganic and organic species at the concentrations indicated and 25°C with ΣTh = 0.01 ppb (from Langmuir and Herman, 1980). Under normal seawater pH conditions, the thorium-organic complexes and $Th(OH)_4^0$ are the dominant dissolved species

chelation pattern of Thorium-organic complexes enhances their stabilities. Figure 2.2 is used to simulate and exemplify the probable role of thorium-organic complexed in natural waters. As shown on Figure 2.2, the thorium-organic complexes dominate over thorium-inorganic complexes below pH 8. Above pH 8, $Th(OH)_4^0$ becomes the dominant species. Therefore, the thorium-organic complexes and $Th(OH)_4^0$ are the dominant dissolved species under normal seawater pH conditions.

These complexes greatly increase the solubility of thorium minerals and the mobility of Th in the water systems. It is informative to compare the solubility of thorianite (ThO_2), which is about $2x10^{-7}$ dpm/L Th ($1x10^{-6}$ ppb) as $Th(OH)_4^0$ at pH 8 (Langmuir and Herman, 1980), with the value of $(1\text{-}5)x10^{-6}$ dpm/L for the concentration of dissolved ^{232}Th in seawater (Huh and Bacon, 1985b). The comparison suggests that complexes can hold thorium in solution and so enhance its solubility and mobility. Thus the tendency of thorium to form strong complexes increases the concentration of dissolved Th and enhances its potential for transport in natural water.

Compared with inorganic ligands, organic ligands greatly enhance the solubility of thorium at pH values below 8. As shown in Fig. 2.3, thorianite (ThO_2) solubility with the organic ligands present is increased five orders of magnitude above the purely inorganic solubility at pH 5. The range of increased solubility extends up to pH 8, whereas inorganic ligands alone significantly effect solubility only below pH 7.

In organic-rich environments, therefore, it seems likely that organic complexes predominate over inorganic complexes of thorium. Thorium is found to be enriched in certain organic matter, particularly that formed from humic substances which are important in complexing and adsorption of the cation of Th from water (Ivanovich and Harmon, 1982). Humic substances contain both

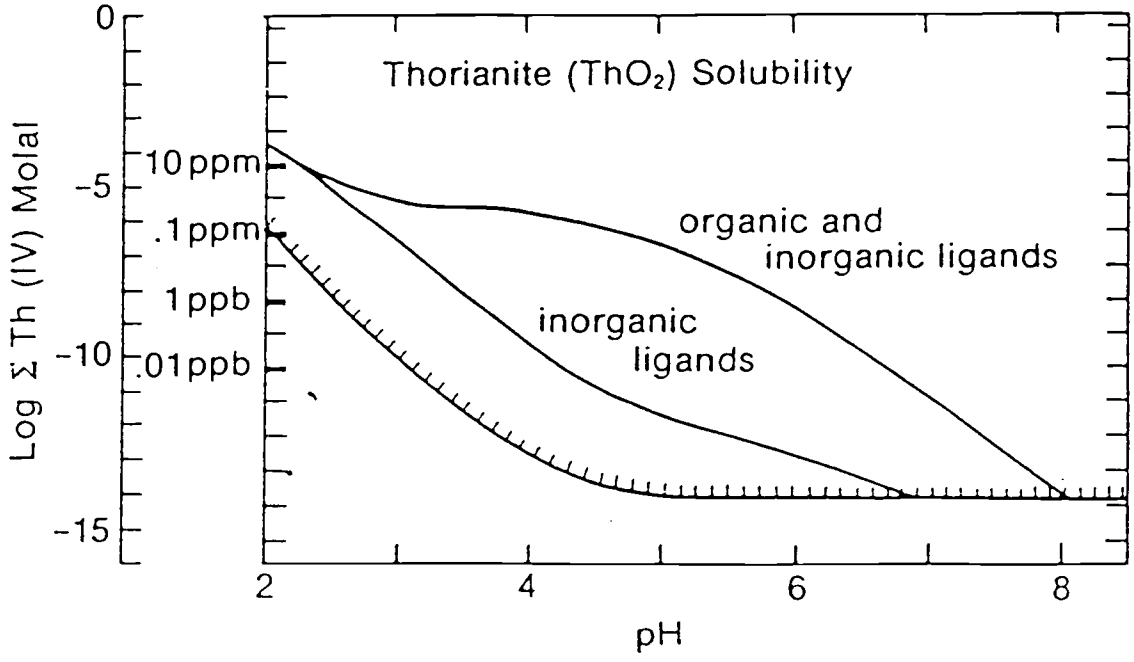

Figure 2.3. The Effect of thorium complexing on the solubility of thorianite, ThO_2(c) as a function of pH at 25°C (from Langmuir and Herman, 1980). The cross-hatched curve denotes the solubility of ThO_2 in pure water. Thorium tends to form strong complexes greatly increasing the solubility of thorium minerals in water systems, especially organic complexes

carboxyl and phenolic hydroxyl groups (Perude, 1978). The humic (acid-insoluble) and fulvic (acid-soluble) acids (Perdue, 1978; Ertel et al., 1986) provide important sources of both dissolved and adsorbed organic ligands in natural water because the acidic character of the humic polymers enables them to interact with cations of heavy metals and form complex linkages of various kinds by ion exchange, surface adsorption and chelation (Reuter and Perdue, 1977). Turner et al. (1981) correlated the stability constants for humic and fulvic acid complexes with the corresponding hydroxide and observed reasonably good correlations between them, indicating that humic substance complexation is most likely to be significant for those cations which are significantly complexed by hydroxide in natural water. Therefore, humic substances can influence markedly the distribution of thorium in aquatic systems through formation of thorium humate complexes.

2.2 Thorium Isotopes and the role of ^{232}Th

Thorium has six naturally occurring isotopes: ^{227}Th, ^{228}Th, ^{230}Th, ^{231}Th, ^{232}Th and ^{234}Th. ^{232}Th is the only non-radiogenic isotope of Th and is the grand-parent of ^{228}Th. All others are derived from the ^{238}U and ^{235}U decay series (Fig. 2.4). All of the elements belong to the actinide family which are the heaviest naturally-occurring elements in the cosmosphere. The natural isotopic abundance (in terms of mass or atom numbers) of ^{232}Th is nearly 100%. However, due to its very long half-life (1.4×10^{10} years), the radioactivity of ^{232}Th in natural environments is often less than activities of other Th isotopes. In seawater, the concentration of ^{232}Th (10^{-5} dpm/L or lower) is extremely low compared with other radiogenic thorium isotopes (e.g. ^{230}Th=10^{-3}-10^{-4} dpm/L), because most Th host minerals are highly resistant to weathering and

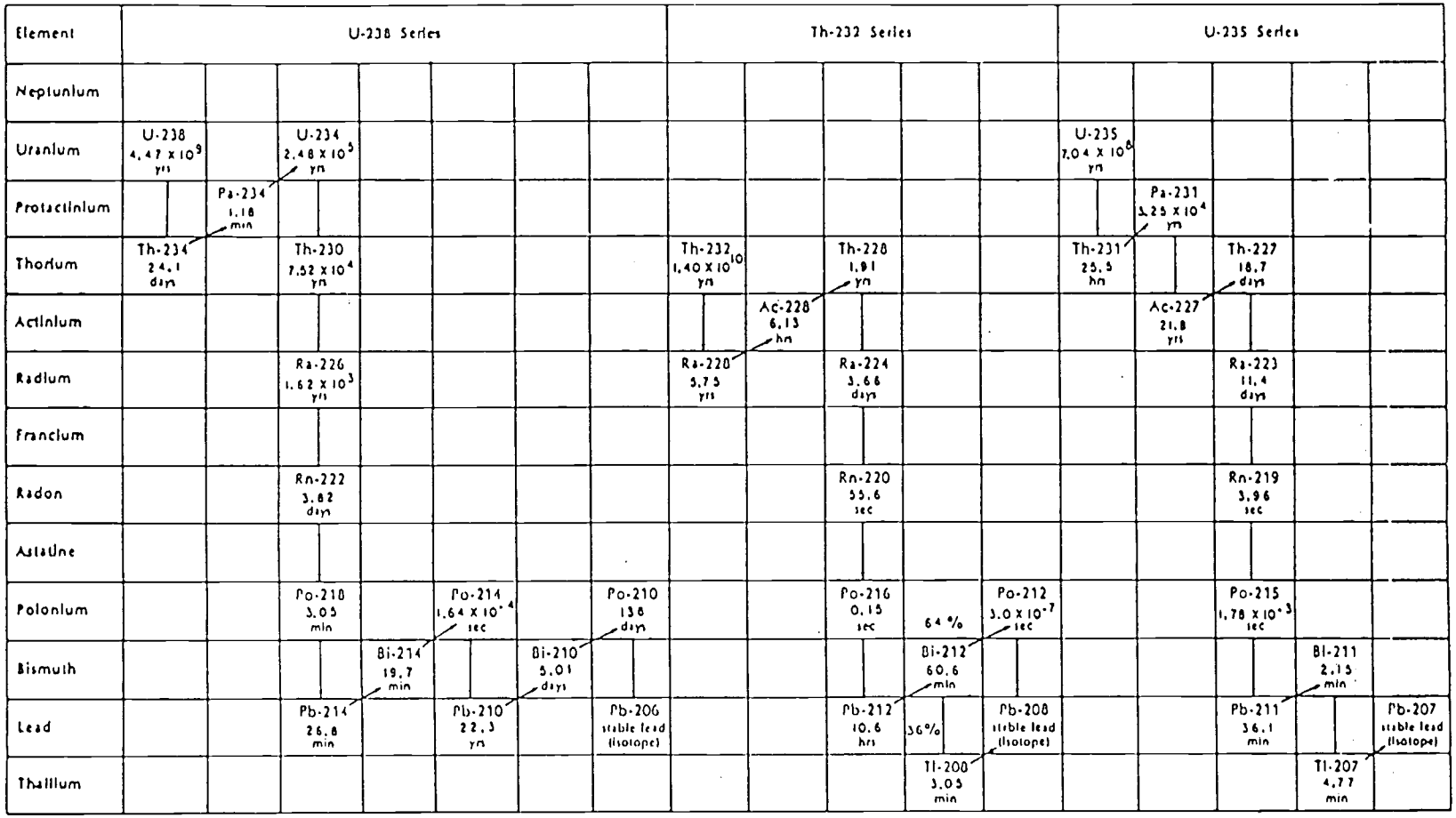

Figure 2.4. Chart showing the decay chain of the uranium and thorium series isotopes and the half-lives of each isotope. Alpha decays are shown by the vertical arrows and beta decays by the diagonal (from Broecker and Peng, 1982)

thorium is very insoluble and immobile in natural waters.

The radiogenic Th isotopes are primarily produced in situ in the ocean by radioactive decay of their dissolved progenitors. Thus, the concentration of these radiogenic Th isotopes in waters can be measured directly or, for very short-lived ones, are determined by the concentration of their parents. Hence their rates of supply can be accurately determined from knowledge of the parent distributions (Bacon and Anderson, 1982) which have been well studied. Generally, uranium in seawater is present in dissolved form (U^{6+}) as a carbonate complex, $UO_2(CO_3)_3^{4-}$, and its concentration is almost constant (on average 3.3 ppb or 2.45 dpm/kg; Huh and Beasley, 1987) in the ocean, except in anoxic environment where a significant portion of U^{6+} may be reduced to U^{4+} and removed from the water column.

Due to their different half-lives (range from one day to ten billion years), thorium isotopes have been used to study processes of various timescales in marine geochemistry and geochronology. ^{230}Th ($T_{1/2}$=75,200 year) has been extensively used to determine accumulation rates of deep-sea sediments and ferromanganese oxide concretions (Ku, 1976; Ivanovich and Harmon, 1982; and references therein). Deficiencies of ^{234}Th ($T_{1/2}$ = 24 day) and ^{228}Th ($T_{1/2}$ = 1.91 year) relative to their soluble parents (^{238}U and ^{228}Ra, respectively) have been applied to index the removal rates of particles and reactive elements in surface ocean and coastal waters (Bhat et al., 1969; Moore, 1969; Broecker et al., 1973; Matsumoto, 1975; Knauss et al., 1978; Li et al., 1979). Excess ^{228}Th (over ^{228}Ra) and excess ^{234}Th (over ^{238}U) have been used to evaluate accumulation rates and mixing rates of near-shore sediments (Koide et al., 1973; Bruland et al., 1981; Huh et al., 1987).

The applications of these parent-daughter pairs ($^{234}Th/^{238}U$, $^{230}Th/^{234}U$ and $^{228}Th/^{228}Ra$) lie in the radioactive disequilibria between the particle

reactive daughters (thorium isotopes) and their soluble non-reactive parents (uranium and radium isotopes) in the water column. In aqueous media above pH = 3, thorium is particularly prone to hydrolysis (Langmuir and Herman, 1980), forming a variety of hydroxide species which are very particle-reactive. Once produced from radioactive decay of their parents, these reactive daughter products can be effectively removed from water columns by adsorption onto particles (i.e. scavenging) to cause radioactive disequilibria within these parent-daughter pairs. The extent of radioactive disequilibria between the particle reactive daughters and their soluble parents makes thorium isotopes amenable to the quantitative study of chemical scavenging and removal rates in the water column (Huh and Bacon, 1985a,b; and references therein).

More recently, studies of the distributions of these isotopes in the water column and between dissolved and particulate forms have led to an increased understanding of the rate and mechanism of deep-sea scavenging (Moore, 1981; Nozaki et al., 1981; Bacon and Anderson, 1982; Anderson et al., 1983a,b; Nozaki and Horibe, 1983; Coale and Bruland, 1985). This scavenging process is believed to be important in regulating the oceanic concentrations and distributions of a large variety of trace metals which form reactive hydrolyzed species, such as Al (Hydes, 1979; Moore, 1983; Measures and Edmond, 1984; Measures et al., 1984), Be (Measures and Edmond, 1982), Co (Knauer et al., 1982), Cr (Murray et al., 1983), Cu (Boyle et al., 1977), Fe (Spencer and Brewer, 1971; Bacon et al., 1980; Landing and Bruland, 1981; Gordon et al., 1982), Mn (Weiss, 1977), the rare-earth elements (Elderfield and Greaves, 1982; de Baar et al., 1983), and Pb (Schaule and Patterson, 1981).

A problem arises in using radiogenic Th isotopes to study the general scavenging of trace metals. Direct comparisons cannot be made because of their very different source functions (Nozaki and Horibe, 1983; Huh and Bacon,

1985). Most trace metals are transported to the ocean through fluvial and aeolian pathways, while radiogenic Th isotopes are produced in situ by radioactive decay of their dissolved progenitors. ^{232}Th is therefore proposed to serve as a link between them, because it is nonradiogenic and is added to the ocean by the same pathways as most of the trace metals.

Furthermore, ^{232}Th has occasionally shown profiles similar to those of the above-mentioned trace metals in which most of them are essential in metal-requiring, metal-activated enzyme systems of organisms (Riley and Chester, 1983; Sunda and Huntsman, 1986). For instance, Al and Fe have displayed the similar surface enrichment and deep water depletion patterns (Moore, 1983) as Th; Mn, Fe and Th show the similar trend across redox boundaries; and the distribution of Be and ^{232}Th in manganese nodules have the similar features. It has often been found that ^{232}Th concentration in nodules first increases downward in the very surface, forming a subsurface maximum, from there it decreases downward (Huh, 1982). Such a feature is also found for ^{9}Be (in nodules) which has somewhat nutrient-like profiles in water columns (Measures and Edmond, 1982, 1984). In view of their quite similar distribution in manganese nodules as an ultimate sink, possibly their distributions in water columns are also similar. All these similarities may imply that the distributions of ^{232}Th and many other trace metals are controlled by the same biogeochemical cycles.

Thus, from the knowledge of ^{232}Th distribution, one could better understand the transport pathways and biogeochemistry of thorium as well as many other particle-reactive trace metals in the ocean. The applications of other Th isotopes to various marine geochemical and geochronological problems can therefore be strengthened (Huh and Bacon, 1985a,b).

Based on a literature survey, a status report on our current knowledge about the distribution and geochemistry of ^{232}Th in seawater is given in section

2.4. The historical ^{232}Th data are reviewed and compared with some added new data. In addition, some postulations on the global distribution pattern of the $^{230}Th/^{232}Th$ activity ratio in the ocean are made from observations on manganese nodules.

2.3 Evolution of Methodology

The data listed in table 3, obtained by using a variety of sampling and measuring methods, show a wide range of concentrations of ^{232}Th, especially near the continents. It is therefore necessary first to discuss the evolution of sampling and analytical methods for the determination of Th in seawater before reviewing the historical data. Conventionally, alpha-emitting Th isotopes in seawater are measured by alpha spectrometry. For ^{228}Th ($T_{1/2}$ = 1.91 years), alpha-spectrometry is still the best means. For long-lived isotopes (^{230}Th and ^{232}Th), however, very large volumes of seawater (~10^3L) are required. To collect large-volume samples for such analysis, marine radiochemists usually deploy MnO_2-coated acrylic fibers in the sea for long periods of time (~months) so that enough thorium can be adsorbed on the fiber. The "effective volume" of a sample is determined using ^{234}Th as a natural tracer, with the assumption that ^{234}Th ($T_{1/2}$ = 24 day) is in equilibrium with ^{238}U in seawater and has an activity of 2.4 dpm/L. Alternatively, submersible pumps are used in conjunction with MnO_2 adsorbers while on station to speed up the collection (~10 hours/deployment). A fairly large set of data on ^{230}Th and ^{232}Th in seawater has been obtained using this method during the past decade (to be reviewed later). In general the quality of the ^{232}Th data has not been satisfactory, primarily because high and uncertain blank levels are often associated with this methodology. In many samples virtually no ^{232}Th could be

detected above even the low end of blank levels.

To circumvent these problems, more sensitive techniques are required, so that one can work on smaller samples and thereby control the blank and contamination problems more efficiently. A neutron activation analysis (NAA) method was developed by Huh and Bacon (1985a) to measure ^{232}Th in 10-L samples. Using this technique, they reported the first profile showing the complete distribution of ^{232}Th in an oceanic water column from the Caribbean Sea (Huh and Bacon, 1985b). Subsequently, a mass spectrometric (MS) technique was developed at Caltech (Chen et al., 1986a), and independently at OSU (Huh and Beasley, 1987). The mass spectrometric method is superior to the NAA in many respects (Table 2). First of all, it measures ^{232}Th as well as ^{230}Th concurrently in the same small-volume samples. Second, it can be used on even smaller sample volumes (~1 L). To date, several water column profiles of ^{232}Th and ^{230}Th have been determined by the MS method. This late technical advancement has made possible rapid sampling and analysis of samples with reduced potential contamination problems. Oceanographically-consistent ^{232}Th data are expected to emerge rapidly in the years to come.

TABLE 2. Comparison of methods for measuring Th isotopes in natural waters

Method	Required sample size	Isotopes measured
α-spectrometry	~ 10^3 L	^{232}Th (?),^{230}Th,^{228}Th
NAA	≤ 10 L	^{232}Th
IDMS	≤ 1 L	^{232}Th & ^{230}Th

TABLE 3. Reported ^{232}Th Content of Ocean Water[a]

Ocean	Sample Location	Depth (m)	Distance to Land (km)	^{232}Th (dpm/10^3-l)	Ref.	Date
Black Sea	43°42'N, 36°33'E	0	~100	0.39	[73]	1961
		2000	~100	0.64	[73]	
	43°26'N, 33°38'E	0	~150	0.73	[73]	
		1000	~150	0.61	[73]	
		2000	~150	0.95	[73]	
	42°44'N, 30°16'E	0	~150	0.34	[73]	
		0	~150	0.56	[73]	
	45°03'N, 32°52'E	0	~50	0.49	[73]	
Azov Sea	45°26'N, 35°44'E	0	<1	2.69	[73]	
	45°36'N, 35°35'E	0	~100	1.71	[73]	
	45°48'N, 36°08'E	0	~150	0.98	[73]	
	46°01'N, 36°39'E	0	~200	0.98	[73]	
	46°17'N, 37°20'E	0	~100	11.98	[73]	
	46°53'N, 37°54'E	0	~50	53.54	[73]	
	45°29'N, 37°20'E	0	<30	2.2	[73]	
N. Atl.	13°31'N, 60°39'W	0	~400	0.16 ±.05	[102]	1964
	32°15'N, 74°47.5'W	4500	~300	1.1 ±.2	[102]	
Caribbean	14°14'N, 64°40'W	0	~450	0.16 ±.05	[102]	
	17°35'N, 65°16'W	800	~750	0.09 ±.04	[102]	
N. Pac.	32°57'N, 127°05'W	0	~600	0.08 ±.01	[120]	1966
		2500	~600	0.16 ±.02	[120]	
	35°36'N, 124°34.4'W	2500	~250	0.05 ±.01	[120]	
	SIO Pier	0	<1	3.2 ±.2	[120]	
World[b]		0		<0.02	[54]	1969
NW Pac.	44°00'N, 150°58'E	0	~600	0.24±.02	[84]	1970
	39°57'N, 151°02'E	0	~1000	0.34 ±.12	[84]	
	32°58'N, 151°06'E	0	~1200	0.29 ±.07	[84]	
	30°00'N, 150°56'E	0	~1300	0.35 ±.07	[84]	
	24°58'N, 151°00'E	0	~1700	0.024 ±.005	[84]	
	31°01'N, 136°19'E	0	~300	0.097 ±.049	[84]	
	30°00'N, 133°40'E	0	~300	0.42 ±.02	[84]	
	28°00'N, 134°33'E	0	~550	0.59 ±.02	[84]	
	33°05'N, 143°15'E	0	~400	0.88 ±.15	[84]	
		1000	~400	0.34 ±.12	[84]	
		3000	~400	0.17 ±.05	[84]	
	40°01'N, 143°31'E	0	~200	1.91 ±.66	[84]	
	39°01'N, 143°28'E	0	~200	1.05 ±.73	[84]	
	37°54'N, 143°50'E	0	~250	0.78 ±.29	[84]	
		500	~250	1.08 ±.27	[84]	
		1000	~250	2.69 ± 1.34	[84]	
		3000	~250	6.85 ± 1.30	[84]	
		5000	~250	1.20 ±.59	[84]	
	30°00'N, 140°00'E	0-6000	~600	0.49 ±.07[c]	[84]	
	30°08'N, 139°37'E	0	<1	2.20 ±.17	[84]	
	(Jogashima Pier)	0	<1	4.89 ±.24	[84]	

TABLE 3. (Cont'd)

Ocean	Sample Location	Depth (m)	Distance to Land (km)	^{232}Th (dpm/10^3-l)	Ref.	Date
	35°05'N, 135°25'E	0	<50	1.22 ±.12	[84]	
	33°27'N, 139°20'E	0	~150	5.38 ±.49	[84]	
Japan Sea	40°36'N, 131°01'E	0	~300	0.81 ±.10	[84]	
		1000	~300	0.61 ±.12	[84]	
	41°16'N, 131°01'E	2000	~150	0.42 ±.05	[84]	
		3000	~150	1.05 ±.15	[84]	
	41°12'N, 132°15'E	0	~300	0.54 ±.22	[84]	
E. China	31°30'N, 128°28'E	0	~250	0.54 ±.07	[84]	
Sea	31°31'N, 128°32'E	0	~200	3.72 ±.32	[84]	
	31°51'N, 129°33'E	0	<100	0.24 ±.05	[84]	
	31°00'N, 126°40'E	0	~350	0.54 ±.05	[84]	
	31°38'N, 127°37'E	0	~300	0.61 ±.07	[84]	
	30°40'N, 118°42'W	0	~200	0.26 ±.09	[49]	1973
N. Pac.	39°02'N, 169°57'W	0	~3000	0.31 ±.15	[49]	
	30°05'N, 170°05'W	0	~4000	0.47 ±.14	[49]	
	31°54'N, 146°06'W	0	~3000	0.21 ±.09	[49]	
	41°22'N, 175°52'W	0	~3000	0.28 ±.12	[49]	
	38°16'N, 156°46'W	0	~1500	0.20 ±.12	[49]	
N. Pac.		3500		0.02	[61]	1976
	34°59'N, 120°43'W	0	<6	0.605 (10)[d]	[56]	1978
	34°59'N, 120°43'W	40	<6	1.56[e] (06)[d]	[56]	
	34°51'N, 121°08'W	70	~60	0.204 (32)[d]	[56]	
	25°42'N, 109°42'W	0	<40	0.40 (21)[d]	[56]	
	34°00'N, 118°57'W	0	<10	0.045 (72)[d]	[56]	
	33°37'N, 120°08'W	150	~100	0.031 (73)[d]	[56]	
	8°48'N, 104°W	0	~850	0.02 ±.02	[89]	1981
	8°48'N, 104°W	~3000	~850	0.02 ±.01	[89]	
	6°30'N, 93°W	0	~900	<0.01	[89]	
	6°30'N, 93°W	~3450	~900	<0.01	[89]	
	11°N, 140°W	0	~3300	0.014	[89]	
	11°N, 140°W	4600-4900	~3300	0.02 ±.01	[89]	
	1°N, 139°W	4150-4450	~4200	0.015±.005	[89]	
	5°6'N, 81°32'W	1500	~250	<0.01	[6]	1982
	5°6'N, 81°32'W	2250	~250	0.09 ±.02	[6]	
	5°6'N, 81°32'W	3000	~250	0.05 ±.02	[6]	
	11°9'N, 87°35'W	2000	~250	0.010±.005	[6]	
	11°9'N, 87°35'W	3000	~250	0.02 ±.01	[6]	
	11°9'N, 87°35'W	4700	~250	1.9 ±.2	[6]	
	9°36'N, 89°8'W	1500	~400	0.05 ±.02	[6]	
	9°36'N, 89°8'W	2250	~400	0.05 ±.01	[6]	
	9°36'N, 89°8'W	2900	~400	<0.02	[6]	
	7°4'N, 91°41'W	1000	~750	0.03 ±.02	[6]	
	7°4'N, 91°41'W	1500	~750	0.08 ±.02	[6]	
	7°4'N, 91°41'W	2250	~750	0.02 ±.01	[6]	
	7°4'N, 91°41'W	3100	~750	0.04 ±.01	[6]	

TABLE 3. (Cont'd)

Ocean	Sample Location	Depth (m)	Distance to Land (km)	^{232}Th (dpm/10^3-l)	Ref.	Date
	4°8'N, 94°22'W	1100-1200	~1200	<0.02	[6]	
	15°21'N, 151°28'W	2778	~4000	<0.002	[4]	1983
N. Atl.	32°05'N, 64°15'W	3200	~1300	0.015±.004[f]	[4]	
	32°05'N, 64°15'W	3200	~1300	0.020±.006[f]	[4]	
	32°05'N, 64°15'W	3200	~1300	0.033±.016[f]	[4]	
	32°05'N, 64°15'W	3200	~1300	0.015±.008[f]	[4]	
	32°05'N, 64°15'W	3200	~1300	0.022±.009[f]	[4]	
NW Pac.	30°N, 146°E	3965-5725	~750	0.007-0.033[g]	[99]	
Caribbean	14°31'N, 66°8'W	10-4782	~370	0.0005-0.087[g,i]	[43]	1985
N. Pac.	21°N, 109°W	~2600	~250	0.024-1.05[h,j]	[18]	1986
N. Atl.	7°44'N, 40°43'W	10-4280	~1000	0.022-0.035[g,j]	[19]	
N. Pac.	33°49'N, 118°42'W	0-855	~50	0.014-0.051[g,j]	[44]	1987
	29°20'N, 144°30'E	1100-5500	~625	0.021-0.116[g]	[103]	
	39°N, 144°20'E	1100-5500	~200	0.023-0.061[g]	[103]	
Japan Sea	42°49'N, 138°06'E	500-3500	~170	0.027-0.130[g]	[103]	
	38°17.5'N, 135°29'E	1100	~145	0.059±.028	[103]	
		2100	~145	0.098±.043	[103]	
	38°17.5'N, 135°29'E	10-2913	~145	0.03-0.09[g,k]	[103]	
	42°49'N, 138°06'E	10-3626	~170	0.01-0.10[g,k]	[103]	
	38°40.6'N, 132°48'E	10-2810	~400	0.03-0.08[g,k]	[103]	
NW Atl.	32°46'N, 70°47'W	0-1300	~550	0.008-0.197[g]	[23]	
	23°11'N, 63°58'W	0-5785	~1800	0.007-0.058[g]	[23]	
N. Pac.	44°40'N, 130°20'W	2000	~550	0.051-1.88[h,j]	[20]	
	11°N, 140°W	0-3969	~3300	0.003-0.009[l]	[47]	1988
	1°N, 139°W	0-4425	~4000	0.003-0.015[l]	[47]	

[a] Data are listed in chronological order of publication.
[b] Integrated result of surface waters from the NW Atlantic, the Gulf of Mexico, the Caribbean Sea, the Equatorial Pacific and the S. Pacific.
[c] Integrated water in the indicated depth range.
[d] Numbers in parentheses indicate maximum contribution of blank in percent.
[e] Particulate contamination, bottom at 45 m.
[f] Obtained from sequential two-month deployments of MnO_2-coated Nitex adsorbers.
[g] Profile available; data show concentration range in the indicated depth range.
[h] Mixture of hydrothermal solutions and seawater.
[i] Determined by neutron activation analysis.
[j] Determined by mass spectrometry.
[k] Reported as total (i.e., particulate + dissolved) ^{232}Th.
[l] MANOP MnO_2 fiber data. The effective volume sampled was estimated by dividing the ^{226}Ra activity measured on the fiber lechate by the known ^{226}Ra concentration in seawater. The ^{232}Th concentration was calculated assuming Th and Ra have the same adsorbing efficiency on the fiber.

2.4 Review and Update of ^{232}Th Data in the Ocean

Seawater concentrations of ^{232}Th have been reported by numerous workers including the following (in chronological order): Koczy et al. (1957); Lazarev et al. (1961); Moore and Sackett (1964); Kuznetsov et al. (1966); Somayajulu and Goldberg (1966); Kaufman (1969); Miyake et al. (1970); Krishnaswami et al. (1972); Imai and Sakanoue (1973); Cherry and Shannon (1974); Knauss et al. (1978); Moore (1981); Nozaki et al. (1981); Bacon and Anderson (1982); Anderson et al. (1983a,b); Nozaki and Horibe (1983); Huh and Bacon (1985b); Chen et al. (1986a); Chen et al. (1986b); Huh and Beasley (1987); Nozaki et al. (1987); Nozaki and Yamada (1987); Cochran et al. (1987); and Chen (1987). The data summarized in Table 3 and Figure 2.5 span a wide range from the order of 10^{-4} dpm/10^3L to 10^0 dpm/10^3L. In most cases ^{232}Th was determined coincidentally with other Th isotopes of prime interest and reported with little discussion. Several intriguing, but not necessarily geochemically accurate, trends appear in the literature data of ^{232}Th in seawater. First, recent measurements are in general significantly lower than older ones by one to two orders of magnitude. This is clearly shown in Fig. 2.5 where nearly all post-1980 data (open symbols) fall below pre-1980 data (solid circles). Second, coastal waters generally have much higher ^{232}Th than open-ocean waters especially for pre-1980 data. And third, samples collected with MnO_2-adsorbers usually result in lower ^{232}Th than those collected with large sample containers. It is suspected that these trends are fortuitous; they are probably due to improvements of analytical techniques with time, to better control of sampling and laboratory contamination in recent years, and to the possible failure to remove fine suspended particulates from bulk water samples.

Because of the need of sampling and processing large-volume samples for

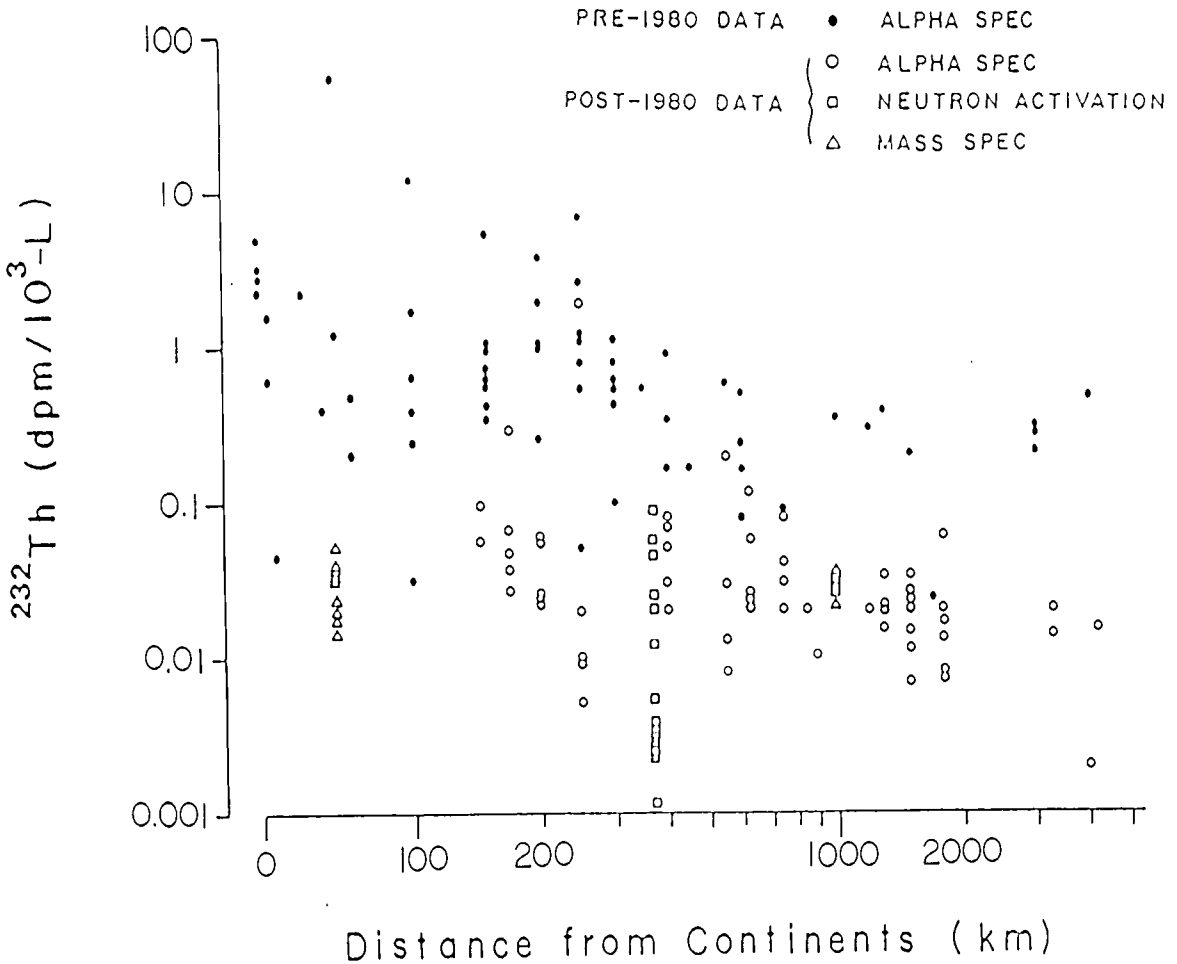

Figure 2.5. Reported ^{232}Th concentration in seawater plotted versus distance from continents (data source given in Table 3). The distance scale is linear from 0 to 100 m and logarithmic thereafter. Various symbols indicate data determined by different analytical techniques. The clear trend that pre-1980 data (solid circles) are substantially higher than post-1980 data (open symbols) is primarily caused by sampling and analytical artifacts

the determination of ^{232}Th by the conventional alpha-particle counting technique, it is difficult to distinguish carefully between the thorium in dissolved form and that associated with suspended matters. Consequently, the reported Th concentrations might be only the upper limit, i.e. maximum possible amounts dissolved. Therefore, extra caution should be taken when using these data to discuss the marine geochemistry of ^{232}Th. With the development of new techniques and more attention paid on the control of contamination, the data quality has been improved lately. The data reported post 1980 are more reliable.

Many, if not most, authors listed in Table 3 have implicitly or explicitly indicated that the data they reported were representative of dissolved ^{232}Th. It should be pointed out that the samples were collected and processed with several different methods, including centrifugation, filtration, leaching of MnO_2 adsorbers, etc. Even with the same methods, the operation conditions may not be the same (e.g., filtration with different pore-sized filters, time of filtration and acidification, etc.). Considering these differences in sample processing, particulate matter was probably not excluded with equal efficiency. These data, therefore, are not directly comparable. In view of the usual observation that nearshore waters have higher productivity and suspended load than open ocean waters, it is very likely that the higher ^{232}Th measured for coastal waters may to some extent reflect the higher particulate concentration included in the sample. The lower ^{232}Th concentrations determined by MnO_2 adsorbers may be explained by the low collection efficiency for particulate Th versus dissolved Th. This differential retention would tend to occur if dissolved Th is irreversibly scavenged, whereas particulate Th may be intermittently caught during passage through the fiber matrix. Therefore, compared with the "container" method, the "fiber" method differentially excluded particulate Th,

and thus resulted in lower ^{232}Th values. As for the small-volume samples collected for the NAA and MS analyses, concentrations of ^{232}Th over $1x10^{-1}$ dpm/10^3L have not so far been detected (except for hydrothermal fluids; to be discussed in Cha. 4). This may be attributed to a clean removal of particulate matter using fine membrane filters and a better control of contamination problems on small-volume samples.

More critical evaluation of dissolved ^{232}Th levels has been given by a few authors as follows. Kaufman (1969) set an upper limit of 0.017 dpm/10^3L for ^{232}Th concentration in surface ocean water based on a composite of 24 analyses of water collected from widely spaced parts of the ocean. Moore (1981) suggested that the ^{232}Th content of surface as well as deep Pacific seawater was 0.01-0.02 dpm/10^3L. Nozaki and Horibe (1983) showed an increase of ^{232}Th with depth, from 0.007 dpm/10^3L to 0.033 dpm/10^3L, in the deep (3965-5725m) western North Pacific, and argued for the existence of a dissolved Th source at the seafloor. Huh and Bacon (1985b) reported a water column profile of dissolved ^{232}Th in the eastern Caribbean Sea which showed relatively high concentrations in the upper 200 m with a maximum of 0.087 dpm/10^3L near the base of the mixed layer. In the deep Caribbean Sea, ^{232}Th concentrations (averaging 0.0027 dpm/10^3L) are one order of magnitude lower than most previously reported open ocean data. In the Santa Monica Basin, 50 km offshore from Southern California coastline, ^{232}Th also showed higher concentration (0.05 dpm/10^3L) at surface and lower concentration (0.01-0.02 dpm/10^3L) at depth (Huh and Beasley, 1987). Note that these values for a coastal environment are not significantly higher than most reported open ocean data (0.007-0.05 dpm/10^3L).

^{232}Th concentrations in coastal water are supposed to be higher than in open ocean. This observed similarity between coastal water and open ocean

may be caused by estuary effects, which means that high riverine input flux of dissolved ^{232}Th is removed rapidly during estuarine mixing. Further discussion about input of ^{232}Th to the ocean and estuarine influence on thorium distribution will be given in section 4.2.1.

2.5 Implications From Manganese Nodules

There is convincing evidence that thorium in manganese nodules and crusts come from seawater. Ku and Broecker (1969) found that, ^{230}Th is considerably enriched on the upper surface of nodules, which implied that ^{230}Th was preferentially added to the nodule surface through chemical precipitates from the water column above. Although most of the ^{232}Th delivered to the ocean may be passively transported in terrigenous detritus, it is possible that a detectable fraction of the ^{232}Th is involved in transport in the dissolved form. The study of Huh and Ku (1984) indicated that the geochemical behavior of ^{232}Th in manganese deposits bears resemblance to that of ^{230}Th, i.e. ^{232}Th in nodules is derived from dissolved ^{232}Th in seawater.

Thus, as with numerous other elements and radionuclides, the source and oceanic distribution of Th can be inferred from ferromanganese nodules and crusts in which the content of Th and its isotopic composition can be easily determined. In other words, these concretions have the potential of indexing the concentration and isotopic composition of thorium in bottom waters. This has been demonstrated by several workers (e.g., Moore, 1981, 1984; Huh, 1982; Huh and Ku, 1984; Nozaki and Yang, 1985). It is informative to update the data base of manganese nodules (and crusts) and make some general inference about the oceanic distribution of the two long-lived Th isotopes, ^{230}Th and ^{232}Th.

From a literature survey and recent work of Huh and Moore (1988), initial

$^{230}Th/^{232}Th$ activity ratios in a large number of manganese deposits from the world oceans have been compiled, as listed in Table 4. In cases where the activity ratios were given in the literature, they are directly adopted in the table. Otherwise, values are derived from the original data set (i.e., profiles of ^{230}Th and ^{232}Th) by linear extrapolation to zero depths. The errors associated with the manipulation are conservatively estimated to be within 50%, but usually much less.

The initial $^{230}Th/^{232}Th$ activity ratios in all samples observed vary by two orders of magnitude, from ~2 to 200. Their geographical variation is mapped in Figure 2.6. As we glance from the North Pacific toward the Atlantic and Indian Oceans, some striking systematics can be noted. There is a general, although weak, trend that the activity ratio of $^{230}Th/^{232}Th$ in nodules/crusts increases southward in the central Pacific. In the central North Pacific red clay area (from 20°N to 40°N and 160°E to 130°W), the $^{230}Th/^{232}Th$ activity ratio falls within a narrow range ($\bar{X}$ = 60±18, n = 10) with the exception of only one sample (viz., KK73; Table 4). In the North Pacific siliceous ooze region (9-16°N, 120-160°W), the mean $^{230}Th/^{232}Th$ ratio based on 14 samples is 83±16. As we proceed further south to ~14°S in the central South Pacific, the highest $^{230}Th/^{232}Th$, around ~200, are found.

$^{230}Th/^{232}Th$ values observed on nodules and crusts from the Atlantic and Indian Oceans are consistently lower. There is no significant difference between values from these two oceans. The mean value based on all 16 samples from these two oceans is 17±10.

Some irregularities can be seen from the above general trend; and they can be attributed to topographic and regional geochemical controls. Lower ratios are encountered in marginal seas, such as those in the South China

TABLE 4. Initial activity ratios of $^{230}Th/^{232}Th$ at top surfaces of manganese nodules or crusts[a]

Sample ID	Location	Water depth (m)	$\frac{^{230}Th}{^{232}Th}$	Ref.
I. Pacific				
MANOP Site-R	30°N, 158°W	5800		
Rama I-15BC			70	[39]
Rama I-18BC			60	[39]
Rama I-20BC			40	[39]
KK73	40°N, 148°W	5163	2-3	[17]
V21-D2a	34°54'N, 160°19'W	5400	58	[17]
KH-80-2 St. 9	30°00'N, 170°01'W	5380	64	[101]
SCHW-1D[b]	30°N, 140°W	3480	50	[67]
V21-71a	27°54'N, 162°31'E	5870	43	[64]
V21-71	27°05'N, 166°04'E	5954	54	[64]
TE8-1[b]	22°N, 159°W	1230	40	[17]
Mn-139[b]	20°01'N, 136°36'W	3916	70	[65]
6A	19°39'N, 113°44'W	4000	48	[64]
Necker Ridge				
L5-83-HW 10-D7[b]	21°47.8'N, 167°37.4'W	2100	80	[46]
L5-83-HW 8-D5[b]	22°18.9'N, 166°53.9'W	2350	80	[46]
Horizon Guyot				
L5-83-HW 24-D17[b]	19°33.2'N, 168°49.9'W	2400	77	[46]
L5-83-HW 21-D14[b]	19°30.7'N, 168°50.1'W	1800	30	[46]
MP-26[b]	19°N, 171°W	1464	25	[9]
MANOP Site-S	11°N, 140°W	4900		
K7905-47BC			60	[39]
K7905-75BC			100	[39]
K7905-91BC[b]			100	[117]
K7905			77±11[c]	[90]
Mn7601-20-2	11°07'N, 140°05'W	4722	66	[93]
C57-58-1	15°19.5'N, 125°54.4'W	4638	95	[62]
A47-16-1	9°2.3'N, 151°11.4'W	5049	86	[62]
A47-16-2			116	[62]
MANOP Site-H	6°30'N, 93°W	3570		
Pluto III-6SBC-1			65	[39]
Pluto III-6SBC-2			63	[39]
Vulcan I-37BC			78	[39]
Pluto III-D11[b]			80	[46]
Carr. 5	9°26.5'N, 113°16.5'W	3700	100	[9]
1052[b]	2°N, 98°W	3150	140	[17]

TABLE 4. (Cont'd)

Sample ID	Location	Water depth (m)	$\frac{^{230}Th}{^{232}Th}$	Ref.
South China Sea				
40 TKD[b]	12°21.4'N, 118°48.9'E	1000	2.2	[77]
44 TKD	12°48.5'N, 118°51.6'E	1900	4.1	[77]
South Pacific				
V18-T119[b]	12°27'S, 159°25'W	~5000	80	[64]
V18-D32	14°18'S, 149°32'W	~2000	200	[64]
Techno[b]	13°09'S, 148°62'W	4020	200	[48]
DW-72	21°31'S, 85°14'W	920	50	[9]
DWHD-47	41°59'S, 102°01'W	4000	50	[9]
E17-36	55°S, 95°W	4770	61	[64]
II. Atlantic				
Blake Plateau				
G74-2374[b]	30°31'N, 79°01'W	876	5-10	[64]
G74-2384[b]	30°53.5'N, 78°44'W	843	12	[64]
A266-41[b]	30°59'N, 78°15'W	830	5-10	[64]
T3-71D 160-10G[b]	30°08'N, 42°29'W		18	[116]
t3-71D 148-2B[b]	26°07'N, 25°21'W		18	[116]
T3-72D 253-13-21[b]	26°08'N, 44°45'W	3400	2-3	[116]
K-9-12[b]	15°20'N, 21°48'W	2800	23	[88]
K-9-13[b]	15°16'N, 21°52'W	990	20	[88]
K-9-21[b]	7°58'N, 21°02'W	1800	16	[88]
Lusiad AD4	6°03'N, 32°22'W	1020	8	[9]
V22-D7[b]	37°33'S, 18°06'E	3040	37	[88]
V16-T3[b]	13°04'S, 24°41'W	4415	22	[64]
III. Indian Ocean				
D6253	2°48'N, 59°51'E	~3600	40	[64]
RC14 D-4[b]	23°26'S, 50°49'E	~4300	10	[88]
V16-T19a	29°52'S, 62°36'E	~4500	10	[64]
V16-T19b			23	[64]

[a] Initial $^{230}Th/^{232}Th$ activity ratios are mostly estimated by extrapolation to zero depths, unless otherwise described in the original papers.

[b] Samples so indicated are manganese crusts; otherwise they are manganese nodules.

[c] Data given is the statistic mean and standard deviation based on seven nodule samples collected from the same location.

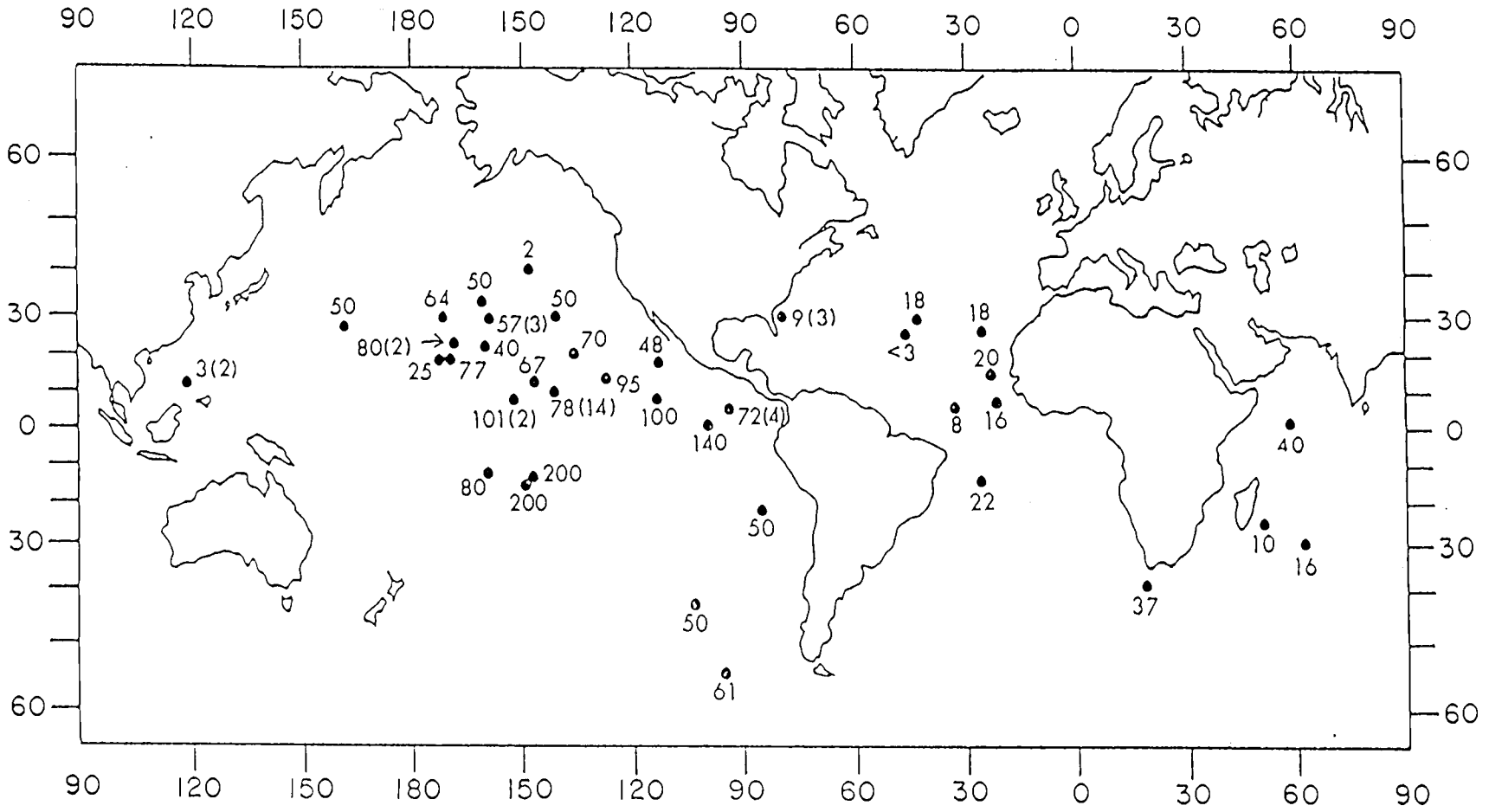

Figure 2.6. Map showing the distribution of initial $^{230}Th/^{232}Th$ activity ratio in manganese nodules and crusts (data source given in Table 4). Where replicate samples were collected and analyzed, mean values are given and the numbers in parentheses indicate number of samples

Sea (2-4) and the Blake Plateau near Florida (5-12), which can be due to lower ^{230}Th and/or higher ^{232}Th concentrations in the ambient seawater. There are two possible causes for the low $^{230}Th/^{232}Th$ ratios. First, compared to their open-ocean counterparts, the samples existed at much shallower water depths, and the water-column geochemistry of thorium in general dictates that ^{230}Th concentration in intermediate waters increases with depth (Huh and Beasley, 1987). Second, and perhaps most importantly, the proximity to land as a source of ^{232}Th could bring down the initial $^{230}Th/^{232}Th$ ratios due to higher supply rate of ^{232}Th.

Some manganese crusts were formed by hydrothermal activities and accumulated rapidly. As a consequence, they bear very different isotopic signatures. The studies of thorium isotopes in manganese nodules have provided important information on the rate of nodule accretion. For instance, sample T3-72D 253-13-21 in Table 4, recovered from the Trans-Atlantic Geotraverse (TAG) area, accumulated at a rate two orders of magnitude faster than hydrogenous manganese deposits (Scott et al., 1974). The initial $^{230}Th/^{232}Th$ activity ratio estimated for that sample (2-3) is low; still it is an upper limit, because most ^{230}Th in the sample is supported by ^{234}U. Since there was no insoluble residue in that sample (Scott et al., 1974), the measured ^{232}Th (2-5 dpm/g) could be of hydrothermal source. Low initial $^{230}Th/^{232}Th$ ratios can also be derived from other hydrothermal crusts (Moore and Vogt, 1976). In addition, $^{230}Th/^{232}Th$ ratios measured on MnO_2 fibers deployed at MANOP site M, an area influenced by hydrothermal activity, showed the lowest values compared with other sites (Moore, 1981). All these strongly suggest that hydrothermal solutions are enriched in ^{232}Th with respect to seawater. This subject will be further discussed with our ^{232}Th data on hydrothermal solution (section 4.2.5).

Small-scale variation in the $^{230}Th/^{232}Th$ can be noted in areas with irregular seafloor topography, such as the area along the Hawaiian Archipelago and Line Islands. For example, three manganese crusts collected from different depths (1464m, 1800m, and 2400m) in the vicinity of the Horizon Guyot showed very different $^{230}Th/^{232}Th$ values (25, 30, and 77, respectively). The increase with depth of the activity ratio may reflect the concentration increase of ^{230}Th with depth at that area. Th isotopes measured on MnO_2 adsorbers deployed at all MANOP sites also showed that the $^{230}Th/^{232}Th$ activity ratios were higher in deep waters than in surface waters (Moore, 1981). In contrast, the $^{230}Th/^{232}Th$ ratio in nodules showed little variation over a large area in the North Pacific central gyre. This is presumably due to the fact that within that region the seafloor is generally flat and the water column hydrographic and geochemical conditions are very similar from place to place.

2.6 Implications From Other Authigenic Deposits

Besides ferromanganese oxide deposits, any other authigenic phases that can concentrate thorium from seawater during their formation may also serve as natural detectors of isotopic composition of Th in seawater. Marine barite, for example, isolated from a sediment core taken from the Walvis Ridge in the Atlantic (31°21'S, 1°58'E) was analyzed for Th isotopes by Somayajulu and Goldberg (1966). They measured very high ^{232}Th concentrations (50-120 ppm) in barite, attesting to the well known chemistry that barium sulphate can scavenge thorium from solution efficiently. Based on the $^{230}Th/^{232}Th$ activity ratio they measured on barite down the core, an initial ratio of 20-30 can be obtained by extrapolation. This value is not inconsistent with those observed on manganese nodules and crusts from the Atlantic Ocean (see Table 4).

METHODS AND MATERIALS

3.1 General Introduction

Studies of trace elements in the ocean environment have long been hampered by analytical problems: contamination, interference of ubiquitous major ions in sea-salt, and the requirement of sensitive methods of detection for concentrations in the nanomolar to sub-picomolar range. Contamination, with all of its possible sources such as sampling and laboratory operations, is the first cause of analytical errors in trace analysis. At the trace level, this error is often of random nature and unpredictable.

To minimize sources of potential contamination for measuring ^{232}Th, the sample size should be as small as possible, and the operating procedure should be as simple as possible. Due to a very long half-life, hence low activity of ^{232}Th, to measure its concentration by the conventional alpha-particle counting method requires processing large volumes (~10^3 L) of water samples, which often results in very high uncertainties and blanks. In order to reduce sample size and simplify the operation procedures, and thereby to better control the blank and the degree of contamination, more sensitive techniques are required for measuring ^{232}Th in natural waters. The neutron activation analysis (NAA) method developed by Huh and Bacon (1985) makes it possible to determine ^{232}Th concentrations in small volume (10 L) seawater samples with sufficient sensitivity. It allows the use of fine membrane filters to remove particulate material more cleanly and efficiently, hence measure ^{232}Th concentrations in dissolved form. However, the separation and purification procedures for NAA method are more sophisticated than for α-spectrometry. The isotope dilution mass spectrometry (IDMS) method, which was developed independently at

Caltech (Chen et al.) and at OSU (Huh) in 1986, has much simpler chemical and detection procedures. The IDMS technique is less prone to interference problems than the NAA method. Furthermore, the IDMS method can measure both ^{230}Th and ^{232}Th on the same sub-liter samples.

These two analytical tools were employed in this research. Despite the reduced sample size, contamination is still the primary cause of analytical errors. For ^{232}Th and ^{230}Th, it is of paramount importance to control the blank properly. To minimize sources of contamination, all labware was washed with 12N HCl before using, and ultrapure reagents were used wherever necessary. Blank and contamination levels were also carefully monitored. Sample blanks were processed in parallel with samples. All the procedures and reagents employed on the samples were also applied to the blanks.

3.2 Sampling and Shipboard Filtration

The sampling operation is executed with great care to prevent contamination. Before use, the sample containers (10 L polyethylene jerricans) were soaked in a 2% microsolution and subsequently in concentrated HCl for two weeks, then rinsed with double distilled/deionized water. Before and after sampling the cleaned containers were covered with polybags to prevent dust collection around container necks.

During R/V Wecoma cruise W8507C in July 1985, water samples were collected by Niskin bottles from seven stations along an offshore transect off the Washington/Oregon coast (46°49.13'-46°50.13'N, 124°15.13'-125°22.42'W; water depth increasing from 42 m to 2035 m). At every station surface waters, integrated over the top 100m, were collected and centrifuged. In addition, a complete profile of 10 samples were collected over the water column at the

deepest station (i.e., STN. 6). Following collection, all the water samples were acidified with triple-purified 6N HCl to lower the pH to ~2.

In a cruise to Saanich Inlet (water depth = 220m) in early August of 1985, the samples across the redox boundary were collected by Niskin bottles. Water samples from the Columbia River, the confluence of the John Day and Columbia Rivers and Lost Lake were collected in May 1987. They were collected directly from the surface and transferred to 10-L acid-cleaned jerricans. Crater Lake samples were collected from the water column in the south basin in August 1987, using Niskin water samplers with CTD capability to measure temperature, conductivity, and depth. The CTD was also outfitted with a transmissometer to measure the water clarity. Upon collection, all water samples mentioned above (except the samples from off the Washington and Oregon coast) were filtered within a few hours by pumping through 0.4-μm pore size Nuclepore filters and acidified immediately with 12N HCl (ULTREX) to bring the pH to ~2. The filters were stored in petri-dishes and kept frozen until analysis.

Five 50-ml hydrothermal solution samples from the Juan de Fuca Ridge (44°40'N, 130°20'W) were collected and supplied by Dr. Kadko. These samples were collected by the deep submersible Alvin near the hydrothermal vents. Compared with the other seawater samples, the hydrothermal sample sizes are much smaller (ca. 50 ml vs. 10 L). In fact, it is the smallest sample size we have ever measured ^{232}Th by mass spectrometry. The samples were unfiltered and acidified with ULTREX HCl.

TABLE 5. Sampling information

Sampling location	Date	depth (m)	Comments
Columbia River, Oregon (Bonnevilley Dam)	May 1987	86	
Confluence of the John Day & Columbia Rivers,Oregon	May 1987		
Lost Lake, Oregon	May 1987	77	Oligotrophic
Crater Lake, Oregon	Aug. 1987	456	Oligotrophic
Washington/Oregon coast	July 1985	2035	75% fresh water input from Columbia River
Saanich Inlet, Vancouver, B.C	Aug. 1985	220	Intermittent anoxic ford
Juan de Fuca Ridge (44°40'N, 130°20'W)		~2000	Hydrothermal solution

In the laboratory, 12.5 mg of iron carrier (Puratronic grade, prepurified of Th by cation exchange chromatography) and about 2 dpm of ^{229}Th spike (1 dpm for hydrothermal solutions) were added to the acidified water samples as the yield tracer. After thorough mixing to attain isotopic equilibration for three days, the waters were adjusted to pH = 8 with ULTREX ammonium hydroxide to effect $Fe(OH)_3$ precipitation. Samples were shaken constantly to facilitate Th adsorption onto the iron hydroxide. After a week, the samples were transferred to a 5-L glass beaker, and heated to accelerate Th scavenging. The supernatant waters were then removed by siphoning and discarded. The hydroxide precipitates were collected by centrifugation, and then washed with deionized/distilled water to remove salts.

Suspended particulate matter caught on Nuclepore filters were digested by soaking in hot concentrated NH_4OH in the presence of the ^{229}Th yield determinant for about 12 hours. After driving off ammonia, HNO_3 + $HClO_4$ were used to decompose organic matter and dissolve particulates. Once the samples were in solution, the subsequent procedures were the same as those discussed previously for the water samples.

After preconcentration and separation by hydroxide precipitation, ion exchange methods were used to remove the remaining major elements and most of the interfering minor elements. All the samples were analyzed by the IDMS method, except those collected off the Washington coast, which were measured by the NAA method.

3.3 Neutron Activation Analysis

3.3.1 Principle

The NAA method is designed to measure ^{232}Th only. ^{232}Th, with a half-life of 14 billion years, can be regarded as a "stable" nuclide. Its weak radioactivity makes ^{232}Th difficult to determine from its primary α-radiation, especially when its concentration is low in the sample of interest such as seawater. Upon irradiation with thermal neutrons, ^{232}Th can be transformed into short-lived daughter products via the reaction:

$$^{232}Th\ (n,\gamma)\ ^{233}Th\ (t_{1/2} = 22.2\ min) \xrightarrow{\beta} {}^{233}Pa\ (t_{1/2} = 27\ d)$$

The induced activities of the daughter products (^{233}Th and ^{233}Pa) can be over five (for ^{233}Pa) to seven (for ^{233}Th) orders of magnitude higher than the target ^{232}Th activity. Accurate and precise determination of ^{232}Th can therefore be attained by measuring, with greatly enhanced sensitivity, activities of the generated products (Huh and Bacon, 1985a).

The immediate product from the irradiation of ^{232}Th is ^{233}Th, it ß-decays with a 22.2-minute half-life to ^{233}Pa which is both ß-active and γ-active. In principle, ^{232}Th concentration in the target sample can be indexed by either ^{233}Th or ^{233}Pa. Although the induced activity of ^{233}Th is normally two orders of magnitude higher than that of ^{233}Pa, ^{233}Pa assay is more desirable for two reasons:

(i) The longer half-life of ^{233}Pa provides greater convenience in working time. It also allows enough "cooling-off" time after irradiation for highly-radioactive, short-lived interfering nuclides to diminish.

(ii) ^{233}Th emits betas only, whereas ^{233}Pa emits both gammas and betas. For a

system involving high interferences (to be discussed later), it would be more advantageous to detect γ-radiations with discrete energies than to detect ß-particles with continuous spectrum.

The generated activity of ^{233}Pa in the course of the irradiation can be described by the equation:

$$\lambda_3 N_3 = \phi\sigma_1 N_1 \left[\frac{1}{\lambda_2-\lambda_3} \exp(-\lambda_2 t) + \left(\frac{1}{\lambda_3-\lambda_2} - \frac{1}{\lambda_3}\right) \exp(-\lambda_3 t) + \frac{1}{\lambda_3}\right]$$

where:

N = the number of atoms;

λ = decay constant;

ϕ = thermal neutron flux;

σ = thermal neutron capture cross section;

t = duration of irradiation;

The subscripts 1, 2 and 3 represent ^{232}Th, ^{233}Th and ^{233}Pa, respectively.

Assuming there are 0.001 dpm (~$1x10^6$ atoms) of ^{232}Th content in the sample, under a neutron flux of $4x10^{12}$ n/cm -sec and 13 hours of irradiation, the sample is able to produce sufficient ^{233}Pa (>250 dpm) for a precise measurement (Huh and Bacon, 1985a).

3.3.2 Possible activation-induced interferences

Because very large amounts of bremsstrahlung activity produced by activation products of major elements (Na, Cl, K, etc.) could completely mask the very low activity of ^{233}Pa, it is necessary that the major elements and/or their activation products must be removed. ^{233}Pa is to be identified by its 312 KeV γ-radiation. When using neutron activation method to convert ^{232}Th to ^{233}Pa, numerous other activation products emitting γ-radiation in the

window of 300-320 KeV will also be induced. Huh and Bacon (1985a) have estimated possible interferences caused by irradiating a typical seawater sample of 100-L equivalent under a neutron flux of $8x10^{12}n/cm^2$-sec for 8 hours, and shown that the induced ^{233}Pa activity is only about 300 dpm, whereas other activation products with -radiation close to 312 keV have activities one to over four orders higher. They include:

10^3-10^4 dpm: ^{203}Hg, ^{160}Tb, ^{177m}Lu, ^{151}Eu

10^4-10^5 dpm: ^{75}Se, ^{143}Ce, ^{169}Yb

10^5-10^6 dpm: ^{140}La, ^{171}Er, ^{175}Yb, ^{177}Lu

$> 10^6$ dpm: ^{51}Cr

Some products (e.g. ^{198}Au and ^{85}Sr) emit characteristic -radiation not very close to this energy but so overwhelmingly high that they may also interfere with ^{233}Pa measurement.

In order to single out the desired 312-keV -radiation of ^{233}Pa, the samples should be as interference-free as possible. In view of the many high-level interferences that may be incurred by activation, radiochemical procedures are certainly necessary. The NAA method therefore involves both preirradiation and postirradiation radiochemical separations and purifications.

3.3.3 Pre-irradiation chemistry

Thorium isotopes were separated from bulk samples and purified during the preirradiation chemistry. The separation and purification schemes include ion exchange chromatography and solvent extraction (Fig. 3.1). After coprecipitation (continue from sampling section), the washed iron hydroxide was dissolved in cincentrated HNO_3 to make a solution in 8N HNO_3, and passed through an anion exchange column (column dimension: 10 mm i.d. and 10 cm

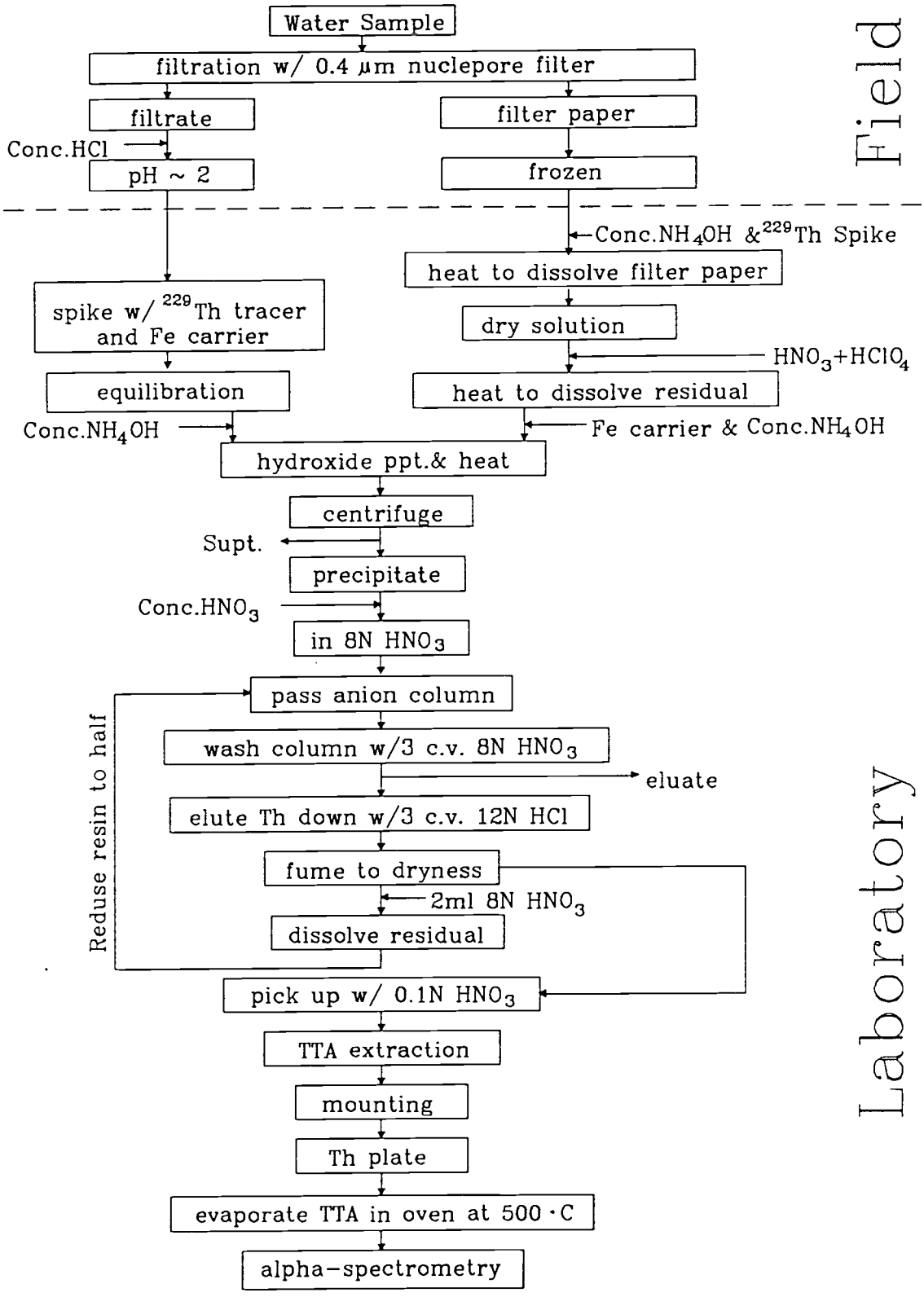

Figure 3.1 Flow diagram for separation and purification of thorium

length). The resin (Dowex AG 1X8, 100-200 mesh, chloride form) was conditioned with 8N HNO_3 beforehand. This clean-up step was performed to isolate Th from the rare earth elements, as they contribute many of the interferences. In 8N HNO_3 medium, thorium has the highest value of the distribution coefficients (Fig. 3.2) and forms a stable anionic nitrate complex, $[Th(NO_3)_6]^-$ (Korkisch, 1969). This hexanitrato complex is strongly adsorbed onto the resin. Under these conditions, rare earth elements were eluted with three column volumes of fresh 8N HNO_3 solution.

Thorium was then eluted from the column with 30 ml of concentrated HCl. Since thorium has no adsorption in hydrochloric acid (Fig. 3.3), it can therefore be separated from most other elements which form anionic chloride complexes (Hf, Au, Bi, Se, Hg ,Ir, etc.) and are retained on column. The same procedure was repeated one more time to further separate and purify thorium isotopes. The eluate was fumed to dryness, picked up with ~2 ml of 8N HNO_3 and passed through the half-reduced column (column dimension: 10 mm i.d. and 5 cm length) in which the resin had been converted to nitrate form again.

Thorium was finally eluted with 3 column volumes of concentrated HCl and dried by evaporating on a hot plate. Upon dryness, Th was taken up with 1-2 ml of 0.1N HNO_3 for TTA/benzene (thiophencarbonyltrifluoroacetone in benzene) solvent extraction. TTA is a ß-diketone and forms a stable chelate complex compound with Th, which is easily extracted by benzene at pH greater than zero (Ryabchikov and Gol'braikh, 1963). The extraction method is particularly effective at a pH of 1-2 for the final separation of small quantities of thorium from a complex mixture of elements such as the alkaline earth and rare earth elements, actinium and several other metal ions. Under our experimental condition, pH = 1, the extraction efficiency of thorium is about 90%. The extraction was repeated three times to ensure that most of Th in the inorganic

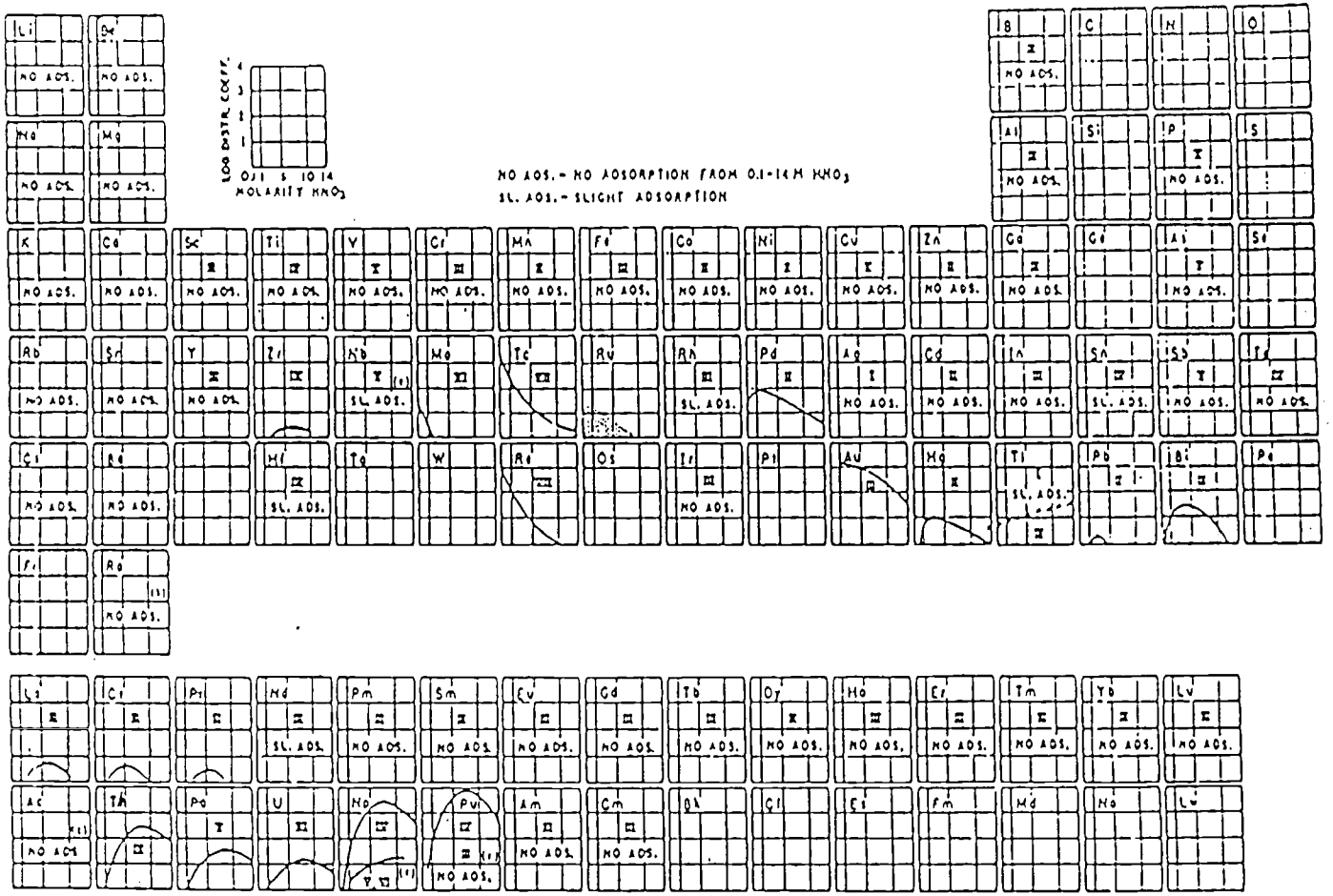

Figure 3.2. Distribution of elements between a strong-base anion-exchange resin and nitric acid solutions. The ordinates are logarithms of the distribution coefficient in milliliters of solution per gram of dry resin (from Faris and Buchanan, 1964)

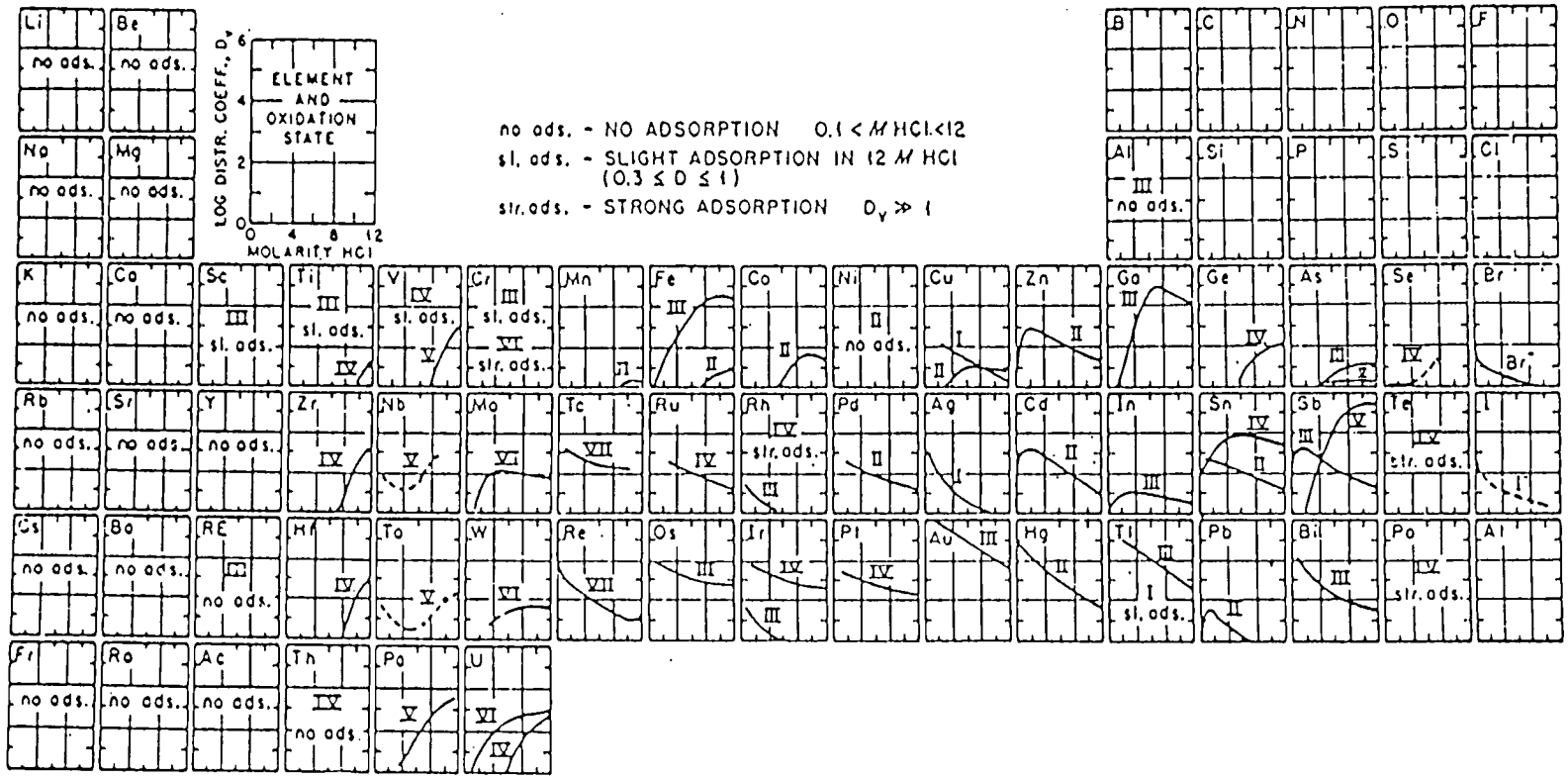

Figure 3.3. Distribution of elements between a strong-base anion-exchange resin with 10% crosslinking and hydrochloric acid (from Kraus and Nelson, 1955)

solution had been exchanged into organic phase.

After the preirradiation procedure, there is virtually only Th left in the sample. The final step of the preirradiation radiochemistry was to mount the purified extracts onto a high-purity (Puratronic, 99.9995% purity) aluminum foil (2 cm diameter, 0.002 cm thickness) for α counting to determine the thorium recovery and for the subsequent irradiation. The complete procedure took about three days for a batch of five samples.

3.3.4 Neutron activation

For activation analysis, we have the advantage of easy access to the Triga reactor in the OSU Radiation Center. After yield was determined by α-spectrometry, the Al foils were packed in double heat-sealed polyethylene vials together with two standards and irradiated on the rotation rack for 13 hours at a thermal neutron flux of $4 \times 10^{12} n/cm^2$-sec. The standards prepared from high-purity ThO_2 (Lindsay Code 116, 99% purity), were used to establish the calibration curve to eliminate the necessity of absolute determination and calibration of various parameters such as flux density, slow neutron capture cross-section, counter efficiency, delay in counting, etc..

Since ^{232}Th concentrations were low in the samples of interest, the resulting initial radioactivity from this irradiation was essentially all ^{28}Al [^{27}Al (n,) ^{28}Al, $t_{1/2}$ = 2.3 min.], which diminished rapidly. After "cooling off" in the OSU Radiation Center for two days, the poly-vials were packed in a lead container and shipped back to the radiochemistry laboratory. There the samples were allowed to cool further for several days before the post-irradiation chemistry.

3.3.5 Post-irradiation chemistry

The post-irradiation procedure was to extract and purify ^{233}Pa for subsequent counting. ^{233}Pa, the radionuclide of interest, is to be identified by its 312 keV -radiation. Without radiochemical processing, the ^{233}Pa signal could be totally swamped by the induced activity of interfering nuclides emitting -radiation in the energy window of 300-320 keV. To single out the desired 312-keV -radiation of ^{233}Pa, this nuclide was separated and purified using ion exchange chromatography and solvent extraction. ^{233}Pa was not prone to contamination and thus the subsequent procedures were no longer disturbed by this cause of error and could be performed using reagent-grade chemicals.

The samples on aluminum foil were dissolved in 10 ml of 12N HCl in Teflon beakers (Fig. 3.4). ^{231}Pa was added to each of the samples as a tracer to monitor their yields. The solution (in 6-12 N HCl) was passed through an anion exchange column (AG 1X8), and then washed with two column volumes of 8N HCl to elute thorium and aluminum. Protactinium was desorbed with two column volumes of 6N HCl + 0.2N HF and evaporated to dryness in the presence of 1 ml of H_2SO_4 to remove HF completely, as HF would interfere with the subsequent separation of Pa. The residues were dissolved in a mixture of concentrated HCl and HNO_3, which were then dried by evaporating on a hot plate. Upon reaching dryness, Pa was picked up with 1-2 ml of 8N HCl and was then extracted twice by shaking with equal portions of DIBK (di-isobutyl ketone). By this step protactinium could be completely exchanged into the organic phase and separated from iron and irradiated thorium (Golden and Maddock, 1956; Korkisch, 1969). The combined Pa-containing extracts were back-extracted into 0.5N HCl. 2 ml HNO_3 and 0.5 ml $HClO_4$ were added to the

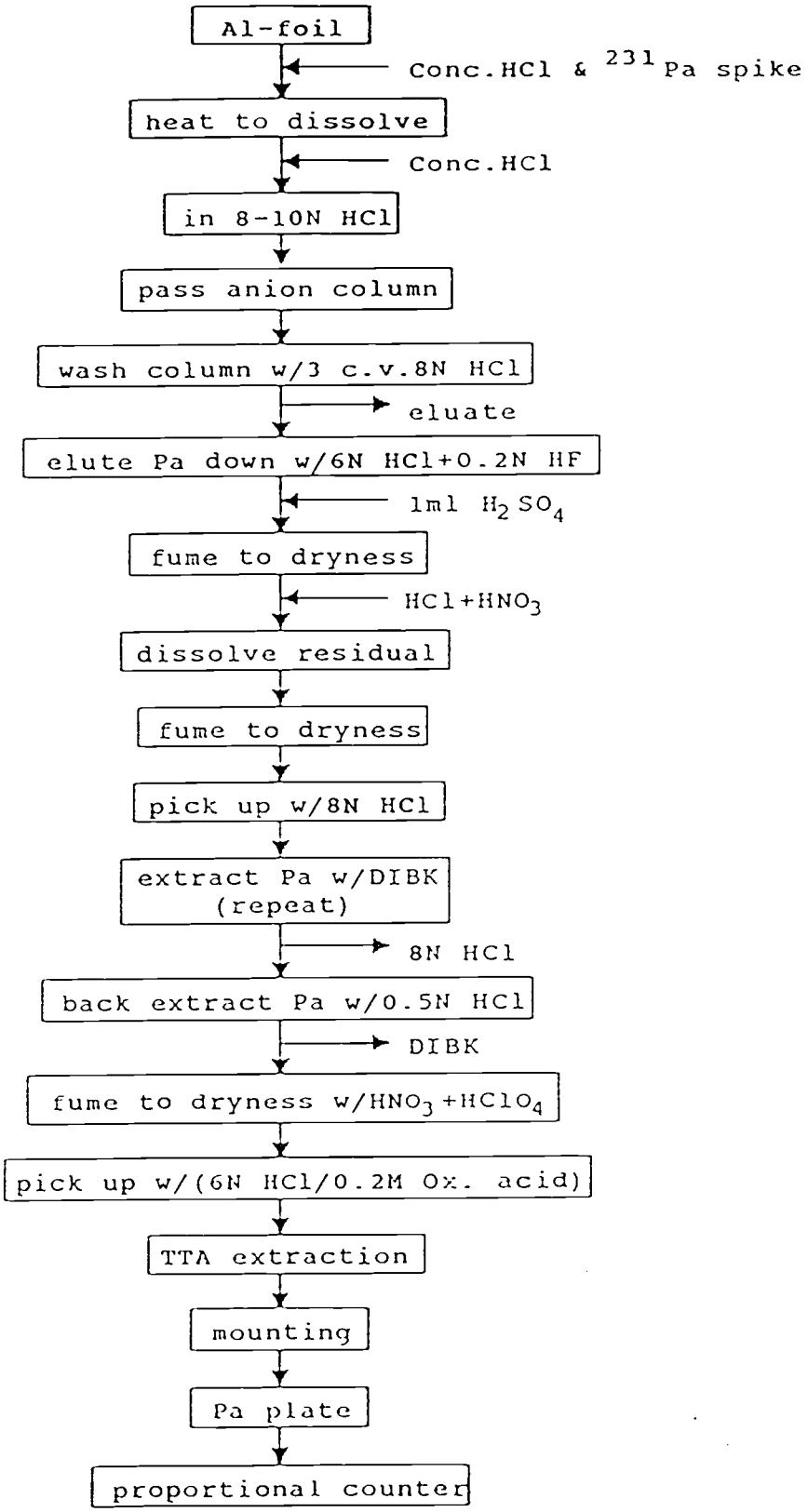

Figure 3.4. Flow diagram for separation and purification of ^{233}Pa

aqueous solution which was then evaporated to dryness. Pa was then picked up with 1 ml of a mixture of 6N hydrochloric acid and 0.2 M oxalic acid and extracted to the extent of about 90% by shaking with three 1-ml portions of 0.5M TTA in benzene (Myasoedov and Muxart, 1962; Korkisch, 1969). The extraction of protactinium performed from the mixture of 6N HCl+0.2M oxalic acid is to decrease the simultaneous extraction of zirconium (Pal'shin and Myasoedov, 1963). Under the conditions of optimum extraction, protactinium can be further separated from the remaining iron, thorium and the radioactive impurities. Finally, the organic phase was evaporated on a stainless steel planchet and counted.

3.3.6 Counting and data processing

The purity of the final Pa sources was confirmed both by γ-spectrometry and by ß-counting. In general, each sample, blank and standard was counted for a day in a gamma spectrometer, which has a Ge(Li) detector interfaced with a Canberra Series-40 MCA (4092-channel) and a DEC PDP-11 computer. A Canberra SPECTRUM-F software package used on this system can perform automatic spectrum analysis and data reduction. The gamma spectra of the samples showed a distinct 312-KeV peak and other characteristic ^{233}Pa peaks, indicating a high degree of ^{233}Pa purification. Time-series ß-counting also reflected the ^{233}Pa half-life of 27 days. Because the low-level beta counter (Tennelec LB-1000 Series) has a much higher counting efficiency (~48%) than the gamma counter (~5%), the quantitative determination was made by ß-counting. The counting efficiency and α/ß cross-talk factors of the beta counter were calibrated with ^{231}Pa and ^{233}Pa standards. The chemical yields of Th were determined right after preirradiation chemistry from the count rates of

^{229}Th in silicon surface-barrier detectors with known efficiencies. The Pa yields were determined by total α-counting in a windowless, gas flow-type proportional scintillation counter.

The results of the two ^{232}Th standards (0.878 dpm and 0.0439 dpm) were used to establish the calibration factor, which was (80.3 ± 1.77) x 10^{-6} (cpm^{233}Pa/dpm^{232}Th). The activities of ^{232}Th in the samples were then calculated using the equation (Huh and Bacon, 1985a):

$$^{232}\text{Th(dpm/kg)} = \frac{(\text{cpm}^{233}\text{Pa})_{\text{corrected}}}{(\%\text{Th yield}/100)(\%\text{Pa yield}/100)(80.3\text{x}10^{-6})(\text{cpm/dpm})\text{sample wt.(kg)}}$$

where: $^{233}\text{Pa}_{\text{corrected}} = {}^{233}\text{Pa}_{\text{measured}} - {}^{233}\text{Pa}_{\text{blank}}$

%Th yield = [^{229}Th(cpm)/^{229}Th(dpm)] ÷ detector efficiency

%Pa yield = ^{231}Pa (cpm)/^{231}Pa spike (cpm)

The counting results showed that the samples had an average γ-counting error of 3% and an average ß-counting error of 8%. The chemical yield is 4-60% (average 22%) for Th and 4-76% (average 56%) for Pa. The sample blanks (reagents + foil) contribute 1.5-71% of the signals detected. The standard deviations of ^{232}Th concentrations range from 3.2% to 34%, and most of them were about 10%. The results are listed in Table 6.

TABLE 6. Data used to calculate total ^{232}Th concentrations off Washington and Oregon Coast (46°49.13'N, 125°22.42'W; water depth 2035m)

Depth (m)	Sample Wt.(kg)	% Th yield	% Pa yield	c.p.m. ^{233}Pa Measured	c.p.m. ^{233}Pa Corrected	Th-232 (dpm/10^6kg)
15	8.31	12.0±0.4	48.4±1.1	30.2± 2.2	27.9± 2.2	269.±22
390	10.38	24.1±0.7	59.9±1.0	5.3± 0.4	1.5± 0.5	12.± 4
590	10.46	7.4±0.4	53.4±0.9	63.4± 5.0	52.5± 5.1	403.±40
890	9.82	29.1±0.9	3.7±0.1	148. ±10	146. ±10	1192.±88
1290	9.89	6.4±0.2	73.6±1.6	126. ± 7	116. ± 7	934.± 6
1540	6.67	28.1±0.9	45.2±1.0	8.8± 0.8	5.0± 0.8	60.±10
1875	10.94	15.3±0.5	62.1±1.4	23.9± 1.6	20.1± 1.6	147.±12
1975	21.20	19.4±0.7	60.1±1.3	22.5± 1.2	11.6± 1.6	97.±14

3.4 Mass Spectrometric Analysis

3.4.1 Basic concepts

Most compounds can produce unique or distinctive patterns in a mass spectrometer, and these substances can be identified from their mass spectra. The signals produced by a mass spectrometer are the direct result of chemical reactions (i.e., ionizations, decompositions, and fragmentations). The technique of mass spectrometry is carried out with sophisticated instrument systems which produce, separate, and detect both positive and negative gas-phase ions. The ion masses (more correctly, their mass-to-charge ratios, M/e's) and their relative abundances are displayed in a "mass spectrum".

Thus, by using the isotope dilution mass spectrometric method (IDMS), it is possible to measure ^{230}Th and ^{232}Th concurrently on the same sub-liter samples. Supposing a water sample has a ^{230}Th concentration of $1x10^{-4}$ dpm/L and a ^{232}Th concentration of $1x10^{-6}$ dpm/L, then in 1-L of such a sample, there are 2.3 fg (femto gram = 10^{-15} g) of ^{230}Th and 4,100 fg of ^{232}Th. These are enormous quantities of both isotopes in terms of measurable amount by mass spectrometry. We have recently improved the ionization efficiency from 0.1% to 7% , which means the sample sizes can be further cut down with the MS method. For ^{232}Th alone, even 10 ml of water sample is enough. The specific activities of ^{230}Th and ^{232}Th in the samples are quantified using ^{229}Th ($t_{1/2}$ = 7341 yr., 0.2 dpm = 420 fg) as a yield monitor.

3.4.2 Chemical procedure

The procedures for the mass spectrometric analysis were in general similar

to those developed for NAA by Huh and Bacon (1985). The thorium isotopes were purified through the anion exchange column (AG 1X8, 100-200 mesh, chloride form). Since the required sample volume was reduced, smaller-scale columns were used. The anion exchange procedures were repeated three times with decreased volumes of ion exchange resin each subsequent time (Fig. 3.5). The first two purification steps used a 12 ml poly-prep column filled with 4 ml and 2 ml resin, respectively. The third purification step was performed in a micro-column with 100 µl of resin. Thorium was finally eluted off the micro-column with ~200 µl of 12N HCl, dripped directly onto a teflon pad (3/4" diameter), and evaporated under a heat lamp to near dryness.

The purified samples were packed into petri-culture dishes (PYREX) by attaching the teflon-pad onto the bottom of the dish, and then sent to the Radiological Sciences Section of Battelle Pacific Northwest Laboratories for mass spectrometric analysis.

3.4.3 Mass spectrometry

At Battelle, the final refinate was dissolved in about 50 µl (one drop) of 8N HNO_3 and evaporated to ~1 µl in the presence of a single 150 µm anion exchange resin bead, so that the Th isotopes are placed onto the resin bead (Huh, 1985). This method is similar to that of Walker et al. (1974). The bead was subsequently recovered using a rhenium wire, loaded onto a rhenium filament and placed into the mass spectrometer.

Following carbonization of the resin bead at low temperatures, thorium was volatilized at high temperatures and the different isotopes were counted in their respective mass regions of the spectrum.

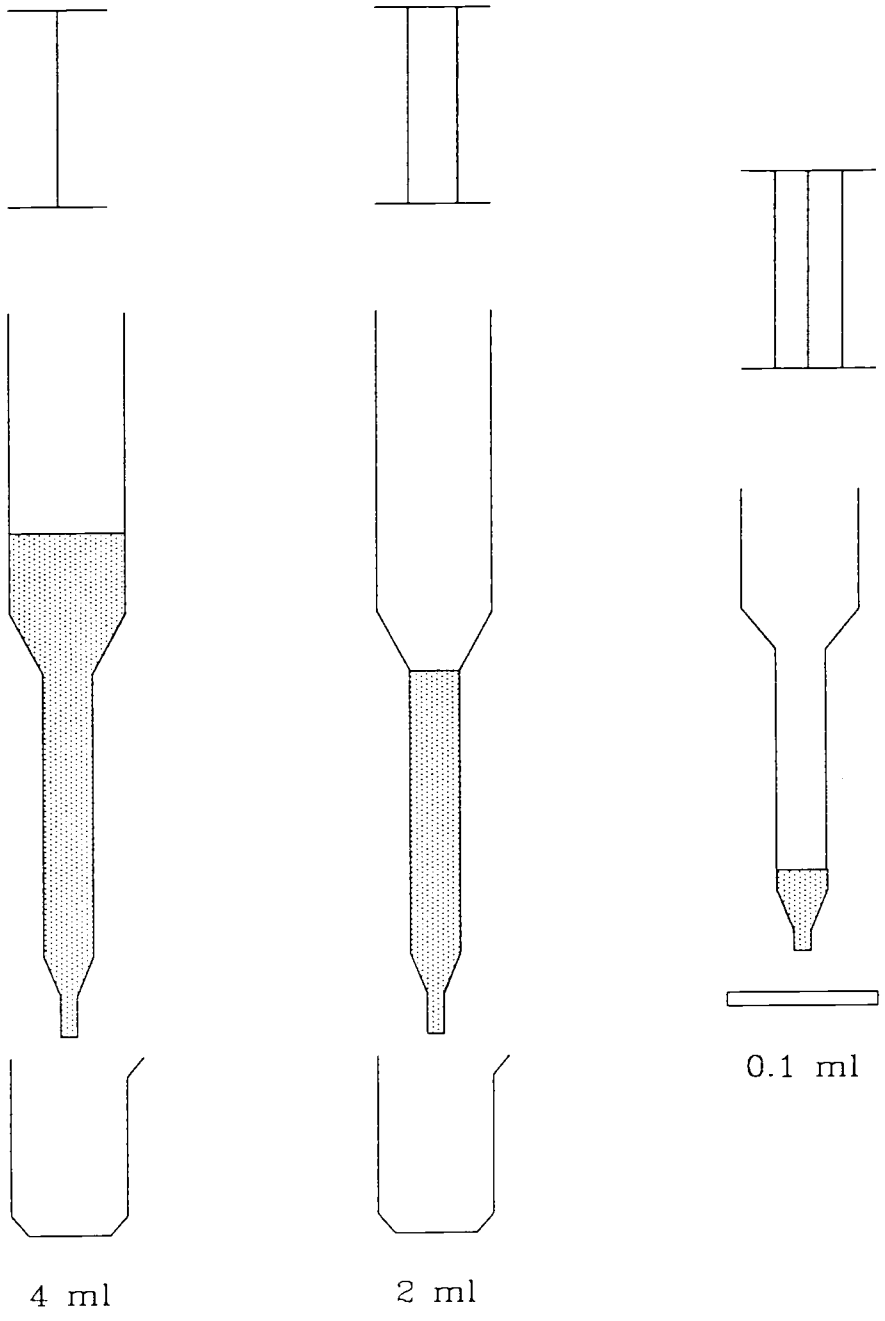

Figure 3.5. Column for AG 1x8 separations in the mass spectrometric analysis. 12 ml Poly-prep column with graduated volume markings provides nominal column calibration at a glance

3.4.4 Counting results and data reduction

The activity (dpm) of a radionuclide is defined by the law of radioactive decay, $A = -dN/dt = \lambda N$; and is proportional to the number of the atoms in the sample at time t. The decay constant λ is a most important characteristic of each radioactive nuclide. In terms of activity ratios between the nuclides of interest and spike ^{229}Th, the equation can be written as:

$$A_{interest}/A_{spike} = (\lambda N)_{interest}/(\lambda N)_{spike}$$

i.e., the activity ratio is proportional to the atom ratio. To calculate the activities of ^{232}Th and ^{230}Th, therefore, we only need to know their atom ratios which are given by the results of mass spectrometry. Based on the atom ratios derived from MS, the contents of ^{230}Th and ^{232}Th, in terms of activities, in the samples can be calculated by these equations:

$$A_1 \text{ (dpm/kg)} = [A_3 \times (\lambda N)_1/(\lambda N)_3] \div \text{Sample Wt. (kg)}$$

$$A_2 \text{ (dpm/kg)} = [A_3 \times (\lambda N)_2/(\lambda N)_3] \div \text{Sample Wt. (kg)}$$

where 1, 2, 3 represent ^{232}Th, ^{230}Th, ^{229}Th, respectively.

The counting results showed that, in spite of the very low yield (<1%), the total ion counts were so high for ^{232}Th that the counting error was well within ±3%. The low recovery of Th was primarily due to the fact that the amount of residue (in the refinate) was too much to be picked up by a single resin bead. As for ^{230}Th, because of its much lower atom number relative to ^{232}Th, its standard deviation varies with chemical recovery and concentration of ^{230}Th in the sample. The counting error decreases as Th recovery and ^{230}Th concentration increase, and is in the range 6.5%-49%. The background appeared

high and variable, probably due to air contamination in the laboratory. Because blanks were closely monitored for each batch of samples, the background was manageable with respect to the levels of ^{232}Th and ^{230}Th measured. The results are presented and discussed in next chapter.

THE DISTRIBUTION AND CONCENTRATIONS OF DISSOLVED AND PARTICULATE THORIUM IN FRESH WATER AND SEAWATER

4.1 General Introduction

The purpose of this chapter is to describe the behavior of ^{230}Th and ^{232}Th in several diverse aquatic environments. The factors controlling the concentrations and distributions of thorium are evaluated. These factors include, principally, the source of supply, physical, chemical and biological processes, and the natural properties of the water (e.g., hydrothermal activity, particle concentration, redox potential, pH, etc.). Although thorium isotopes have been studied intensively in the ocean, very little is known about the distribution and partitioning of Th isotopes in continental waters which have different chemistries (such as pH and alkalinity) and compositions from seawater. In order to evaluate the supply of Th isotopes from continents to the ocean and to understand the marine geochemical cycle of long-lived Th isotopes, the knowledge about the concentration levels of thorium in continental water and seawater is necessary. Concentrations and distributions of ^{230}Th and ^{232}Th, as well as their partitioning between dissolved and particulate forms were obtained for samples from the Columbia River, the confluence of the John Day and Columbia Rivers, Crater Lake and Saanich Inlet (Table 7). The total ^{232}Th concentration were determined for samples off the coast of Washington and Oregon (Table 6) and at the Juan de Fuca Ridge (Table 10, presented in section 4.2.5). The data set represents the distributions of thorium in natural waters of diversified chemical make-up and thus allows us to study the behaviors of Th isotopes in those environments, and the relationship of ^{230}Th and ^{232}Th.

4.2 Results and Discussion

4.2.1 Transport of thorium from continents to the ocean and interactions at land-sea and air-sea interfaces

4.2.1.1 Comparison of Th concentrations and partitions between dissolved and particulate forms in fresh water and seawater

Due to its continental source, ^{232}Th concentrations in rivers and lakes are expected to be higher than in the ocean and our results support this. Table 7 lists the concentrations of dissolved and particulate forms of ^{230}Th and ^{232}Th measured in samples from surface of rivers, lakes and the ocean. Because the water samples collected off the Washington/Oregon coast were unfiltered and measured by the NAA method, only the total ^{232}Th content (i.e., dissolved + particulate) in the water column are reported; hence, this set of data is not comparable directly with others.

Dissolved ^{232}Th concentrations in the Columbia River and Lost Lake are one order of magnitude higher than in seawater; yet the dissolved ^{232}Th accounts for only about 5% of the total ^{232}Th concentrations in these samples. Exceptionally high concentrations of thorium are observed at the confluence of the John Day and Columbia rivers. One possible explanation for this is the tendency of thorium to form strong organic complexes. During sampling at this site, phytoplankton was observed on the water surface and the water sample was very difficult to filter. Perhaps the high level of organic matter at this site enhanced the degree of Th complexation, greatly increasing the solubility of thorium.

Particulate Th concentrations in the rivers and Lost Lake are a factor of

TABLE 7. Surface concentrations of ^{230}Th and ^{232}Th, and their partitioning in some rivers, lakes and seawater.

Sampling site	^{232}Th (dpm/10^6kg)[a] Diss.	Part.	Part.[b] (%)	^{230}Th (dpm/10^6kg) Diss.	Part.	Part. (%)
Bonneville Dam	585±16	18100±531	97	798±32	17519±788	96
Confluence of John Day & Columbia Rivers	708±20	18653±565	96	917±54	51750±1653	98
Lost Lake	256±7	4160±130	94	2766±16	12288±410	98
Crater Lake	27.8±.9	8.3±1.1	23	38.5±6.7	n.d.[c]	
Saanich Inlet	20.7±.4	16.9±.6	45	63.0±5.0	29.9±5.8	32
Santa Monica Basin	59.6±1.0	2.5±.2	5	161±31	n.d.	

TABLE 8. Concentrations of Th in Crater Lake (water depth = 450m)

Depth (m)	^{232}Th (dpm/10^6kg) Dissolved	Particulate	^{230}Th (dpm/10^6kg) Dissolved	Particulate	$^{230}Th/^{232}Th$ (Activity)
10	27.75±0.85	8.30±1.13	38.45± 6.65	n.d.	1.39±0.24
90	92.58±2.61	8.09±1.07	181.8± 8.63	n.d.	1.96±0.06
230	30.09±0.93	3.77±0.58	39.22±19.21	n.d.	1.30±0.64
444	19.96±0.65	9.02±0.67	31.87± 4.83	n.d.	1.60±0.25
I[d]	0.00184	0.00028			

[a] 1 dpm ^{232}Th = 4.09 μg = 0.0176 μmol; 1 dpm ^{230}Th = 21.8 pg = 0.0947 pmol.

[b] Percentage of thorium on particulate form.

[c] n.d.-- not detectable; due to large errors in ion counting.

[d] I = water column inventories (dpm/cm^2); estimated by integrating over the profiles.

thousand to ten thousand higher than those observed in Saanich Inlet and the Santa Monica Basin. This is due to two reasons: (i) total ^{232}Th concentrations in continental waters are enormously higher than in seawater, (ii) particulate concentrations are much higher (~1 to 5 orders) in rivers than in open oceans (Salomons and Förstner, 1984) (Fig. 4.1). Since thorium is a very particle reactive element, the concentration of particulate Th in rivers and lakes is expected to be higher than in the ocean.

The adsorption of thorium depends on the adsorbent surface sites available. Due to its particle-reactive nature, the rate of removal of dissolved Th, hence, partitioning of Th between dissolved and particulate form, depends on particle concentrations. High partitioning of thorium in particulate form in the Columbia River and Lost Lake are therefore expected. Our results show that, in the Lost Lake and Columbia River surface waters, more than 94% of the thorium present was found in particulate form. In contrast, 45% in Saanich Inlet, and only 4.7% of ^{232}Th in the Santa Monica Basin, were found in particulate form.

Crater Lake samples show very low particulate thorium. The lake water is extraordinarily clear and can be characterized as being low total-dissolved-solids water containing less then 100 ppm dissolved solids and less than 1 ppm of suspended solids (Williams and Von Herzen, 1983). Input of water is mainly in the form of snowfall directly onto the lake surface and this would contain low concentrations of thorium. These unique features were reflected by our data on Th distributions in the lake (Table 8). The dissolved Th concentration (28 dpm/10^6kg) in the surface of Crater Lake was much lower than in Lost Lake and the rivers studied, and was even lower than in the Santa Monica Basin (Table 7). Because of low particle concentration of the lake water, the partitioning of ^{232}Th on particulate form was also much lower (only 27%) than

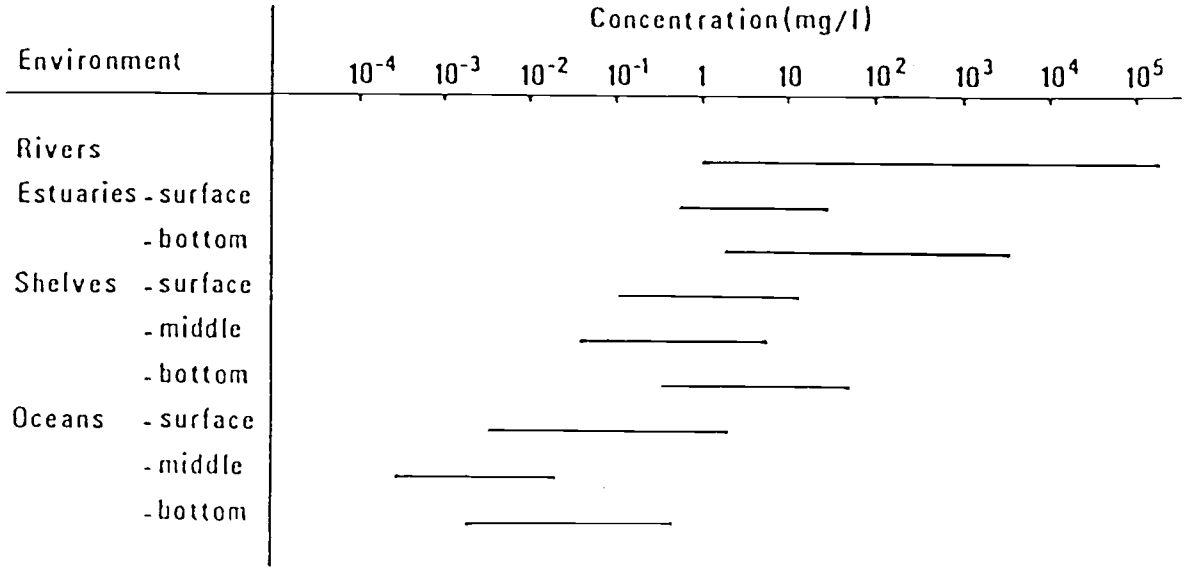

Figure 4.1. Particulate concentrations in the hydrological cycle (from Kranck, 1980)

in the Columbia River and Lost Lake. On the average, only about 13% of ^{232}Th in the water column was found on particulate form, whereas there were 50% of ^{232}Th on particulate form in the water column of the Santa Monica Basin (Huh and Beasley, 1987). It further reflects the low particle concentration in Crater Lake and demonstrates the dependence of Th partitioning on particle concentration.

4.2.1.2 Removal of fluvial ^{232}Th in estuarine and coastal regions

There are two sources of ^{232}Th to the ocean, fluvial and aeolian inputs. The observed surface enrichments of dissolved ^{230}Th (50.6 dpm/10^6 kg) and ^{232}Th (161 dpm/10^6 kg) in the Santa Monica Basin (Fig. 4.2), which is 50 km offshore from Southern California coastline, strongly suggests a terrestrial input for both isotopes (Huh and Beasley, 1987). It is possible that both Th isotopes are transported into the sea in dissolved form, and/or by leaching of terrestrial detritus on contact with seawater. It should be pointed out that input of ^{232}Th from aeolian and fluvial sources would also deliver ^{230}Th. According to the study of Nozaki and Yamada (1987) in North Pacific, they suggested a fluvial source of ^{230}Th to surface waters in the Japan Sea as well. A surface enrichment of total ^{232}Th (269 dpm/10^6kg) is also observed off the coast of Washington/Oregon (Fig. 4.3). A recent study of Jones and Murray (1985) on the same area showed a Mn profile (Fig. 4.3) with a similar feature as total ^{232}Th (these figures will be further discussed). They ascribed this surface enrichment to fluvial inputs, especially from the Columbia River. The fact that Th is scavenged by hydrous Mn and Fe oxide means Mn and Th came from the same source, i.e. the Columbia River. Hence, terrestrial waters are important source of thorium, at least to coastal regions.

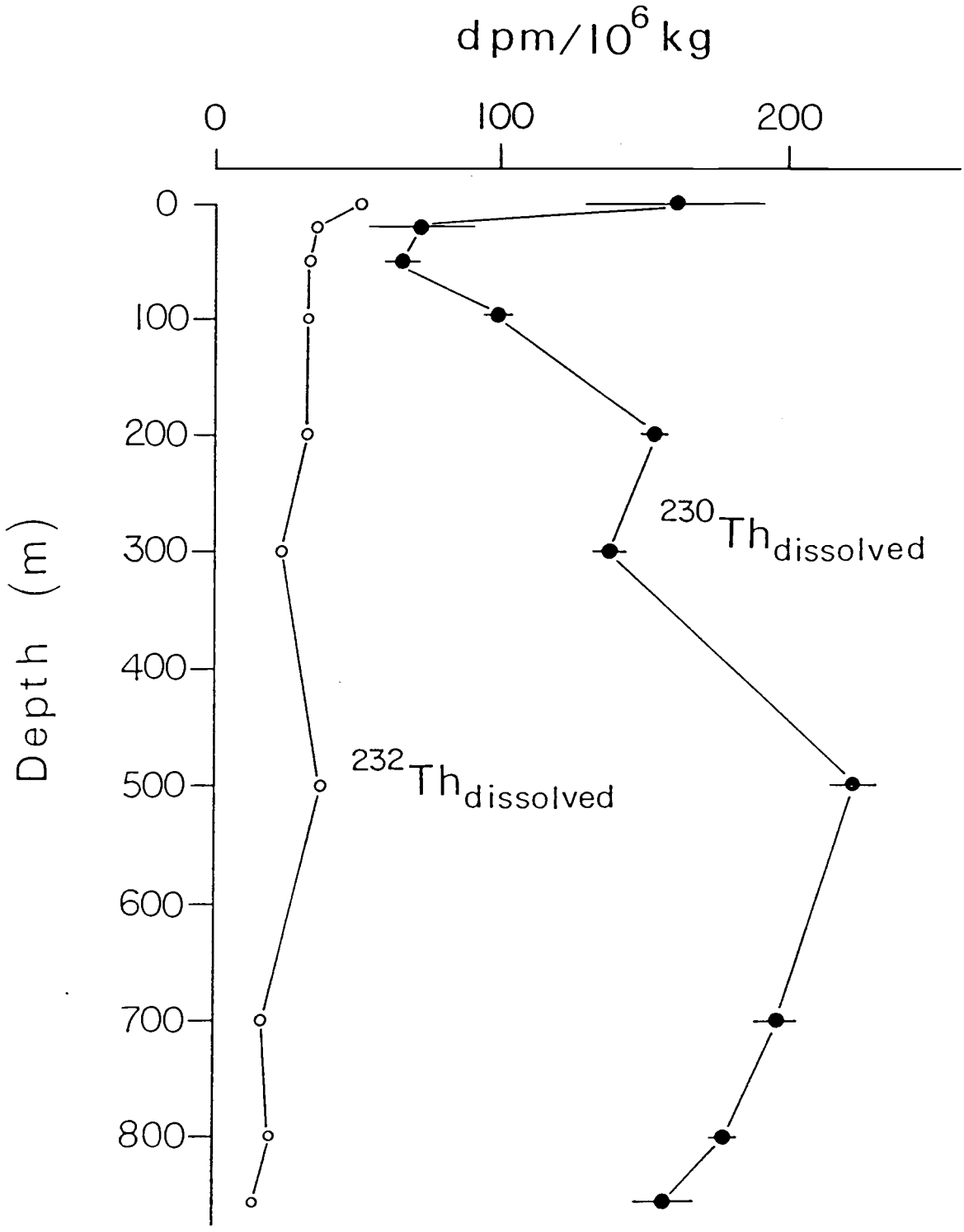

Figure 4.2. Profiles of dissolved ^{232}Th and ^{230}Th in the Santa Monica Basin off Los Angeles (from Huh and Beasley, 1987). The surface enrichment strongly suggests a terrestrial input for both isotopes

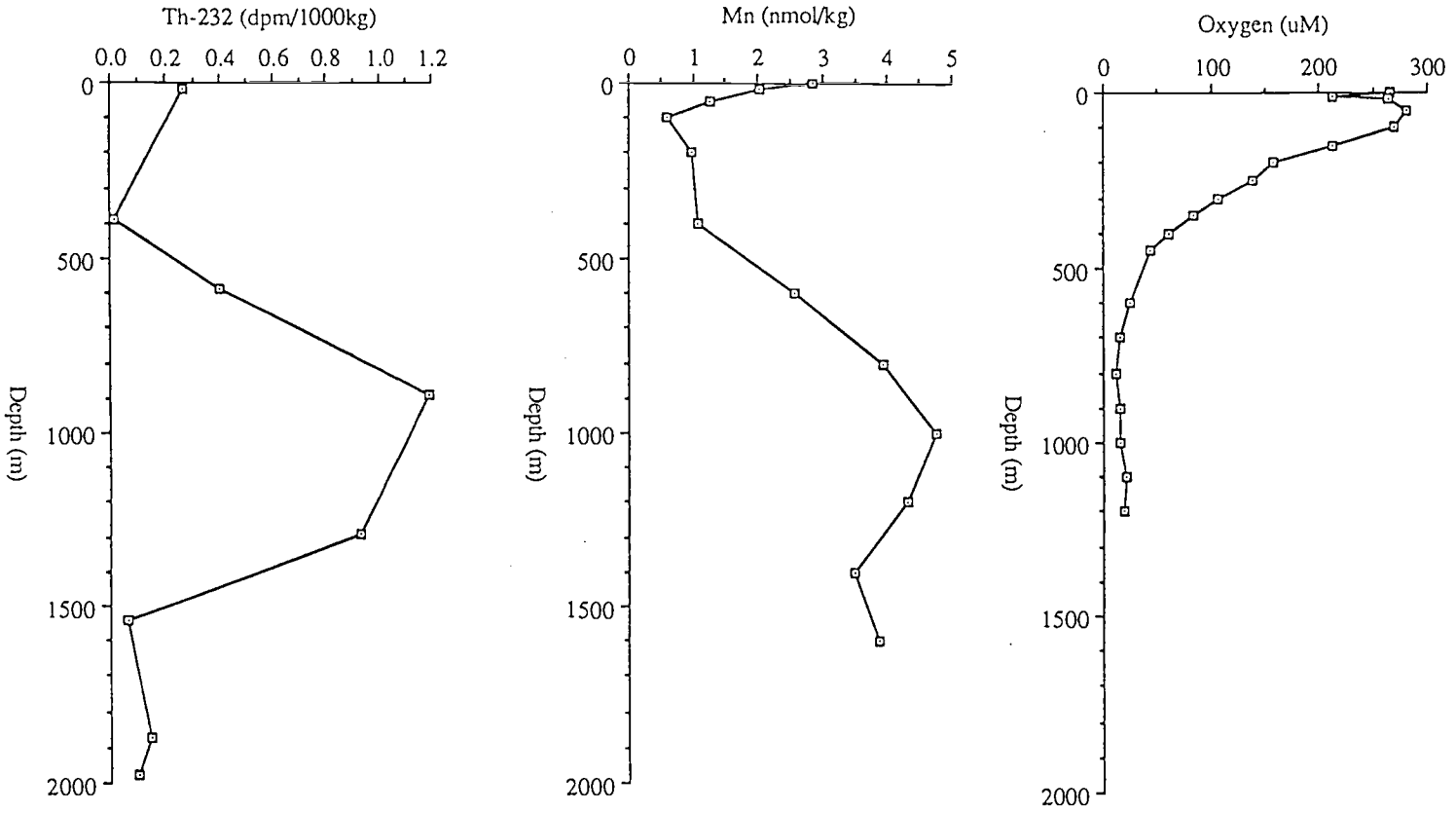

Figure 4.3. Distribution of ^{232}Th, Mn and dissolved O_2 in the water column off Washington and Oregon Coast. The similar distribution of ^{232}Th and Mn in this particular area suggests that both elements may come from the same source(s) and have participated in common geochemical cycles. (Mn and O_2 data from Jones and Murray, 1985)

The very high concentrations of thorium in continental waters, as discussed in last section, could forward a substantial flux of thorium to the estuaries. The observed values in the coastal region, however, are not very high, comparatively. This means that dissolved riverine Th is nearly quantitatively removed during estuarine mixing, as observed in coastal waters of the Santa Monica Basin. The data from samples collected off the Washington coast also shows evidence of the effect of estuarine mixing on Th distribution (Table 6).

There are two possible sources of thorium to the Washington and Oregon coastal area. One is the riverine input from the Columbia River; another is the advective-diffusive transport from reducing nearshore sediments (Jones and Murray, 1985). The Columbia River discharges 6.3×10^8 m^3/day (over 75% of the freshwater input) into the northeast Pacific Ocean (Jay and Sherwood, 1984). With such high Th concentrations in the Columbia River, the discharge of the river water could contribute a considerable flux of thorium to the estuaries. The concentrations of total ^{232}Th in surface waters of the coastal area, however, are relatively low compared with high Th concentrations in the Columbia River. It reveals that Th exported by the Columbia River is probably diluted and removed on the way through estuarine to oceanic waters. The removal is possibly caused by enhanced scavenging of Th during the estuarine mixing. Estuaries are often a sink for reactive metals which form strong complexes with humic acids and iron hydrous oxides (Sholkovitz, 1976; Salomons and Förstner, 1984; Li et al., 1984). In a natural estuarine environment, the increase in both pH and salinity and the existence of suspended particles all enhance the coagulation of metals with iron hydrous oxides. The flocculation of metal-$Fe(OH)_3$ and of organic matter from solution in estuarine mixing zones may serve to remove additional amounts of dissolved constituents from river

water and keep them in the estuaries, and consequently further reduces the amount of metals transported into the ocean.

Therefore, the fluvial source of ^{232}Th is important to the coastal waters, but seems insignificant to the open oceans. In other words, atmospheric input of ^{232}Th is probably more important to the open ocean, like Al, for instance. The study of Orians and Bruland (1986) has shown that the external source of dissolved Al to the open ocean is primarily by leaching of dust delivered from the atmosphere. The similar profiles of these two particle reactive elements are observed in the open ocean. It has also been noted that the crust ratio of Th/Al ($1.2x10^{-4}$) is very close to the weight ratio of Th/Al ($1.3\text{-}2 \times 10^{-4}$) in some deep seawater (Huh, 1985). These may mean that these two elements have certain similar source terms and transport pathways. The coherence of the Al input pattern and distribution pattern of the initial $^{230}Th/^{232}Th$ activity ratio observed on manganese nodules and crusts may further support this possibility, as discussed in section 2.5. The aeolian input of dissolved Al is higher in the Atlantic than in the Pacific. As shown in Figure 2.6, the $^{230}Th/^{232}Th$ activity ratios in Mn nodules (and presumably also in seawater) in the Atlantic are lower than in the Pacific. Because the production rate of ^{230}Th is nearly constant everywhere, it is reasonable to presume that the variation in $^{230}Th/^{232}Th$ in the open ocean is primarily controlled by ^{232}Th. This means there is higher dissolved ^{232}Th content in the Atlantic than in the Pacific. In the Pacific, lowest aeolian input of Al is found in the South Pacific central gyre, where the highest $^{230}Th/^{232}Th$ activity ratio are also found. The same trends of Al and ^{232}Th in global ocean distribution may mean they have similar aeolian input pattern.

4.2.1.3 Interactions at the continental margin and seafloor

The vertical distribution pattern of ^{232}Th (Fig. 4.3) on continental slope off the Washington and Oregon coast, approximately 160 km northwest of the mouth of the Columbia River, reveals the scavenging processes and boundary effects. The profile of total ^{232}Th concentration showed a mid-depth maximum at 890 m and a decrease toward the bottom water. The maximum concentration of thorium probably resulted from a combined effect of (i) scavenging and remineralization processes of thorium in the water column; (ii) offshore advection of water enriched in ^{232}Th from reducing sediments; and (iii) lateral advection of particles from slope. The processes of Th scavenging onto particles and removal from the surface water column requires time and distance to achieve. As transport time and distance increase, more Th is scavenged by particles and removed from the water column. When particles sink to the depth of the maximum, they are concentrated there by certain as yet unclear physical and/or geochemical causes, but probably not by biological process. It has been suggested that the predominant scavenging reactions off Washington/Oregon coast are inorganic rather than biological (Beasley et al. 1982). In addition to the water column scavenging of ^{232}Th, the incident of the maximum ^{232}Th concentration in the deep water should also consider the effect of continental margin as possible sources of thorium. Since this sampling site is on the continental slope, the reducing sediments enriched in Th possibly run off from the shelf and are concentrated in the deep water at the maximum depth. The diffusive fluxes of Th from the upper continental slope sediments could be another possible source. It has been observed that Mn distributions along an offshore transect in this area exhibit a plume originating from the slope (Jones and Murray, 1985). Moreover, their profile of Mn at a nearby station showed a

remarkable resemblance to our ^{232}Th profile (Fig. 4.3), i.e. both profiles are characterized by high concentrations in a broad oxygen minimum centered around 1000 m. Mn oxide acts as a carrier of Th. Therefore, offshore advection of Mn along with ^{232}Th remobilized from reducing sediments may support these maxima.

The decrease of ^{232}Th from the mid-deep water maximum toward the bottom is possibly due to resuspension of slope and bottom sediments resulting in enhanced Th scavenging, and rapid particle removal. Whether there were nepheloid layers existing or not in the bottom water, it could not be indicated by our total Th data, because nepheloid layers could only result in a decrease of dissolved Th. Without additional data, the profile can not be definitively explained.

4.2.2 Subsurface maxima of ^{232}Th in water columns: a common feature

Several Th profiles from different environments, such as Crater Lake (Fig. 4.4), the Caribbean sea (Fig. 4.5) (Huh & Bacon, 1985b), and Saanich inlet (Fig. 4.6a and 4.7), show similar subsurface maximum features. There are two possibilities for this feature: (i) vertical particulate transport and release of thorium at the depth of the maximum, (ii) advective transport from a remote source (Huh and Bacon, 1985b). In Crater Lake, the profiles of both dissolved ^{230}Th and ^{232}Th (Fig. 4.4) show a subsurface enrichment around the pycnocline. The subsurface Th maximum in the lake, which only has a surface area of 53 km^2, is probably from vertical and side transport and concentrated at the pycnocline. The minimal light transmission, which caused by high phytoplankton concentrations, is observed at the depth of the maximum dissolved Th concentrations (Fig. 4.4). However, the particulate Th showed no correlation

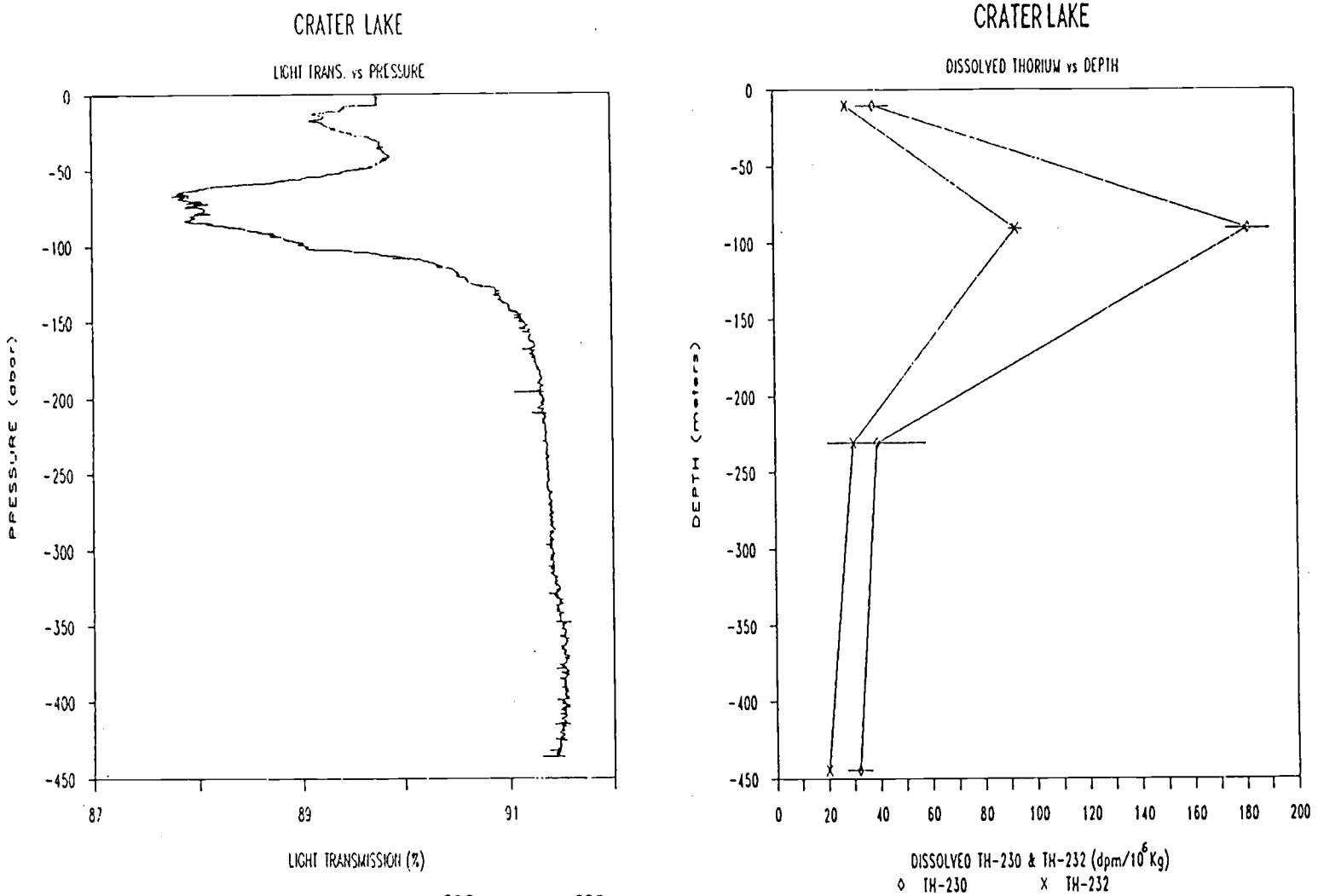

Figure 4.4. Profiles of dissolved ^{232}Th and ^{230}Th in Crater Lake. The subsurface maximum of thorium are coincident with minimal light transmission, indicating that the vertical particulate transport is the cause of these feature. (light transmission data from Collier, unpublished.)

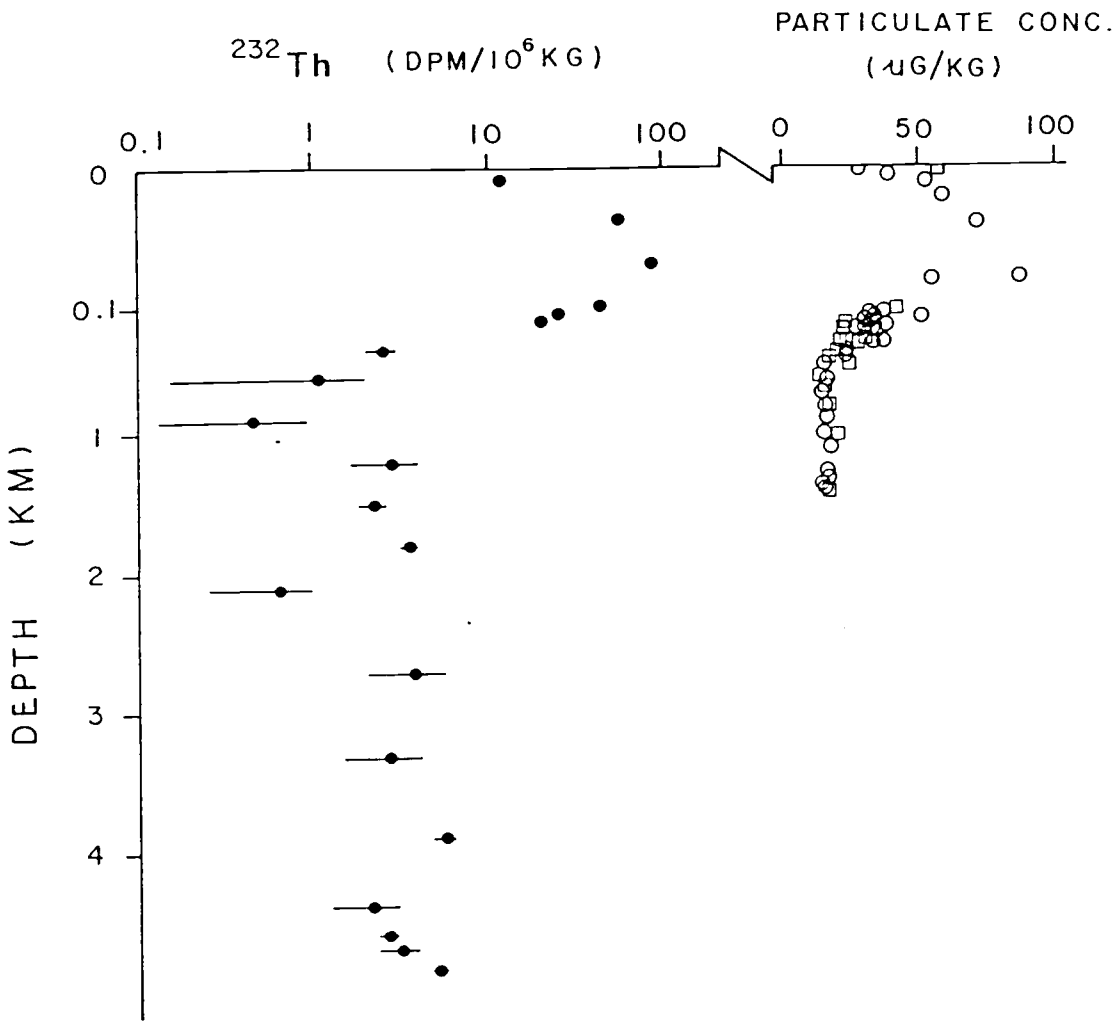

Figure 4.5. Profile of dissolved ^{232}Th in the Caribbean Sea (from Huh and Bacon, 1985). The subsurface maximum of dissolved ^{232}Th also correlates with the maximum particulate concentration

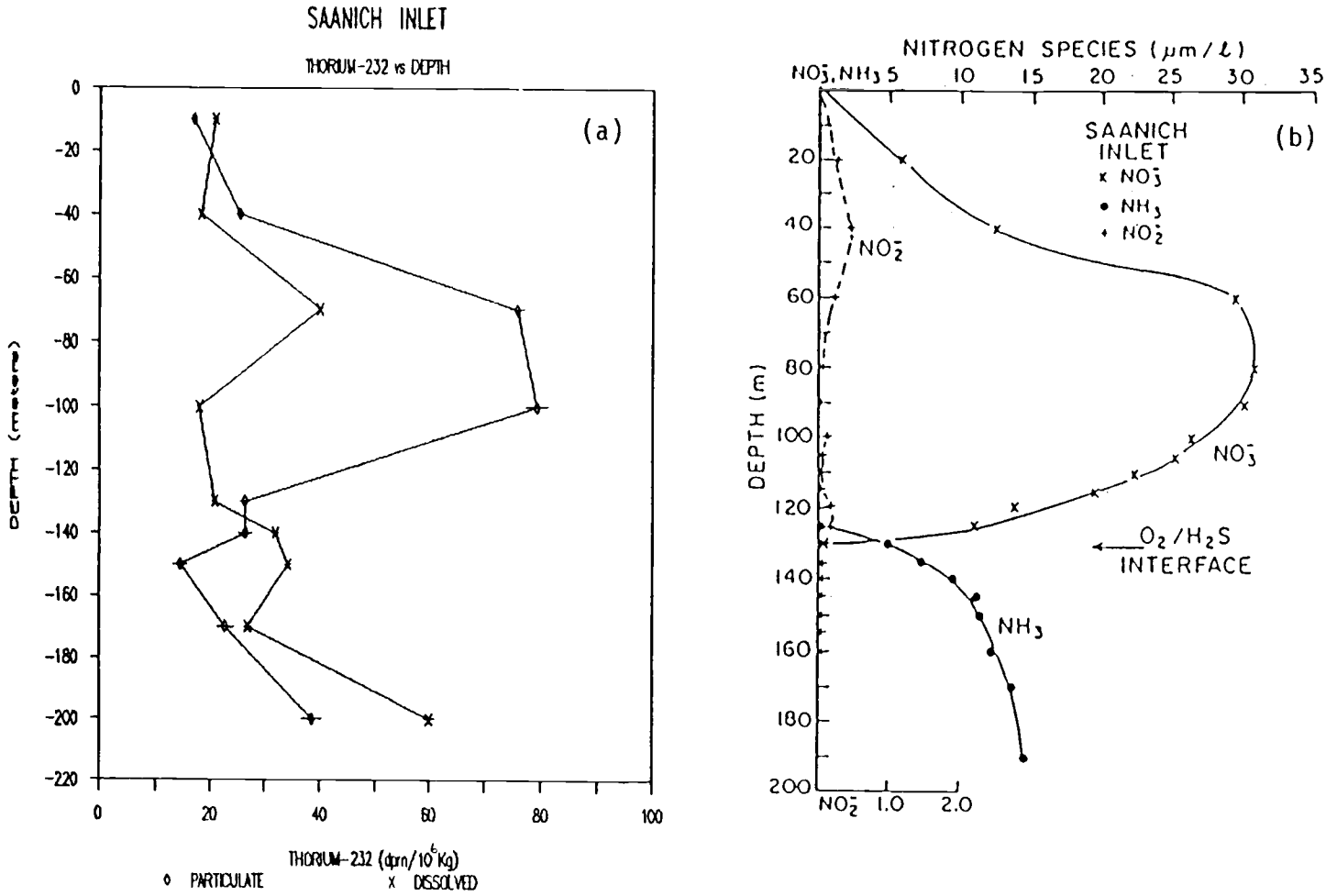

Figure 4.6. (a) Profiles of dissolved and particulate ^{232}Th in Saanich Inlet. Above the O_2-H_2S boundary (at 135m) particulate ^{232}Th is higher than dissolved ^{232}Th; below the redox boundary, concentrations of particulate and dissolved ^{232}Th were reversed. (b) Profiles of nitrogen species in Saanich Inlet (from Emerson et al., 1979). The coincidence of the NO_3^- and Th maxima shows that the subsurface maximum in Saanich Inlet is closely related to biochemical processes and vertical particle transport

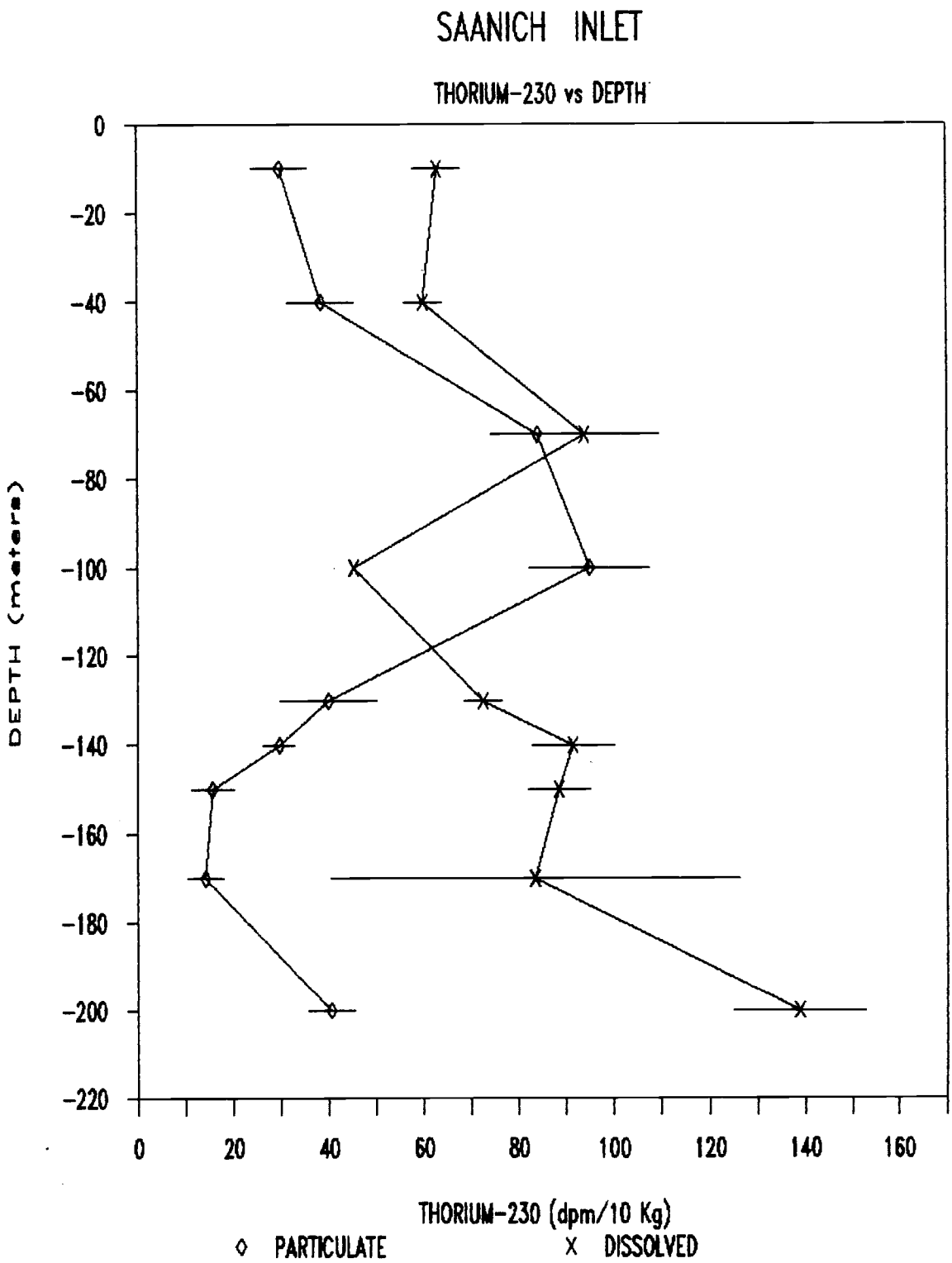

Figure 4.7. Profiles of dissolved and particulate ^{230}Th in Saanich Inlet. The dissolved ^{230}Th is higher than particulate ^{230}Th in the entire water column, demonstrating the source terms of dissolved ^{230}Th

with phytoplankton concentrations in the lake because particulate Th concentrations were very low (Table 8) and almost no change in the water column.

The Caribbean Sea profile, with a more detailed sampling, exhibits a subsurface maximum at the base of the mixed layer. The dissolved ^{232}Th maximum also correlates with the maximum particulate concentration at about 80 m, similar to the case with Crater Lake. This feature may be explained by disaggregation of particulate matter packaged in the upper euphotic zone. The reduced particle size results in longer residence times at that layer, where a large fraction of the "leachable Th" may be released. In addition, it is also possible that the subsurface maximum observed in Caribbean Sea was partially due to advective transport from a remote source (Huh and Bacon, 1985b).

As for the similar feature observed in Saanich Inlet, whether it was only due to the reason (i) or both (i and ii) cannot be determined without additional information. Nevertheless, it is certain that the subsurface maximum in Saanich Inlet is closely related to biochemical processes and vertical particle transport. In Saanich Inlet, the subsurface maximum of Th coincides approximately with the NO_3^- maximum (Emerson et al., 1979) (Fig. 4.6b). The low concentrations of NO_3^- in the surface water indicate high biological activities there which used up the nutrient. The produced organic particles enhanced Th scavenging and removed Th out of the surface water as the particles sink to the depth of maximum. The more pronounced subsurface maximum of particulate Th (Fig. 4.6a and 4.7) is the evidence of the scavenging processes. The regeneration of the organic particles at the depth of maximum makes up the high concentrations of NO_3^- and dissolved Th. Thereafter the removal of dissolved Th onto particles from 70 m to 100 m is caused by increased particulate Mn (IV) concentrations (Fig.4.8b) in that region, which is also due

to biological catalysis. The studies on microbial mediation of Mn (II) precipitation in Saanich Inlet (Tebo et al., 1984; Tebo and Emerson, 1986) demonstrated a two step process of manganese oxidation and concluded that the rate of oxidation in the low oxygen containing waters above the O_2-H_2S interface is catalyzed by bacteria. The Mn oxide which are continuously formed just above the interface has large "fresh" surface area and may be a very efficient scavenger for adsorption of thorium. The observed maximum of particulate Mn correlated well with the maximum of particulate Th, indicating the enhanced scavenging of dissolved thorium by particulate Mn in this region. Therefore, the similar trends of NO_3^- and Th profiles and the correlation of Mn and Th in the upper water column of Saanich Inlet suggest that biochemical process is one of the major factors controlling distribution of thorium.

4.2.3 Redox reaction of thorium

Concentrations of ^{230}Th and ^{232}Th and activity ratios of $^{230}Th/^{232}Th$ in Saanich Inlet are listed in Table 9. The oxic-anoxic boundary indicated by the co-existence of low concentrations of oxygen and hydrogen sulfide was found around 135 m (Fig. 4.8, data from Tebo, personal communication). The profiles of ^{230}Th and ^{232}Th, both in dissolved and particulate forms, exhibited interesting systematic trends with depth in the redox water environment (Fig. 4.6a and 4.7). The concentrations of Th increased with depth down to 70 m, then dissolved Th decreased to 100 m while particulate Th continually increased toward a subsurface maximum above the oxic water. Around the redox boundary, the behaviors of dissolved and particulate Th were reversed. The particulate Th decreased with depth while the dissolved Th were increasing across the O_2-H_2S interface. Below ~150 m, both particulate and dissolved Th

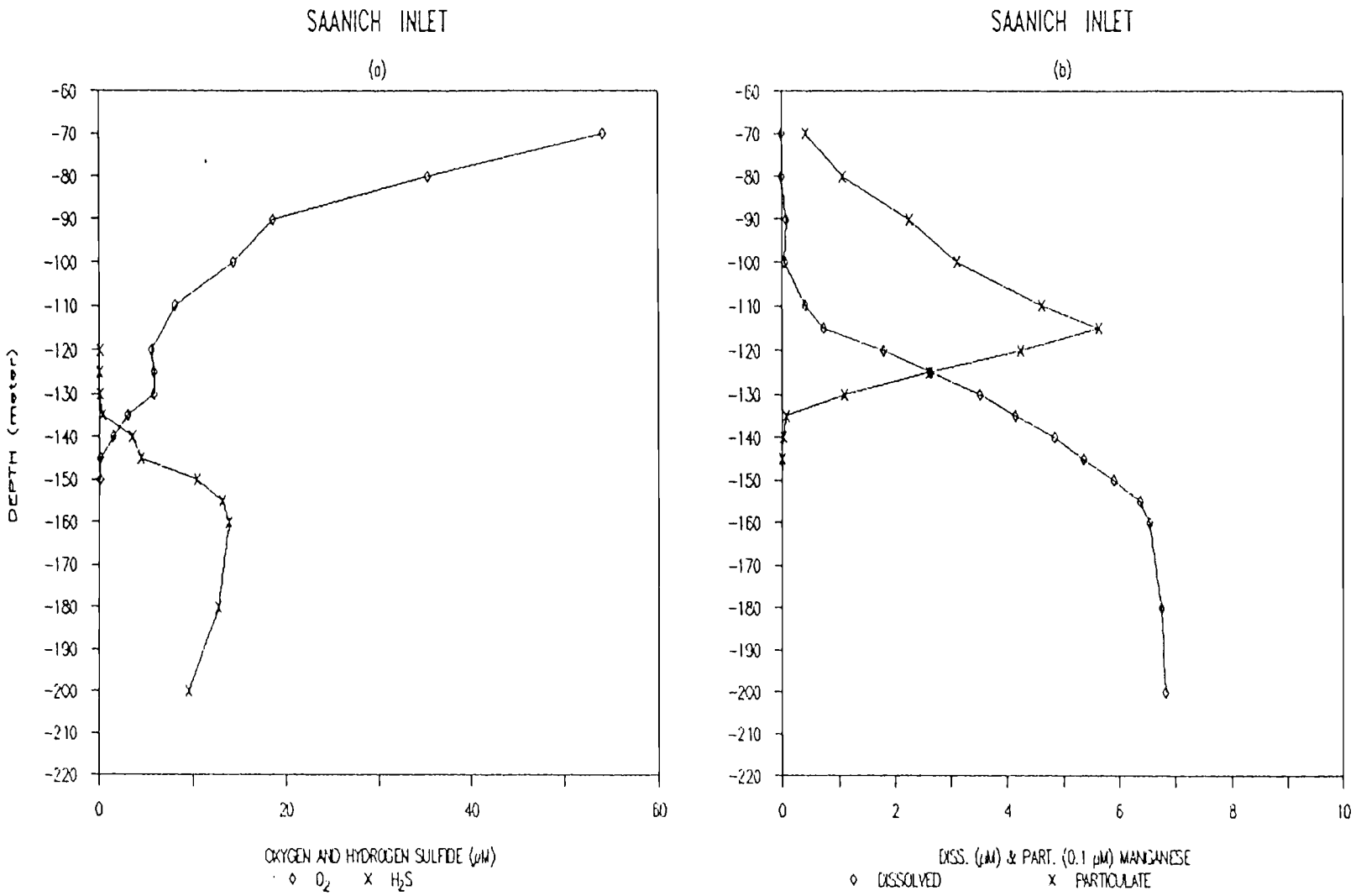

Figure 4.8. Oxygen and hydrogen sulfide (a), and manganese (b) distribution in Saanich Inlet. The O_2-H_2S boundary is at 135m. (Data from Tebo, personal communication)

TABLE 9. Concentrations of ^{230}Th and ^{232}Th and their activity ratio at the Saanich Inlet (water depth 220m)

	DISSOLVED		
DEPTH	^{232}Th	^{230}Th	$^{230}Th/^{232}Th$
(m)	(dpm/10^6kg)	(dpm/10^6kg)	(Act. ratio)
10	20.7 ± 0.4	63.0 ± 5.0	3.04 ± 0.22
40	18.2 ± 0.4	60.0 ± 4.0	3.30 ± 0.23
70	40.0 ± 0.5	93.9 ± 15.6	2.27 ± 0.38
100	18.0 ± 0.4	45.4 ± 4.0	2.52 ± 0.23
130	20.7 ± 0.4	72.5 ± 4.0	3.50 ± 0.20
140	31.9 ± 0.6	91.5 ± 8.5	2.87 ± 0.27
150	34.2 ± 0.6	88.5 ± 6.5	2.59 ± 0.20
170	26.9 ± 0.5	83.5 ± 43.0	3.11 ± 1.60
200	60.0 ± 1.0	139 ± 14	2.32 ± 0.24
	PARTICULATE		
DEPTH	^{232}Th	^{230}Th	$^{230}Th/^{232}Th$
(m)	(dpm/10^6kg)	(dpm/10^6kg)	(Act. ratio)
10	16.9 ± 0.6	29.9 ± 5.8	1.77 ± 0.35
40	25.3 ± 0.7	38.5 ± 7.0	1.52 ± 0.28
70	75.6 ± 1.3	84.1 ± 9.9	1.10 ± 0.14
100	79.2 ± 2.0	95.0 ± 12.5	1.20 ± 0.16
130	26.3 ± 0.9	40.0 ± 10.2	1.52 ± 0.39
140	26.4 ± 1.3	29.6 ± 3.3	1.12 ± 0.14
150	14.4 ± 1.2	15.6 ± 4.4	1.08 ± 0.32
170	22.7 ± 1.4	14.2 ± 3.7	0.62 ± 0.17
200	38.6 ± 1.8	40.5 ± 4.9	1.05 ± 0.14

showed increases in concentrations in the bottom reducing waters. The high concentrations of Th near the bottom might indicate a bottom source of Th. The study of Nozaki and Horibe (1983) in the western North Pacific suggested the same possibility.

The very different Th profile in Saanich Inlet demonstrates the additional effects of oxidation and reduction reactions. The denser sampling near the oxic-anoxic boundary made it possible to determine the detailed structure of Th profiles in the oxidized and reduced environments. Th-Fe hydroxyl complexes are different in the oxidizing and reducing waters because of the redox sensitivity of iron. In oxidizing water, iron exists entirely as Fe^{3+} due to rapid oxidation rate of Fe^{2+}. Upon crossing the redox boundary, ferric iron is first reduced to ferrous iron (Fe^{2+}) in the form of $Fe(OH)_2$ which is more soluble than $Fe(OH)_3$. Subsequently, Fe^{2+} can form a soluble complex with ammonium ions $[Fe(NH_3)_6]^{2+}$ in absolute reducing water. Below the oxygen-hydrogen sulfide interface in Saanich Inlet, ammonia concentrations showed trend similar to Th (Fig. 4.6b), increasing with the depth, indicating an abundance of complexing ligand available in the bottom water.

The chemical properties of ferric-ferrous ions change in the redox boundary, directly affecting the partitioning of Th between solution and suspended particles. Above the oxygen-hydrogen sulfide boundary area, concentrations of particulate ^{232}Th were higher than those of dissolved ^{232}Th (Fig. 4.6a); the opposite is true below the oxygen-hydrogen sulfide interface. This implies that thorium on particles are released into solution when settling across the redox boundary. The manganese profile (Fig. 4.8) measured in Saanich Inlet on the same cruise showed a trend similar to the ^{232}Th (and ^{230}Th) profiles. Above the redox boundary, particulate Mn^{4+} was dominant and increased with depth, reaching a maximum at ~115 m. Concentrations of Mn^{4+}

then decreased to below the detection limit near the redox boundary, while dissolved Mn^{2+} increased and gradually became the dominant species in the reducing water column. The sharp decrease in Mn^{2+} concentration above 120 m indicated its removal in the region of high particulate Mn (more details in section 4.2.2). It seems likely that, in addition to Th-Fe hydroxyl complexes, Th is also associated with Mn on particles in the upper water column. As the particles settle across the redox boundary, the elements are remobilized. Thus, thorium is remobilized by reductive dissolution of Fe-Mn oxyhydroxides in the anoxic water. This same contention has been advanced by Todd et al. (1988) based on ^{228}Th data measured in Saanich Inlet and can be further supported by ^{234}Th data measured by Bacon (unpublished). The profile of ^{234}Th in Saanich Inlet showed sharp increase in dissolved concentration and decrease in particulate concentration below the oxygen-hydrogen sulfide interface (at ~130 m), similar to ^{230}Th and ^{232}Th behaviors.

The profiles (Fig. 4.7) of dissolved and particulate ^{230}Th in Saanich Inlet reflect the source terms of ^{230}Th. The concentrations of ^{230}Th in dissolved form were in general higher than in particulate form, except in the region (80-125 m) of high particulate Mn concentration (discussed above). This is because there are two sources of dissolved ^{230}Th: leaching of detrital ^{230}Th and in-situ product of ^{230}Th from the radioactive decay of ^{234}U. The second source is responsible for the high concentrations of dissolved ^{230}Th. In addition, the dissolution of particulate ^{232}Th as settling across the redox boundary further increases the differentiation between the concentrations of dissolved and particulate ^{230}Th in the anoxic water.

4.2.4 Correlation between ^{230}Th and ^{232}Th and its implications

Very little is known about the internal geochemical cycle of ^{232}Th in the ocean. Although the source terms of dissolved ^{230}Th and ^{232}Th are very different, there is reason to believe that both isotopes have participated in common geochemical cycle(s) in the water column. A correspondence on the distributions of dissolved ^{230}Th and ^{232}Th is clearly shown on the profiles (Fig. 4.2 & 4.4), in Crater Lake and Santa Monica Basin (Huh and Beasley, 1987). This may mean that these two isotopes have similar geochemical behaviors in the water column. A high degree of correlation between the distributions of both dissolved and particulate ^{230}Th and ^{232}Th are also observed in the water column of Saanich Inlet (Fig. 4.9), further signifying their similarities in geochemical cycle. This is very important information on applying radiogenic Th isotopes to study the general scavenging of non-radiogenic trace metals, since ^{232}Th is proposed as a link between them. The data available at present, however, is not sufficient to determine whether dissolved ^{232}Th in deep sea is in equilibrium with particulate ^{232}Th with respect to adsorption/desorption, as it is with ^{230}Th (Nozaki et al., 1981; Bacon and Anderson, 1982). To answer this question, more detailed study on ^{232}Th distribution and partitioning is needed.

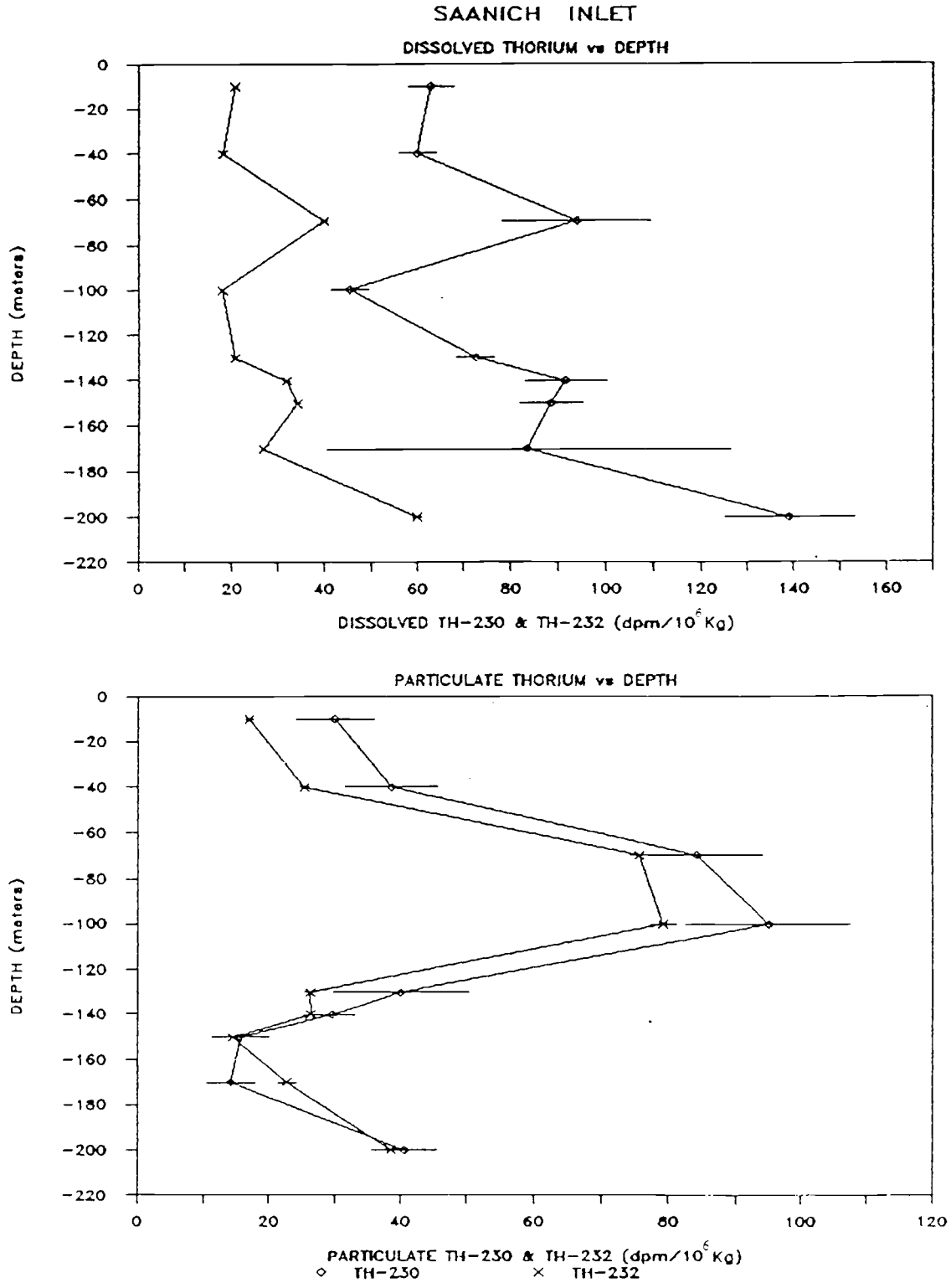

Figure 4.9. Distributions of both dissolved and particulate ^{230}Th and ^{232}Th in Saanich Inlet. The parallel trends of ^{230}Th and ^{232}Th mean these two isotopes have similar geochemical behaviors in the water column

4.2.5 Hydrothermal influence on Th distribution

Studies of hydrothermal processes have indicated that hydrothermal input is an important source of certain metals, such as Mn, Pb, rare earth elements, etc. (Edmond et al., 1979a,b, 1982; Chen et al, 1986a, and references therein) to the natural waters. When the primary hot, acidic, metal-rich hydrothermal solution flows toward the bottom water, it encounters the cold, alkaline overlying water column, resulting in precipitation of its carried metals. This process may remarkably alter the rate of metal scavenging. Therefore, the hydrothermal fluid, which carries high concentrations of dissolved metals and other salts, may significantly affect the composition and chemistry of natural waters. The influence of hydrothermal processes on Th distribution is not yet understood.

Recent studies of Collier and Dymond (1987) in Crater Lake show evidence of hot spring activity in the Lake. Their profiles of some metals (Mn and Fe) in Crater Lake show abrupt increase of concentrations at bottom water indicating a possibility of hydrothermal input. It can be supported by their CTD and light transmission data. The conductivity increases with water temperature in the bottom water, suggesting an increase in dissolved solids in the hot spring. As mentioned above, the interaction of the lake water with hot spring can result in precipitation. However, the light transmission of the warm water at the bottom (Collier and Dymond, 1987) was relatively constant, suggesting that large amounts of dissolved solids do not precipitate during this mixing process; concentrations of trace metals (Mn, Fe) are therefore enriched in the bottom water of the Lake.

The behavior of thorium in Crater Lake is different from those metals, however. As shown on the profile (Fig. 4.4), Th concentrations are almost

unchanged from 230 m to the bottom, unlike the other metals in Crater Lake. This indicates that the hydrothermal activity has very little contribution to the concentrations of both Th isotopes in the Lake. This result is in agreement with the study of Chen et al. (1986a) on the East Pacific Rise (21°N). Their results showed that concentrations of total ^{232}Th (<0.02-1.1 dpm/10^3L) in the hydrothermal solution was extremely low and was close to its concentration (0.04 dpm/10^3L) in the ambient seawater. They concluded that the hydrothermal Th flux to the seawater is negligible compared with the global river Th flux.

The recent study of Chen (1987) in hot springs on the Juan de Fuca ridge showed high concentrations of thorium (0.05-1.9 dpm/10^3L), indicating that Th was highly enriched in the hydrothermal solutions relative to ambient seawater. Because the samples were acidified prior to filtration, Chen suggested that leaching of ^{232}Th associated with particles might contribute a part of the thorium in the hydrothermal solution. Our results of ^{232}Th concentrations in hydrothermal solutions, collected by Dr. Kadko from the Juan de Fuca Ridge, range from 0.08 to 3.1 dpm/10^3 L, in general agreement with Chen's data. There are distinct relationships between ^{232}Th concentration and other properties of the sample solution. As shown on Table 10, the ^{232}Th concentration correlates positively with temperature, ^{226}Ra and ^{222}Rn; but negatively with pH and alkalinity. These relationships strongly indicate that, compared with seawater, the hydrothermal end-member is highly enriched in ^{232}Th. Thus, hydrothermal vents should constitute a source of ^{232}Th to the ocean. Because of few data are available at the present time, it is not possible to assess how large this source is. More unequivocal measurements are required to evaluate this source term.

TABLE 10. ^{232}Th concentrations in hydrothermal solution from Juan de Fuca Ridge (44°40'N, 130°20'W; water depth ~2000 m). Other data are from Kadko (unpublished).

Sample number	^{232}Th (dpm/10^3-l)	T°C	pH	Alk (meq/l)	^{226}Ra (dpm/l)	^{222}Rn (dpm/l)
1915m12	0.0816±.0040	6	6.85	2.37	---	---
1915m13	0.0823±.0052	24	7.45	2.37	---	---
1920m15	0.0812±.0042	27	4.93	2.10	---	---
1915m16	0.343 ±.007	244	6.05	1.39	5.1	96
1917m16	3.12 ±.05	326	3.70	0.19	28.8	649

4.3 Conclusion

1. Distributions and partitioning of thorium between dissolved and particulate forms in natural water systems are at least controlled by a number of biogeochemical factors, which vary with environmental setting.
2. Fluvial input is an important source of ^{232}Th in coastal regions.
3. The subsurface maximum of dissolved ^{232}Th in Saanich Inlet was possibly caused by the vertical transport of biogenic particles and its regeneration at the depth of the maximum; and its particulate maximum may be due to both the vertical transport of biogenic particles and the oxidation of manganese (II) catalyzed by bacteria in the suboxic water.
4. Thorium is strongly affected by the chemical changes across the redox boundary. Particulate Th tends to be released into water when particles settle across the O_2-H_2S interface, resulting in the enrichment of dissolved Th in reducing waters.
5. The correspondence observed in the distributions of ^{230}Th and ^{232}Th suggests that these two radioisotopes are involved in common geochemical cycles in the water column.
6. Seafloor hydrothermal vents are likely to constitute a source of ^{232}Th to bottom waters, but the magnitude of this input appears to be site-specific and remains to be evaluated.

SUMMARY

Based on data available at the present time, we can draw some conclusions about the fundamental behavior of ^{232}Th in the natural water system. The controlling factors on thorium distributions is the environmental setting, as indicated by the higher concentrations of thorium and its particle association in continental water than in seawater. The surface enrichment of dissolved ^{232}Th in seawater is evidence of its surface source and subsequent removal with depth, similar to that of many trace metals (Orians and Bruland, 1986; Schaule and Patterson, 1981; Nozaki et al., 1980; Bowen et al., 1980).

As with numerous trace metals, fluvial and aeolian inputs should be the two major sources of ^{232}Th to the ocean. Fluvial source may be more important in coastal regions, whereas atmospheric input is certainly dominant in the open ocean. Due to tremendously high concentrations of dissolved ^{232}Th in continental waters relative to in seawater, the discharge of river water could contribute a considerable flux of ^{232}Th to estuaries. From the relative low ^{232}Th observed in coastal waters, the dissolved riverine ^{232}Th is nearly quantitatively removed during rapid scavenging in estuary; it is unlikely that this source of ^{232}Th can be carried farther out into the open oceans. It means that the primary source of dissolved ^{232}Th to surface waters in the open oceans is probably from aeolian input.

It has been noted that input of ^{232}Th from aeolian and fluvial sources may also deliver ^{230}Th. The strong correspondence between the distribution of ^{230}Th and ^{232}Th in the water column implies that both isotopes may have a similar behavior and be involved in common geochemical cycles.

The occurrence of thorium subsurface maxima in several environments are probably caused by vertical scavenging processes involving biological activity.

From the similar distributions of ^{232}Th and NO_3^- in Saanich Inlet, and of ^{232}Th and ^{9}Be in manganese nodules (Huh, 1982), some insinuative information about the biochemical cycle of ^{232}Th may be gained. The similarities observed from the profiles of ^{232}Th and some trace metals in the water column also suggest that Th distribution is strongly dominated by the biochemical cycle.

The oxidation and reduction reactions are another controlling factor on Th distributions. Particulate ^{232}Th is higher than dissolved ^{232}Th above the oxygen-hydrogen sulfide interface, but lower in the underlying anoxic water. The reductive dissolution of Fe-Mn oxyhydroxides regulates the behavior of thorium in the anoxic water. In addition, thorium is released into the water from particles by formation of a soluble complex with $[Fe(NH_3)_6]^{2+}$ in absolute anoxic environment. As a result, dissolved Th concentration tends to increase toward bottom in extremely reducing water, unlike the profiles in the Panama/Guatemala Basins (Bacon and Anderson, 1982) and the Santa Monica Basin (Huh and Beasley, 1987). These basins are underlain by reducing sediments, too. However, ^{230}Th showed a decrease toward the bottom from a mid-depth maximum. Bacon and Anderson (1982) suggested that the decrease was caused by enhanced scavenging in the reducing environment, which disagrees with our observations in Saanich Inlet. Therefore, whether seafloor sediments act as a net sink or source of dissolved ^{232}Th in the overlying water column requires more study. The most rigorous approach to answer the above question would be to study sediment pore water.

The fate of thorium is closely correlated with the fate of manganese. The coincidences of the similar trends in the water column observed from Saanich Inlet and Washington and Oregon coast indicate that ^{232}Th may be tightly coupled with Mn in continental margin waters; and suggest that Mn and ^{232}Th may have participated in common geochemical cycles to a very large extent.

BIBLIOGRAPHY

1. Anderson, J.J. and Devol, A.H. (1973). Deep water renewal in Saanich Inlet, an intermittently anoxic basin. Estuarine Coastal Mar. Sci. 1, 1-10

2. Anderson, R.F. (1982). Concentration, vertical flux, and remineralization of particulate uranium in seawater. Geochim. Cosmochim. Acta 46, 1293-1299

3. Anderson, R.F., Bacon, M.P. and Brewer, P.G. (1982). Elevated concentrations of actinides in Mono Lake. Science 216, 514-516

4. Anderson, R.F., Bacon, M.P. and Brewer, P.G. (1983a). Removal of ^{230}Th and ^{231}Pa from the open ocean. Earth Planet. Sci. Lett. 62, 7-23.

5. Anderson, R.F., Bacon, M.P. and Brewer, P.G. (1983b). Removal of ^{230}Th and ^{231}Pa at ocean margins. Earth Planet. Sci. Lett. 66, 73-90.

6. Bacon, M.P. and Anderson, R.F. (1982). Distribution of thorium isotopes between dissolved and particulate forms in the deep sea. J. Geophys. Res. 83, 2045-2056

7. Bacon, M.P., Brewer, P.C., Spencer, D.W., Murray, J.W. and Goddard, J. (1980). Lead-210, polonium-210, manganese and iron in the Cariaco Trench. Deep-Sea Res. 27A, 119-135

8. Baker, E.T. (1976). Distribution, composition, and transport of suspended particulate matter in the vicinity of Willapa submarine canyon, Washington. Geol. Soc. America. Bull. 87, 625-632.

9. Barnes, S.S. and Dymond, J.R. (1967). Rates of accumulation of Ferro-manganese nodules. Nature 213, 1218-1219.

10. Beasley, T.M., Carpenter, R. and Jennings, C.D. (1982). Plutonium, ^{241}Am and ^{137}Cs ratios, inventories and vertical profiles in Washington and Oregon continental shelf sediments. Geochim. Cosmochim. Acta 46, 1931-1946

11. Bhat, S.G., Krishnaswami, S., Lal, D., Rama, M. and Moore, W.S. (1969). ^{234}Th/^{238}U ratios in the ocean. Earth Planet. Sci. Lett. 5, 483-491

12. Bowen, V.T., Noshkin, V.E., Livingston, H.D. and Volchok, H.L. (1980). Fallout radionuclides in the Pacific Ocean: vertical and horizontal distributions, largely from GEOSECS stations. Earth Planet. Sci. Lett. 48, 411-434

13. Boyle, E.A., Sclater, F.R. and Edmond, J.M. (1977). The distribution of dissolved copper in the Pacific. Earth Planet. Sci. Lett. 37, 38-54

14. Broecker, W.S., Kaufman, A. & Trier, R.M. (1973). The residence time of thorium in surface sea water and its implications regarding the rate of reactive pollutants. Earth Planet. Sci. Lett. 20, 35-44

15. Bruland, K.W., Franks, R.P., Landing, W.M. and Soutar, A. (1981). Southern California inner basin sediment trap calibration. Earth Planet. Sci. Lett. 53, 400-408

16. Bruland, K.W. (1983). Trace metals in sea-water. In; Chemical Oceanography, Vol.18, 157-220 (Editors: J.P. Riley and R. Chester) Academic Press.

17. Burnett, W.C. and Morgenstein, M. (1976). Growth rates of Pacific nodules as deduced by uranium-series and hydration-rind dating techniques. Earth Planet. Sci. Lett. 33, 208-218.

18. Chen, J.-H and Wasserburg, G.J., von Damm, K.L. and Edmond, J.M. (1986a). The U-Th-Pb systematics in hot springs on the East Pacific Rise at 21°N and Guaymas Basin. Geochim. Cosmochim. Acta 50, 2467-2479

19. Chen, J.-H, Edwards, R.L., Wasserburg, G.J. (1986b). ^{238}U, ^{234}U and ^{232}Th in seawater. Earth Planet. Sci. Lett. 80, 241-252

20. Chen, J.H. (1987). U, Th, and Pb isotopes in hot springs on the Juan de Fuca Ridge. J. Geophysical Res. 92, 11411-11415.

21. Cherry, R.D. and Shannon, L.V. (1974). The alpha-radioactivity of marine organisms. Atomic Energy Review 12, 3-45

22. Coale, K.H. & Bruland, K.W. (1985). ^{234}Th:^{238}U disequilibrium within the California Current. Limnol. Oceanogr. 301, 22-33

23. Cochran, J.K., Livingston, H.D., Hirschberg, D.J. and Surprenant, L.D. (1987). Natural and anthropogenic radionuclide distributions in the Northwest Atlantic Ocean. Earth Planet. Sci. Lett. 84, 135-152.

24. Collier, R. & Dymond, J. (1987). Studies of hydrothermal processes in Crater Lake: A preliminary report of field studies conducted in 1987 for Crater Lake National Park.

25. Cotton, F.A. and Wilkinson, G. (1972). Advanced inorganic chemistry, (3rd ed.) Eiley-Interscience, New York.

26. Dahm, C.N., Gregory, S.V. and Park, P.K. (1981). Organic carbon transport in the Columbia River. Est. Coast. Shelf Sci. 13, 645-658

27. deBaar, H.J.W., Bacon, M.P. and Brewer, P.G. (1983). Rare-earth distributions with a positive Ce anomaly in the Western North Atlantic Ocean. Nature 301, 324-327

28. Edmond, J.M., Measures, C.I., McDuff, R.E., Chan, L.H., Collier, R., Grant, B., Gordon, L.I. and Corliss, J.B. (1979a). Ridge crest hydrothermal activity and the balances of the major and minor elements in the ocean: the Galapagos data. Earth Planet. Sci. Lett. 46, 1-18

29. Edmond, J.M., Measures, C.I., Mangum B., Grant, B., Sclater, F.R., Collier, R., Hudson A., Gordon, L.I. and Corliss, J.B. (1979b). On the formation of metal-rich deposits at ridge crests. Earth Planet. Sci. Lett. 46, 19-30

30. Edmond, J.M., von Damm, K.L., McDuff, R.E. and Measures, C.I. (1982). Chemistry of hot springs on the East Pacific Rise and their effluent dispersal, Nature 297, 187-191

31. Elderfield, H. and Greaves, M.J. (1982). The rare earth elements in seawater. Nature 296, 214-219

32. Emerson, S., Cranston, R.E. and Liss, P.S. (1979). Redox species in a reducing fjord: equilibrium and kinetic considerations. Deep-Sea Res. 26A, 859-878

33. Ertel, J.R., Hedges, J.I., Devol, A.H., Richey, J.E. and Ribeiro, M.N.G. (1986). Dissolved humic substances of the Amazon River system. Limnol. Oceanogr. 31(4), 739-754

34. Fuger, J. and Oetting, F.L. (1976). The chemical thermodynamics of actinide elements and compounds. Part 2, The Actinide Aqueous Ions, part 2, pp. 16-60. Int. At. Energy Agency.

35. Golden, J. and Maddock, A.G., (1956). Protactinium - I, analytical separations. J.Inorg. Nucl. Chem. 2, 46-59

36. Gorden, R.M., Martin, J.H. and Knauer, G.A. (1982). Iron in Northeast Pacific waters. Nature 299, 611-612.

37. Harvey, G.R., Boran, D.A., Chesal, L.A. & Tokar, J.M. (1983). The structure of marine fulvic and humic acids. Mar. Chem. 12, 119-132.

38. Higashi, S. (1959). Estimation of the microgram amount of thorium in sea water. J. Oceanog. Soc. Japan, 15, 1-4

39. Huh, C.-A. (1982). Radiochemical and chemical studies of manganese nodules from three sedimentary regimes in the North Pacific. Ph.D. Thesis, University of Southern California, Los Angeles, 305pp.

40. Huh, C.-A. (1985). Unpublished data.

41. Huh, C.-A. and Ku, T.L. (1984). Radiochemical observations on manganese nodules from three sedimentary environments in the north Pacific. Geochim. Cosmochim. Acta 48, 951-963

42. Huh, C.-A. and Bacon, M. P., (1985a). Determination of thorium concentration in seawater by neutron activation analysis. Analyt. Chem. 57, 2138-2142

43. Huh, C.-A. and Bacon, M. P., (1985b). Thorium-232 in the eastern Caribbean Sea. Nature 316(22) 718-721

44. Huh, C.-A. and Beasley, T. M., (1987). Profiles of dissolved and particulate thorium isotopes in the water column of coastal Southern California. Earth Planet. Sci. Lett. 85, 1-10

45. Huh, C.-A., Zahnle, D.L., Small, L.F. and Noshkin, V.E. (1987). Budgets and behaviors of uranium and thorium series isotopes in Santa Monica Basin sediments. Geochim. Cosmochim. Acta 51, 1743-1754

46. Huh, C.A. and Manheim, F.T., unpublished data.

47. Huh, C.A. and Moore, W.S. (1988). Oceanic distribution of ^{232}Th: a reconnaissance and implications from manganese nodules. Submitted to Earth Planet. Sci. Lett.

48. Hydes, D.J. (1979). Aluminum in seawater: Control by inorganic processes. Science 205, 1260-1262

49. Imai, T. and Sakanoue, M. (1973). Content of plutonium, thorium, and protactinium in sea water and recent coral in the north Pacific. J. Oceanogr. Soc. Japan 29, 76-82.

50. Ivanovich,M. and Harmon, R.S. (Editor). Uranium Series Disequilibrium: Applications to Environmental Problems (1982).

51. Jay, D. and Sherwood, C.R. (1984). The Columbia River estuary. in Columbia River Estuary Data Development Program, Cha. I (Editors: Fox, D.S., Vell, S., Nehlsen, W. and Damron, J.)

52. Jones, C. J. and Murray, J. W. (1985). The geochemistry of manganese in the northeast Pacific Ocean off Washington. Limnol. Oceanogy. 30. 81-92

53. Katz, A. and Kaplan, I.R. (1981). Heavy metals behavior in coastal sediments of southern california: a critical review and synthesis. Mar. Chem. 10, 261-299

54. Kaufman, A. (1969). The ^{232}Th concentration of surface ocean water. Geochim. Cosmochim. Acta 33, 717-724.

55. Knauer, G.A., Martin, J.H. and Gordon, R.M. (1982). Cobalt in north-east Pacific waters. Nature 297, 49-51

56. Knauss, K.G., T.L. Ku and W.S. Moore (1978). Radium and thorium isotopes in the surface waters of the East Pacific and coastal Southern California. Earth Planet. Sci. Lett. 39, 235-249.

57. Koczy, F., Picciotto, E., Poulaert, G. and Wilgain, S. (1957). Mesure des isotopes du Th dans l'eau de mer. Geochim. Cosmochim. Acta 11, 103-129

58. Koide, M., Bruland, K.W. and Goldberg, E.D. (1973). $^{228}Th/^{232}Th$ and ^{210}Pb geochronologies in marine and lake sediments. Geochim. Cosmochim. Acta 37, 1171-1181

59. Korkisch, J. (1969). Modern methods for the separation of rarer metal ions. Pergamon Press.

60. Krishnaswami, S., Lal, D., Somayajulu, B.L.K. Dixon, F.S., Stonecipher, S.A. and Craig, H. (1972). Si, Ra, Th, and Pb in seawater: in-situ extraction by synthetic fiber. Earth Planet. Sci. Lett. 16, 84-90

61. Krishnaswami, S., Lal, D., Somayajulu, B.L.K. Weiss, R.F. and Craig, H. (1976). Large volume in situ filtration of deep Pacific waters: mineralogical and radioisotope studies. Earth Planet. Sci. Lett. 32, 420-429.

62. Krishnaswami, S. and J.K. Cochran (1978). Uranium and thorium series nuclides in oriented ferromanganese nodules: growth rates, turnover times and nuclide behavior. Earth Planet. Sci. Lett. 40, 45-62.

63. Ku, T.L. (1976). The uranium-series methods of age determination. Annual review of Earth and planetary Sciences 4, 347-379

64. Ku, T.L. and Broecker, W.S. (1969). Radiochemical studies on manganese nodules of deep-sea origin. Deep-Sea Research 16, 625-637.

65. Ku, T.L., Omura, A. and Chen, P.S. (1979). ^{10}Be and U-series isotopes in manganese nodules from the central North Pacific. in: Marine Geology and Oceanography of the Pacific Manganese Nodule Province (Eds. Bischoff, J.L. and D.Z. Piper), Plenum Publishing Co.

66. Kunzendorf, H. and Friedrich, G.H. (1976). The distribution of U and Th in growth zones of Manganese nodules. Geochim. Cosmochim. Acta 40, 849-852

67. Kusakabe, M. and Ku, T.L. (1984). Incorporation of Be isotopes and other trace metals into marine ferromanganese deposits. Geochim. Cosmochim. Acta 48, 2187-2193.

68. Kuznetsov, Y., Simonyak, Z., Elizarova, A. and Lisitsyn, A. (1966). Content of Pa and Th isotopes in ocean water. Radiokhimiya 8, 455-458

69. LaFlamme, B.D. & Murray, J.W. (1987). Solid/solution interaction: The effect of carbonate alkalinity on adsorbed thorium. Geochim. Cosmochim. Acta 51, 243-250

70. Lalou, C., Ku, T.L., Brichet, E., Poupeau, G. and Romary, P. (1979). Techno encrustation, Part I: Radiometric studies. in: Collques Int'l du CNRS 289, La Genese Nodules de Manganese, 261-269.

71. Landing, W.M. and Bruland, K.W. (1981). The vertical distribution of iron in the Northeast Pacific. EOS. 62, 906

72. Langmuir, D. & Herman, J.S. (1980). The mobility of thorium in natural waters at low temperatures. .Geochim. Cosmochim. Acta 44, 1753-1766

73. Lazarev, K.F., Nikolaev, D.S. and Grashchenko, S.M. (1961). Concentration of thorium isotopes in sea water. Radiokhimiya, III (5), 623-635.

74. Li, Y.-H., Feely, H.W. and Santschi, P.H. (1979). ^{228}Th-^{228}Ra radioactive disequilibrium in the New York Bight and its implications for coastal pollution. Earth Planet. Sci. Lett. 42, 13-26

75. Li, Y.-H., Birkhardt, L. and Teraoke, H. (1984). Desorption and coagulation of trace elements during estuarine mixing. Geochim. Cosmochim. Acta 48, 1879-1884

76. Mangini, A. and Key, R.M. (1983). A Th-230 profile in the Atlantic Ocean. Earth Planet. Sci. Lett. 62, 377-384.

77. Mangini, A., Segl, M., Kudrass, H., Wiedicke, M., Bonati, G., Hoffman, H.J., Morenzoni, E., Nessi, M., Suter, M. and Wölfli, W. (1986). Diffusion and supply rates of ^{10}Be and ^{230}Th radioisotopes in two manganese encrustations from the South China Sea. Geochim. Cosmochim. Acta 50, 149-156.

78. Matsumoto, E. (1975). ^{234}Th-^{238}U radioactive disequilibrium in the surface layer of the ocean. Geochim. Cosmochim. Acta 39, 205-212

79. McKee, B.A., DeMaster, D.J. and Nittrouer, C. A. (1984). The use of ^{234}Th/^{238}U disequilibrium to examine the fate of particle-reactive species on the Yangtze continental shelf. Earth Planet. Sci. Lett. 68, 431-442

80. Measures, C.I. and Edmond, J.M. (1982). Beryllium in the water column of the central North Pacific. Nature 297, 51-53

81. Measures, C.I. and Edmond, J.M. (1984). The geochemical cycle of ^{9}Be: a reconnaissance. Earth Planet. Sci. Lett. 66, 101-110

82. Measures, C.I. and Edmond, J.M. (1984). Aluminum in the Panama Basin and the North East Atlantic. EOS 65, 967

83. Measures, C.I., Grant, B., Khadem, M., Lee, D.S. and Edmond, J.M. (1984). Distribution of Be, Al, Se and Bi in the surface waters of the western North Atlantic and Caribbean. Earth Planet. Sci. Lett. 71, 1-12

84. Miyake, Y., Sugimura, Y. and Yasujima, T. (1970). Thorium concentration and the activity ratios ^{230}Th/^{232}Th and ^{228}Th/^{232}Th in sea water in the western North Pacific. J. Oceanogr. Soc. Japan 26(3), 130-136.

85. Moore, R.M. (1983). The relationship between distributions of dissolved cadmium, iron and aluminum and hydrography in the Central Arctic Ocean. in Trace Metals in Sea Water (ed. by Wong, Bayle, Bruland, Burton and Goldberg). Plenum Publishing Corp.

86. Moore, W.S. (1967). Amazon and Mississippi River concentrations of U, Th, and Ra isotopes. Earth Planet. Sci. Lett. 2, 231-234.

87. Moore, W.S. (1969). Measurement of ^{228}Ra and ^{228}Th in sea water. J. Geophys. Res. 74, 694-704

88. Moore, W.S. (1974). Accumulation rates of manganese crusts on rocks exposed on the sea floor. in: Inter-university Program of Research on Ferromanganese Deposits of the Ocean Fllor: Phase I Report, 93-97.

89. Moore, W.S. (1981). The thorium isotope content of ocean water. Earth Planet. Sci. Lett. 53, 419-426.

90. Moore, W.S. (1984). Thorium and radium isotopic relationships in manganese nodules and sediments at MANOP Site S. Geochim. Cosmochim. Acta 48, 987-992.

91. Moore, W.S. and W.M. Sackett (1964). Uranium and thorium series inequilibrium in seawater. J. Geophys. Res. 69, 5401-5405.

92. Moore, W.S. and Vogt, P.R. (1976). Hydrothermal manganese crusts from two sites near the Galapagos spreading axis. Earth Planet. Sci. Lett. 29, 349-356.

93. Moore, W.S., Ku, T.L., MacDougall, J.D., Burns, V.M., Burns, R., Dymond, J., Lyle, M.W. and Piper, D.Z. (1981). Fluxes of metals to a manganese nodule: radiochemical, chemical, structural, and mineralogical studies. Earth Planet. Sci. Lett. 52, 151-171.

94. Murray, J.W., Spell, B. and Paul, B. (1983). The contrasting geochemistry of manganese and chromium in the Eastern Tropical Pacific Ocean. in Trace Metals in Sea Water (ed. by Wong, Bayle, Bruland, Burton and Goldberg). Plenum Publishing Corp.

95. Myasoedov, B.F. and Muxart, R. (1962). An extraction photometric method for the determination of quinquevalent protoactinium by means of thenoyltrifluoroacetone. Zhur. Anal. Khim. 17, 340-342

96. Nittrouer, C.A., Sternberg, R.W., Carpenter, R. and Bennett, J.T. (1979). The use of ^{210}Pb geochronology as a sedimentological tool: application to the Washington continental shelf. Mar. Geol. 31, 297-316

97. Nozaki, Y., Turekian, K.K. and Von Damm, K. (1980). ^{210}Pb in GEOSECS water profiles from the north Pacific. Earth Planet. Sci. Lett. 49, 393-400.

98. Nozaki, Y., Horibe, Y. & Tsubota, H. (1981). The water column distributions of thorium isotopes in the western North Pacific. Earth. Planet. Sci. Lett. 54, 203-216

99. Nozaki, Y. & Horibe, Y. (1983). Alpha-emitting thorium isotopes in northwest Pacific deep waters. Earth Planet. Sci. Lett. 65, 39-50

100. Nozaki, Y. and Nakanishi T. (1985). Pa-231 and Th-230 profiles in the open ocean water column. Deep-Sea Res. 32, 1209-1220.

101. Nozaki, Y. and Yang, H.-S. (1985). Non-destructive alpha-spectrometry and radiochemical studies of deep-sea manganese nodules. Geochim. Cosmochim. Acta 49, 1765-1774.

102. Nozaki, Y. and Yamada, M. (1987). Thorium and protactinium isotope distributions in waters of the Japan Sea. Deep-Sea Res. 34(8), 1417-1430.

103. Nozaki, Y. Yang, A.-S. and Yamada, M. (1987). Scavenging of thorium in the ocean. J. Geop. Res. 92, 772-778

104. Orians, K.J. and Bruland, K.W. (1986). The biogeochemistry of aluminum in the Pacific Ocean. Earth Planet. Sci. Lett. 78, 397-410.

105. Pal'shin, E.S.and Myasoedov, B.F. (1963). Separation of protoactinium from other elements by extraction with thenoyltrifluoroacetone. Zhur. Anal. Khim. 18,750-756

106. Perdue, E.M. (1978). Solution thermochemistry of humic substances--I. Acid-bace equilibria of humic acid. Geochim. Cosmochim. Acta 42, 1351-1358

107. Pruter, A.T. and Alverson, D.L. (1972). The Columbia River estuary and adjacent ocean waters. University of Washington Press, Seattle.

108. Reuter, J.H. and Perdue, E.M. (1977). Importance of heavy metal-organic matter interactions in natural waters. Geochim. Cosmochim. Acta 41, 325-334

109. Richards, H.G. and Strens, M.R. (1985). Ocean floor hot springs. Sci. Prog., Oxf. 69, 341-358

110. Riley, J.P. and Chester, R. (Editors). in Chemical Oceanography, Vol.l8, 157-220 (1983). Academic Press.

111. Rogers, J.J.W. and Adams, J.A.S. (1969). Handbook of geochemistry, ed. K.H. Wedepohl. Springer-Verlag, Berlin.

112. Ryabchikov, D.I., Gol'braikh, E.K. (1963). The analytical Chemistry of Thorium. The Macmilian Company, new york

113. Salomons, W. & Förstner, U. (1984). Metals in the Hydrocycle. Press by Springer-Verlag, Berlin Heidelberg New York Tokyo.

114. Sanchez, A. L., Murray, J.W., Schell, W.R., and Miller, L.G., 1986. Fallout plutonium in two oxic-anoxic environments. Limnol. Oceanogr. 31(5), 1110-1121

115. Schaule, B.K. and Patterson, C.C. (1981). Lead concentrations in the northeast Pacific: evidence for global anthropogenic perturbations. Earth Planet. Sci. Lett. 54, 97-116.

116. Scott. M.R., Scott, R.B., Rona, P.A. and Butler, L.W. (1974). Rapidly accumulating manganese deposit from the median valley of the Mid-Atlantic Ridge. Geophysical Research Letters 1(8), 355-358.

117. Sharma, P. Rama and Moore, W.S. (1984). Spatial variation of U-Th series radionuclides and trace metals in deep-sea manganese encrustations. Earth Planet. Sci. Lett. 67, 319-326.

118. Sholkovitz, E.R. (1976). Flocculation of dissolved organic and inorganic matter during the mixing of river water and seawater. Geochim. Cosmochim. Acta 40, 831-845

119. Simpson, H.J. (1970). Tritium in Crater Lake, Oregon. J. Geophys. Res., 75(27), 5195-5205

120. Somayajulu, B.L.K. and Goldberg, E.D. (1966). Thorium and uranium isotopes in seawater and sediments. Earth Planet. Sci. Lett. 1, 102-106.

121. Spencer, D.W. and Brewer, P.G. (1971). Vertical advection diffusion and redox potentials as controls on the distribution of manganese and other trace metals dissolved in waters of the Black Sea. J. Geophys. Res. 76, 5877

122. Sposito, G. (1985). Sorption of trace metals by humic materials in soils and natural waters. CRC Critical Reviews in Environmental Control Vol. 16, Issue 2

123. Sunda, W.G. and Huntsman, S.A., 1986. Relationships among growth rate, cellular manganese concentrations and manganese transport kinetics in estuarine and oceanic species of the diatom thalassiosira. J. Phycal. 22, 259-270

124. Tebo, B.M., Personal communication.

125. Tebo, B.M. and Emerson, S. (1986). Microbial manganese (II) oxidation in the marine environment: a quantitative study. Biogeochemistry 2, 149-161

126. Tebo, B.M., Nealson, K.H., Emerson, S. and Jacobs, L. (1984). Microbial mediation of Mn (II) and Co (II) precipitation at the interfaces in two anoxic fjords. Limnol. and Oceanogr. 29, 1247-1258

127. Thompson, J.M., White, L.D. and Nathenson, M. (1987). Chemical analyses of waters from Crater Lake, Oregon, and nearby springs. U.S. Geological Survey, Open-File Report 87-587

128. Todd, J.F., Elsinger, R.J. and Moore, W.S. (1988). The distributions of uranium, radium and thorium isotopes in two anoxic fjords: Framvaren Fjord (Norway) and Saanich Inlet (British Columbia). *Mar. Chem.* 23, 393-415

129. Turner, D.R., Whitfield, M. and Dickson, A.G. (1981). The equilibrium speciation of dissolved components in freshwater and seawater at 25°C and 1 atm pressure. Geochim. Cosmochim. Acta 45, 855-881

130. Volchok, H.L., Feiner, M., Simpson, H.J., Broecker, W.S., Noshkin, V.E., Bowen, V.T. and Willis, E. (1970). Ocean fallout--the Crater Lake experiment. J. Geophys. Res. 75(6), 1084-1091

131. Walker, R.L., Eby, R.E., Pritchard, C.A. and Carter, J.A., (1974). Simultaneous plutonium and uranium isotopic analysis from a single resin bead--a simplified chemical technique for assaying spent reactor fuels. Anal. Lett. 7, 563-574

132. Weiss, R.F. (1977). Hydrothermal manganese in the deep sea: scavenging residence time and Mn/He^3 relationships. Earth Planet. Sci. Lett. 37, 257-262

133. Williams, D.L. and Von Herzen, R.P. (1983). On the terrestrial heat flow and physical limnology of Grater Lake, Oregon. J. Geophys. Res. 88(B2), 1094-1104